

Assessing the Performance of Polymer-Bentonite Mixtures for
Hydraulic Barrier Applications

By

Weijuan Geng

A dissertation submitted in partial fulfillment of
the requirements for the degree of

Doctor of Philosophy

(Civil and Environmental Engineering)

at the

UNIVERSITY OF WISCONSIN-MADISON

2018

Date of final oral examination: 05/24/2018

The dissertation is approved by the following members of the Final Oral Committee:

William J. Likos, Professor, Civil and Environmental Engineering

Craig H. Benson, Dean of School of Engineering and Applied Science, University
of Virginia

Tuncer H. Edil, Professor Emeritus, Civil and Environmental Engineering

James M. Tinjum, Associate Professor, Engineering Professional Development

Greeshma Gadikota, Assistant Professor, Civil and Environmental Engineering

© Copyright by Weijuan Geng 2018

All Right Reserved

ABSTRACT

ASSESSING THE PERFORMANCE OF POLYMER-BENTONITE MIXTURES FOR HYDRAULIC BARRIER APPLICATIONS

WEIJUAN GENG

Under the Supervision of Professor William J. Likos
at the University of Wisconsin-Madison

Geosynthetic clay liners (GCLs) containing polymer-modified bentonite (PMB) are increasingly being applied as components of hydraulic barrier systems in lieu of conventional sodium bentonite (Na-B) GCLs for improved performance in the presence of chemically aggressive leachates. A comprehensive suite of laboratory experiments was conducted to evaluate the physio-chemical properties of various types of polymers and PMBs. The overall objective of the testing series has been to develop more fundamental understanding of the physical and chemical mechanisms by which PMBs maintain low hydraulic conductivity to aggressive permeant solutions, the limits of this performance, and alternative tests methods by which this performance may be assessed. Conventional index tests including free swell, liquid limit, and fluid loss are not reliable for screening hydraulic performance and chemical compatibility of PMB-GCLs. Experiments were conducted to evaluate viscosity as an alternative index test for screening hydraulic performance and chemical compatibility of PMB-GCLs. Viscosity of representative polymer and polymer-bentonite suspensions is influenced by polymer loading, ionic strength, and chemistry of the test solution. Viscosity of polymer-bentonite suspensions correlates to hydraulic conductivity of PMB-GCLs, where higher viscosity of PMB

corresponds to lower hydraulic conductivity of PMB-GCL permeated with the same solution. A threshold viscosity at 200 cP is identified to correlate to nominally “low” hydraulic conductivity ($<10^{-10}$ m/s). Elution of polymer from PMB-GCLs during permeation is observed to correspond to lower viscosity of PMB in suspension with the same solution, indicating a more mobile polymer phase and high hydraulic conductivity resulting from formation of preferential flow paths as polymer is eluted. Based on these observations, viscosity can potentially be used as an alternative index test in lieu of conventional indices such as free swell, liquid limit, and fluid loss for evaluating hydraulic conductivity and chemical compatibility of PMB-GCLs.

The conformation (shape and structure) of polymer chains in solution is sensitive to environmental conditions such as pH, ionic strength, temperature, electrical potential, and photo-irradiation. Low pH and/or high ionic strength generally result in a coiled polymer conformation, whereas high pH and/or low ionic strength generally result in an extended polymer conformation that forms a well-developed polymer gel upon swelling. Polymer in PMBs ideally forms a hydrogel upon exposure to aqueous solution, clogs bentonite macropores, and results in low hydraulic conductivity of PMB GCLs. Turbidity of polymer and polymer-bentonite suspensions and a modified water content tests were evaluated as potential index measurements to assess polymer conformation and hydrogel formation. Turbidity of polymer suspensions is influenced by solution chemistry and generally decreases with increasing ionic strength. Presence of divalent cations in solution promotes polymer precipitation and affects polymer-bentonite interaction. Solutions rich in SO_4^{2-} have a thickening effect and increase the turbidity of polymer suspensions in comparison to solutions rich in Cl^- . A modified water content test

developed to quantify the water-holding capacity of PMBs is directly correlated to turbidity in solutions where bentonite exhibits comparable swelling. High modified water content of PMB in test solutions systematically correlates to lower hydraulic conductivity of PMB-GCLs permeated with the same solutions. A threshold modified water content value at 230% is required for achieving hydraulic conductivity lower than 10^{-10} m/s for the PMB-GCL.

Previous studies have shown that the magnitude of hydraulic gradient (i) used in laboratory permeation tests does not have a significant effect on measured hydraulic conductivity (k) of conventional NaB GCLs. However, there is a potential effect on hydraulic conductivity of PMB GCLs due to mobilization and elution of polymer. Two sets of hydraulic conductivity tests were performed for PMB GCLs permeated with (1) pure divalent cation-chloride solution (50 mM CaCl_2), and (2) high sodic-sulfate synthetic leachate (Trona) using various hydraulic gradients ($10 \leq i \leq 380$) and at comparable effective stress. Uniformity of post-test polymer distribution within the GCLs was quantified by loss on ignition (LOI) testing to assess polymer elution and preferential flow path development. Results indicate that high hydraulic gradient promotes polymer elution and formation of preferential flow paths. Higher hydraulic gradient tends to elute polymer from PMB GCLs and increases hydraulic conductivity. Results support the hypothesis that polymer clogging in the bentonite macropores is a primary mechanism for low hydraulic conductivity of PMB GCLs.

Anion species have generally not been considered to influence the hydraulic conductivity of conventional NaB-GCLs but have been found in previous studies to affect hydraulic conductivity of PMB-GCLs. Experiments were conducted to evaluate the

turbidity, viscosity, free swell, and modified water content of polymer and polymer-bentonite suspensions and the hydraulic conductivity of PMB-GCLs for a suite of single species anion solutions selected from the Hofmeister anion ranking series. Turbidity and viscosity of polymer suspensions showed similar trends according to anion type. Free swelling, viscosity, and modified water content for polymer-bentonite mixtures also showed consistent trends, but different than those observed for the polymer suspensions. Results suggest that polymer-bentonite interaction is the dominating factor that determines these characteristics of polymer-bentonite suspensions and that this behavior is affected by anion type. Hydraulic conductivity of PMB-GCLs is dominated by bentonite fraction at the initial stage of permeation, then by polymer-bentonite interaction as permeation continues, and ultimately by polymer elution. Anion type influences all three factors, and thus is considered an essential factor in influencing the hydraulic conductivity of PMB-GCLs.

A final suite of tests was determined to quantify the location and characteristics of the polymer fraction in PMBs. Nitrogen sorption isotherms measured for a commercially available PMB and BET (Brunauer-Emmett-Teller) analysis of the isotherms shows that polymer is present in the bentonite inter-aggregate voids. The presence of the polymer increases the meso-pore fraction by decreasing the volume of macropores. Results from the sorption-based pore size analysis were combined with pore size distributions (PSD) available in the literature from mercury intrusion porosimetry (MIP) for conventional bentonite to propose a tri-modal PSD for dry-blended PMBs.

ACKNOWLEDGEMENTS

First and foremost, I would like to thank Professor Bill Likos, my advisor, for his guidance and support throughout my years at the University of Wisconsin-Madison. This document would not exist without you. I would also like to thank Professor Craig Benson for his advice, comments and good discussions during our weekly research meetings. Also, many thanks to my committee: Professor Tuncer Edil, Professor Greeshma Gadikota, and Professor James Tinjum for their help and support. Special thanks to Professor Greeshma Gadikota for providing laboratory equipment and valuable suggestions regarding the sorption-based pore size analysis.

Thank you to Xiaodong Wang for his assistance in the lab. Thank you to undergraduate students including Lauren Thomas, Adrienne Fedora, James Schmidt, Adam Fiore, and Ross Koderl for helping me in the lab.

Thanks to my fellows, Hulya Salihoglu, Will Reybrock, Idil Akin, Alex Michaud, and Jun Yao who have contributed in one way or another to this work. Thanks are extended to all GLE friends for help, discussions, greetings, jokes, funs, etc. Thanks to my friends in Evanston and Madison, particularly Yuli Liu. Thanks to GDZ Production and FanTennis Club for providing me the chance to do the things I love beyond the research life. Thank you all, I had an enjoyable and memorable time along this journey.

Most importantly, I would express gratitude to my parents Hanjun Geng and Xiaoyu Li for their endless love and support.

Financial support of this research work was provided by Colloid Environmental Technologies Co. (CETCO). This support is gratefully acknowledged.

TABLE OF CONTENTS

ABSTRACT	i
ACKNOWLEDGEMENTS	v
TABLE OF CONTENTS	vi
LIST OF FIGURES.....	xiv
LIST OF TABLES.....	xx
CHAPTER ONE	1
EXECUTIVE SUMMARY.....	1
1.1 INTRODUCTION	1
1.2 GEOSYNTHETIC CLAY LINERS	3
1.3 LABORATORY HYDRAULIC CONDUCTIVITY.....	3
1.4 MAJOR FINDINGS	5
1.5 TABLES.....	10
1.6 REFERENCES	11
CHAPTER TWO.....	14
MICROSTRUCTURE INVESTIGATION OF POLYMER-MODIFIED BENTONITE USING BET PORE SIZE ANALYSES	14
ABSTRACT	14
2.1 INTRODUCTION	15
2.2 BACKGROUND.....	16

2.2.1. Pore Size Distribution of Bentonite.....	16
2.2.2. Sodium Bentonite and Implication of Swelling on Bentonite Pores	17
2.3 MATERIALS AND METHODS	19
2.3.1. Polymer Modified Bentonite (PMB) and PMB-GCLs	19
2.3.2. Gas sorption, BET Surface Area, and BJH Pore Volume Measurements	20
2.4 RESULTS AND DISCUSSION	21
2.4.1. BET Specific Surface Area and Porosity.....	21
2.4.2. Pore Size Distribution of PMBs	22
2.5 SUMMARY AND CONCLUSIONS.....	23
2.6 REFERENCES	25
2.7. FIGURES.....	30
CHAPTER 3	38
VISCOSITY AS AN ALTERNATIVE INDEX TEST FOR POLYMER-MODIFIED GEOSYNTHETIC CLAY LINERS.....	38
ABSTRACT	38
3.1 INTRODUCTION	40
3.2 BACKGROUND	44
3.2.1. Polymers, Polymer Conformation, and Bentonite-Polymer Interaction.....	44
3.2.2. Limitations of Conventional Index Parameters	45
3.2.3. Viscosity as an Alternative Index Test.....	47

3.3 MATERIALS AND METHODS	48
3.3.1. Test Solutions	48
3.3.2. Polymer Modified Bentonite (PMB) Geosynthetic Clay Liner	49
3.3.3. Polyacrylamide (PAM) Polymer.....	50
3.3.4. Mixtures of PAM Polymer and Na-B.....	50
3.3.5. Viscosity Testing	51
3.3.6. Hydraulic Conductivity Testing	52
3.4 RESULTS AND DISCUSSION	53
3.4.1. Viscosity of PAM Polymer	53
3.4.2. Viscosity of PAM Polymer and Na-B Mixtures.....	54
3.4.3. Viscosity and Hydraulic Conductivity of PMB-GCL	57
3.4.4. Viscosity and Polymer Elution	58
3.5 SUMMARY AND CONCLUSIONS.....	59
3.6 REFERENCES	62
3.7 TABLES.....	72
2.8 FIGURES.....	73
CHAPTER 4	83
TURBIDITY AND MODIFIED WATER CONTENT OF POLYMER-MODIFIED BENTONITE.....	83
ABSTRACT	83

4.1 INTRODUCTION	84
4.2 BACKGROUND	85
4.2.1. Polymer Conformation and Polymer Swelling	85
4.2.2. Precipitation and Turbidity of Polymer Suspensions	86
4.2.3. Modified Water Content (Rationale)	87
4.3 MATERIALS AND METHODS	88
4.3.1. Polymer and Polymer Modified Bentonite	88
4.3.2. Turbidity Measurement	88
4.3.3. Modified Water Content Measurement.....	89
4.3.4. Hydraulic Conductivity Measurement.....	90
4.4 RESULTS AND DISCUSSION	91
4.4.1. Turbidity of Polymer Suspensions.....	91
4.4.2. Turbidity of Polymer Suspensions and Modified Water Content of PMB.....	93
4.4.3. Modified Water Content and Hydraulic Conductivity of PMB-GCL	93
4.5 SUMMARY AND CONCLUSIONS.....	94
4.6 REFERENCES	96
4.7 FIGURES.....	99
CHAPTER FIVE	110
EFFECT OF HYDRAULIC GRADIENT ON HYDRAULIC CONDUCTIVITY OF POLYMER MODIFIED GEOSYNTHETIC CLAY LINERS	110

ABSTRACT	110
5.1 INTRODUCTION	111
5.2 BACKGROUND	112
5.2.1. Hydraulic Gradient Employed in Previous Hydraulic Conductivity Tests....	112
5.2.2. Implications of Hydraulic Gradient on PMB GCLs.....	113
5.3 MATERIALS AND METHODS	114
5.3.1. Geosynthetic Clay Liners	114
5.3.2. Permeant Liquids	115
5.3.3. Hydraulic Conductivity Testing	115
5.3.4. Termination Criteria.....	117
5.3.5. Total Organic Carbon (TOC) Analysis.....	117
5.3.6. Loss on Ignition (LOI).....	118
5.4 RESULTS AND DISCUSSION	119
5.4.1. PMB GCLs permeated with 50 mM CaCl ₂	120
5.4.2. PMB-GCLs permeated with Trona leachate.....	124
5.5 POST-PERMEATION POLYMER CONTENT	126
5.6 POLYMER ELUTION INDEX.....	130
5.7 CONCLUSIONS AND RECOMMENDATIONS.....	132
5.8 REFERENCES	136
5.9 TABLES.....	141

5.10 FIGURES.....	144
CHAPTER SIX	159
EFFECT OF ANIONS ON HYDRAULIC CONDUCTIVITY OF POLYMER MODIFIED BENTONITE GEOSYNTHETIC CLAY LINERS	159
ABSTRACT	159
6.2 BACKGROUND	160
6.2.1. Anion Fraction in Leachates.....	160
6.2.2. Hofmeister Series on Anion Rank	161
6.3 MATERIALS AND METHODS	161
6.3.1. Geosynthetic Clay Liner	161
6.3.2. Testing Liquids	162
6.3.3. Hydraulic Conductivity Testing	162
6.3.4. Total Organic Carbon Analysis.....	163
6.3.5. Viscosity Testing	164
6.3.6. Modified Water Content Testing.....	164
6.3.7. Turbidity Testing.....	164
6.4 RESULTS AND DISCUSSION	165
6.4.1. Behavior of Polymer Suspensions	165
6.4.2. Anion Effect on Behaviors of Polymer Bentonite Suspensions	166
6.4.3. Implication of Anion Ratio on Polymer Bentonite Interaction.....	167

6.5 SUMMARY AND CONCLUSIONS.....	168
6.6 REFERENCE.....	170
6.7 TABLES.....	172
6.8 FIGURES.....	173
CHAPTER 7	178
EFFECT OF ANION TYPE ON HYDRAULIC CONDUCTIVITY OF SODIUM BENTONITE GEOSYNTHETIC CLAY LINERS.....	178
ABSTRACT	178
7.1 INTRODUCTION	179
7.2 MATERIALS AND METHODS.....	179
7.2.1. Geosynthetic Clay Liners	179
7.2.2. Testing Liquids	180
7.2.3. Free Swell Test	180
7.2.4. Hydraulic Conductivity Testing	180
7.3 RESULTS AND DISCUSSION	181
7.3.1. Swell Index of Sodium Bentonite.....	181
7.3.2. Hydraulic Conductivity of Na-B GCLs	181
7.3.3. Sodium Elution	182
7.4 CONCEPTUAL FRAMEWORK.....	183
7.5 REFERENCE.....	184

7.6 FIGURES..... 185

LIST OF FIGURES

Figure 2.1. Evolution of pore size distribution (PSD) for FEBEX bentonite (from Romero et al. 2005) and a conceptual multi-modal PSD for a typical bentonite.	30
Figure 2.2. (a) SEM image of Wyoming bentonite. Parts b-e are conceptual diagrams of pore spaces on the (b) inter-aggregate scale, (c) intra-aggregate scale, (d) quasicrystal scale, and (e) interlayer scale. (From Likos and Wayllace, 2010).	31
Figure 2.3. Fourier transform infrared spectroscopy (FTIR) of polymer used in this study and commercial PAM.	32
Figure 2.4. Photograph of Quantachrome Autosorb-1-C N ₂ porosimetry.	33
Figure 2.5. Measured N ₂ isotherms for bentonite and polymer bentonite mixture.	34
Figure 2.6. BET surface area for bentonite and polymer bentonite.	35
Figure 2.7. (a) Cumulative pore volume, and (b) pore size density function for bentonite and polymer bentonite mixture.	36
Figure 2.8. Evolution of PSDs combined by N ₂ porosimetry and mercury intrusion porosimetry showing tri-modal PSD for bentonite and polymer bentonite mixture.	37
Figure 3.1. Conceptual illustration of polymer-clay interactions in composite forms (adapted from Kim and Palomino 2011).	73
Figure 3.2. Relations between hydraulic conductivity and (a) swell index, (b) liquid limit, and (c) fluid loss compiled for enhanced bentonites and sodium bentonite (Na-B) from the literature. Enhanced bentonites include Multiswellable Bentonite (MSB) (Onikata et al. 1996), Hyper Clay (HC) (Di Emidio et al. 2010, 2011), Bentonite-polyacrylic-acid composite (BPC) (Scalia et al. 2014), dense prehydrated GCL (DPH-GCL) (Kolstad et al.	

2004), and contaminant resistant clay (CRC) as defined and compiled by Scalia et al. (2018).....	74
Figure 3.3. Swell index tests for polymer modified bentonite in salt solutions. Rhodamine WT dye (pink color) indicates a boundary between free solution and solution containing polymer dissociated from the bentonite.....	75
Figure 3.4. Conceptual illustrations of (a) extended polymer conformation resulting in high viscosity and (b) coiled polymer conformation resulting in low viscosity.....	76
Figure 3.5. Brookfield DV-I PRIME Viscometer (Middleboro, MA) and spindle set.	77
Figure 3.6. Viscosity versus ionic strength for polymer suspensions in NaCl and CaCl ₂ . Polymer concentrations vary from 2% to 5% by mass.	78
Figure 3.7. Viscosity of polymer (PAM)-bentonite suspensions (total solid-liquid ratio of 10%), in (a) NaCl at P/B (polymer-to-bentonite ratio) ranging from 0 to 10%, (b) in various salt solutions at P/B = 5%.....	79
Figure 3.8. Viscosity of polymer-bentonite mixture in 300 mM K ⁺ and Na ⁺ solutions, and 50 mM Mg ²⁺ solutions as a function of anion ratio (R = molar concentration ratio of Cl ⁻ to SO ₄ ²⁻).	80
Figure 3.9. Hydraulic conductivity versus viscosity: (a) PMB-GCLa and PMB suspensions, (b) NaB-GCLs and NaB suspensions.....	81
Figure 3.10. (a) Cumulative polymer elution as function of pore volumes of flow (PVF) for PMB-GCLs, and (b) Steady state polymer elution versus viscosity of PMB suspensions.	82

Figure 4.1. Schematic representation of polymers used in PMB GCLs (1) skeletal structure, (2) polymer swelling in good solvent, (3) polymer collapse in poor solvent for (a) linear, (b) branched and (c) network polymers.....	99
Figure 4.2. Photograph of networked polymer suspension for a networked polymer (at solid-to-liquid ratio of 0.5%) in DI water and 50 mM CaCl ₂	100
Figure 4.3. Conceptual illustration of polymer suspension in good and poor solution upon mixing and after sitting.	101
Figure 4.4. Conceptual illustration of polymer-bentonite suspension in good solution and poor solution.....	102
Figure 4.5. Photographs of Hach 2100N Laboratory Turbidity Meter and end-over-end rotation for preparing polymer suspension.	103
Figure 4.6. Schematic illustration of modified water content test procedures.....	104
Figure 4.7. Turbidity of networked polymer suspension in DI water and 50 mM CaCl ₂ with time.	105
Figure 4.8. Turbidity of networked polymer suspensions in various single species salt solutions.	106
Figure 4.9. Turbidity of networked polymer suspension in 300 mM K ⁺ , 300 mM Na ⁺ , 50 mM Mg ²⁺ solutions and EPRI leachates as a function of anion ratio (R=molar concentration ratio of Cl ⁻ to SO ₄ ²⁻).....	107
Figure 4.10. Modified water content of PMB suspensions versus average turbidity of polymer suspensions.....	108
Figure 4.11. Hydraulic conductivity of PMB-GCL versus modified water content of PMB suspensions.	109

Figure 5.1. Hydraulic gradients used in previous studies and this study for conventional bentonite GCLs and enhanced bentonite GCLs.....	144
Figure 5.2. Photograph with main components of constant-flow pump apparatus	145
Figure 5.3. Hydraulic conductivity values plotted with PVF at varying average hydraulic gradients for PMB GCLs permeated with 50 mM CaCl ₂	146
Figure 5.4. Chemical analysis data of effluents from hydraulic conductivity tests on (a) EC ratio (b) pH ratio, (c) concentration of Ca ratio, and (d) concentration of Na permeated to 50 mM CaCl ₂	147
Figure 5.5. Hydraulic Conductivity (a) and cumulative polymer elution (b) of PMB GCLs permeated with 50 mM CaCl ₂	148
Figure 5.6. Hydraulic Conductivity versus cumulative polymer elution of PMB GCLs permeated with 50 mM CaCl ₂	149
Figure 5.7. Hydraulic conductivity (a) and hydraulic gradient (b) plotted with PVF with falling head methods at varying average hydraulic gradients for PMB GCLs permeated with Trona leachate.....	150
Figure 5.8. Chemical analysis data of effluents from hydraulic conductivity tests on (a) EC ratio, and (b) pH ratio permeated to Trona leachate.	151
Figure 5.9. Photographs of polymer clogging observed: (a) in GCL specimen with dye marking preferential flow path, (b) in outflow fitting/tube, (c) in inflow fitting/tubes, (d) in geosynthetic fabric, (e) in outflow plate, and (f) in inflow burette.....	152
Figure 5.10. Polymer elution in effluents and declogging liquids (a), hydraulic conductivity (b) and cumulative polymer elution (c) plotted with pore volume of flow permeated with Trona.....	153

Figure 5.12. Pictures of PMB GCL taken after permeation with Rhodamine dye staining and polymer loss calculated from post-permeation LOI permeate to Trona at hydraulic gradients of 40, 90, and 120.....	155
Figure 5.13. Hydraulic conductivity versus standard deviation of polymer loss after permeation on PMB GCLs.	156
Figure 5.14. Hydraulic conductivity versus elution index of polymer bentonite mixture.	157
Figure 5.15. Conceptual representation of polymer modified bentonite in poor solutions (i.e. high ionic strength, low RMD), indicating the polymer conformation, polymer bentonite interaction and potential flow path in relationship with elution index.....	158
Figure 6.1. Summary of anion ratio and ionic strength of coal mine, copper mine, gold mining, lead/zinc mine, uranium mine, hazardous waste, coal combustion ash, incinerator ash, and TRC leachate. (From Tian et al. 2017)	173
Figure 6.2. Turbidity of polymer suspension at 0.5% in anion series solutions at ionic strength of 150 mM, 300 mM and 600mM.....	174
Figure 6.3. Viscosity of polymer suspension at 0.5 % in anion series solutions at ionic strength of 150 mM, 300 mM and 600mM.....	175
Figure 6.4. Summary of test results with polymer bentonite suspensions and hydraulic conductivity with PMB-GCLs in anion series solutions.....	176
Figure 6.5. Modified water content of polymer bentonite suspension at solid-to-liquid ratio of 10% in 300 mM K ⁺ and Na ⁺ solutions, and 50 mM Mg ²⁺ solutions as a function of anion ratio.	177

Figure 7.1. Swell index of Na-B in 300 mM cation with single species anion solutions.	185
Figure 7.2. Hydraulic conductivity of Na-B permeated with a fixed 300 mM Na ⁺ and K ⁺ solutions with various anion ratios, along with pure Cl ⁻ and SO ₄ ²⁻	186
Figure 7.3. Chemical equilibrium condition, ratio of incremental outflow to inflow, pH and EC from tests on Na-B permeated to 300 mM K solutions (a), and 300 mM Na solutions (b).....	187
Figure 7.4. Eluted Na as a function of cumulative inflow (mL) for Na-B permeated with 300 mM K ⁺ anion ratio solutions (a), and cumulative Na elution as a function of cumulative inflow (mL) permeated with 300 mM K ⁺ anion ratio solutions (b).....	188
Figure 7.5. Conceptual framework of Na in bentonite interlayer space (a), and enhanced osmotic swelling caused by anion adsorption effect (b).	189

LIST OF TABLES

Table 1.1. Index Properties, Cation Exchange Capacity and Bound Cations of PMB and Na-B	10
Table 3.1. Properties of chemical solutions used in the study	72
Table 5.1. Characteristics of Trona Leachate.....	141
Table 5.2. Effective Stress Conditions of Tests with Different Gradient	142
Table 5.3. Hydraulic conductivity of GCLs permeated at different hydraulic gradient .	143
Table 6.1. Tests results with PMBs in Anion Solutions.....	172

CHAPTER ONE

EXECUTIVE SUMMARY

1.1 INTRODUCTION

Geosynthetic Clay Liners (GCLs) were developed for use in hydraulic barrier applications (e.g., landfills) in lieu of compacted clay liners (CCL) and have advantages including easy installation and low cost. Conventional GCLs are thin, layered systems comprised of a layer of sodium bentonite (Na-B) (7-10 mm) sandwiched between two geotextiles. Pronounced swelling of sodium bentonite when hydrated and corresponding low hydraulic conductivity ($\sim 10^{-11}$ m/s to water) makes GCLs an effective barrier in many liquid containment applications, especially with leachates of low ionic strength (I) (Shackelford et al. 2000, Jo et al. 2004, Bradshaw and Benson 2014).

In aggressive leachates, however, Na-B GCLs can encounter limitations due to potential chemical incompatibility between Na-B and solutions having high I, extreme pH, or low ratio of monovalent to divalent cations (RMD). Demand from the industry for more chemically resistant GCLs has motivated development of polymer-modified bentonite (PMB) GCLs, in which bentonite is amended with polymers either physically or chemically using a variety of different procedures (Lin et al. 2000, Trauger and Darlington 2000, Ashmawy et al. 2002, Kolstad et al. 2004, McRory and Ashmawy 2005, Katsumi et al. 2008, Benson et al. 2010, Di Emidio et al. 2011, Scalia et al. 2011, Benson et al. 2013, Scalia and Benson 2014, Scalia et al. 2014). While there are numerous types of PMBs, dry-blended mixtures of polymer and bentonite, where the polymer and bentonite remain phase separated, have become commercially viable because of the relatively low cost to

produce them and their good hydraulic performance for a wide range of pore fluid chemistries.

New index methods for assessing chemical compatibility and hydraulic conductivity of PMB-GCLs are needed. Improved basic understanding of the basic physical and chemical mechanisms that govern liquid flow and solute transport for PMBs is required. This study has five main objectives:

1. Quantify the pore structure of polymer modified bentonite in the range of meso- and micro-pores to clarify where and in what form the polymer fraction in PMB is located and to evaluate corresponding pore size distribution (PSD) of PMB over a wide range.
2. Develop and evaluate new index tests for potential use as preliminary screening tools to assess chemical compatibility and hydraulic conductivity of PMB-GCLs.
3. Assess polymer conformation (shape and structure) and polymer hydrogel development in different aqueous chemistries and relate polymer conformation and quality of polymer gel to the hydraulic behavior of PMB.
4. Evaluate the effect of hydraulic gradient on hydraulic conductivity of PMB-GCLs and identify corresponding implications of polymer elution/clogging, which is potentially affected by hydraulic gradient, to the hydraulic conductivity of PMB-GCLs.
5. Evaluate the effects of anion type on index properties of polymers and polymer bentonite mixtures and on the hydraulic conductivity of PMB GCLs.

While the above objectives were evaluated using a variety of materials and laboratory testing approaches, the general materials and methods among the different studies had some commonalities. These are summarized below. Specific methods and materials that deviated from these common approaches are summarized in each respective chapter of this dissertation.

1.2 GEOSYNTHETIC CLAY LINERS

Two types of geosynthetic clay liners (GCLs) were used in this study: a Wyoming sodium bentonite (Na-B) GCL and a commercially available PMB GCL containing a phase-separated blend of granular Na-B and a proprietary polymer. The Na-B and PMB in each respective chase was encapsulated between a woven and a nonwoven geotextile by needle punching to form a GCL. Mass per unit area, moisture content, thickness, cation exchange capacity (CEC), bound cations (Ca^{2+} , Na^+ , Mg^{2+} , K^+), granule size distribution (D10, D30, D60) of GCLs, and polymer content of the PMB-GCL are summarized in Table 1.1. CEC and the initial distribution of bound cations (i.e., prior to permeation) were determined by ammonium acetate extraction (ASTM D7503). Polymer content of the PMB was quantified by loss on ignition (LOI) conducted according to ASTM D7348 accounting for loss of strongly bound water molecules, calcite, and organic matter associated with the bentonite fraction (Scalia et al., 2014; Tian et al., 2016). Quantitative X-ray diffraction (XRD) analysis showed that the NaB and PMB contained 84% and 79% montmorillonite respectively, along with measureable quantities of quartz, feldspar and mica (Chen et al. 2015).

1.3 LABORATORY HYDRAULIC CONDUCTIVITY

Hydraulic conductivity tests for GCLs including Na-B and PMB were conducted according to ASTM D6766. Influent permeant solution was contained in 50-mL graduated glass pipettes. Effluent was collected in 60-mL polyethylene bottles. Effective stress was maintained around 20 kPa during permeation. Average hydraulic gradient of ranging from 40-190 was used in flexible-wall permeameters using the falling headwater-constant tailwater method, and average hydraulic gradient of 15 was applied by using a flow pump with constant flow method.

GCL specimens were prepared by cutting a circular sample directly from a roll provided by the manufacturer using a razor knife and steel ring following the procedures in Jo *et al.* (2001). Paste prepared with sodium bentonite and permeant solution was placed around the perimeter of the specimen to prevent loss of the mixture during handling and preferential flow along the edge during permeation. Initial thickness of each GCL specimen was measured with calipers at six equidistant points. Prior to permeation, GCL specimens were hydrated with permeation leachate for 48 h without a hydraulic gradient applied. Permeation followed immediately after the hydration phase.

All tests were continued until the hydraulic and chemical termination criteria in ASTM D6766 were met. Electrical conductivity (EC), pH, and cation concentration of the effluent were measured periodically to assess chemical equilibrium. Hydraulic equilibrium was defined as steady hydraulic conductivity for three consecutive measurements with ratio of incremental volumetric outflow to inflow (flow ratio) within 1.00 ± 0.25 . Chemical equilibrium was assumed when the ratio of effluent to influent electrical conductivity (EC_{out}/EC_{in}) and effluent to influent pH (pH_{out}/pH_{in}) were steady and within 1.0 ± 0.1 . The

burettes and bottles were covered with parafilm to minimize evaporation and atmospheric interaction.

For tests conducted with NaB-GCLs, concentrations of major cations (Ca^{2+} , Mg^{2+} , Na^+ , K^+) are also required to be within 1.0 ± 0.1 . These were analyzed using Varian MPX inductively couple plasma atomic emission spectroscopy (ICP-AES) in accordance with method 6010B defined by the U.S. Environmental Protection Agency (EPA). For tests conducted with PMB-GCLs, total organic carbon (TOC) concentrations were analyzed using a Shimadzu TOC-VCSH (Shimadzu Scientific Instruments, Columbia, MD) with a measurement range for NPOC from 4 ppb to 25000 ppm in accordance with ASTM D4839-03. Calibration curve was set manually with dilution from a standard 100 ppm glucose ($\text{C}_6\text{H}_{12}\text{O}_6$) consisting five points (5, 10, 25, 50, and 100 ppm) with a blank (UHP Milli-Q water). Calibration curve fit was linear with a minimum R^2 accepted at 0.999. The total carbon of sample contains the inorganic content in solution and organic content from polymer backbone chain. Prior to measurement, inorganic carbon content was removed by sparging with CO_2 -free gas. The total organic carbon content was measured by detecting the amount of CO_2 , which was converted by combusting the sample. Thus, the TOC measured herein was considered as polymer concentration (organic content of solution). Standard solution (100 ppm glucose) was checked for every 20 measurements to ensure the accuracy of measurement. The injection volume used was the same as used for calibration curve (50 μL).

1.4 MAJOR FINDINGS

This dissertation is presented in seven chapters. Chapter 2, titled “Microstructure investigation of polymer modified bentonite using BET-BJH analyses”, presents a quantitative study of microstructure of PMB using nitrogen adsorption measurement by BET (Brunauer-Emmett-Teller). The polymer was found to exist in the bentonite inter-aggregate voids, which decreases the volume of relatively large macro-pores and consequently increases the volume of relatively small meso-pore. Combined with a literature review including previous microstructure studies for conventional bentonite by mercury intrusion porosimetry (MIP), the chapter provides an interpretation of the pore size distribution (PSD) of PMB over a wide range of pore sizes.

Chapter 3, titled “Viscosity as an alternative index test for polymer modified geosynthetic clay liners,” provides an overview of limitations encountered using conventional index tests to evaluate PMBs, including free swell, liquid limit, and fluid loss for evaluating hydraulic conductivity and chemical compatibility. Viscosity is evaluated as an alternative index test for screening hydraulic performance and chemical compatibility of PMB-GCLs. Viscosity of polymer-bentonite mixtures systematically decreases with decreasing polymer loading (mass ratio of polymer to bentonite) and with increasing ionic strength of test solution. Viscosity is lower in solutions having multivalent cations and increasing concentrations of chloride anions over sulfate anions. Higher viscosity of PMB systematically corresponds to lower hydraulic conductivity of PMB-GCLs permeated with the same solutions. A threshold viscosity at 200 cP is required for achieving hydraulic conductivity lower than 10^{-10} m/s for the PMB-GCL evaluated in this study. Results indicate that viscosity can potentially be used as an effective index for evaluating hydraulic conductivity and chemical compatibility of PMB-GCLs.

Chapter 4, titled “Turbidity and modified water content for polymer modified bentonite”, qualitatively evaluates polymer conformation and the quality of polymer gel in different aqueous chemistries. Turbidity measurements indicate that solutions containing divalent cations promote polymer precipitation (coiling) and reduce polymer-bentonite interaction. Solutions rich in SO_4^{2-} rather than Cl^- have a thickening effect by forming strong polymer gels and increase the turbidity of polymer suspensions through more polymer-solvent interaction. A modified water content test developed to quantify the water-holding capacity for PMBs is correlated to the turbidity in solutions where Na-B exhibits comparable swelling. High modified water content of PMB in test solutions systematically correlates to lower hydraulic conductivity of PMB-GCLs permeated with the same solutions. A threshold modified water content value of 230% is required for achieving hydraulic conductivity lower than 10^{-10} m/s for the PMB-GCL evaluated in this study.

Chapter 5, titled “Effect of hydraulic gradient on hydraulic conductivity of polymer modified geosynthetic clay liners,” summarizes the range of hydraulic gradients used in previous studies on conventional NaB-GCLs and PMB-GCLs. Two sets of hydraulic conductivity tests were performed on PMB GCLs permeated with (1) pure divalent cation-chloride solution (50 mM CaCl_2), and (2) high sodic-sulfate synthetic leachate (Trona). Hydraulic gradient ranging from 10 to 380 were used in suite of laboratory tests at comparable effective stress. Results show that hydraulic gradient has a significant effect on laboratory test results of PMB GCLs. Uniformity of post-test polymer distribution within the GCLs was quantified by loss on ignition (LOI) testing to assess polymer elution and preferential flow path development. Results indicate that higher hydraulic gradients

promote polymer elution and formation of preferential flow paths. Higher hydraulic gradient tends to elute polymer from PMB GCLs and increases corresponding hydraulic conductivity. Results support a hypothesis that polymer clogging in bentonite macropores is a primary mechanism for low hydraulic conductivity of PMB GCLs and that high hydraulic gradient and chemical conditions that promote contracted polymer conformation promote polymer mobilization and elution. Chapter 6, titled “Effect of anions on hydraulic conductivity of polymer modified geosynthetic clay liners” evaluates the effects of seven anions from the Hofmeister anion ranking series on the behavior of polymer suspensions, polymer bentonite suspensions, and the hydraulic conductivity of PMB-GCLs. Turbidity and viscosity of pure polymer suspensions (no bentonite fraction) showed similar trends according to anion type. Free swelling, viscosity, and modified water content for polymer-bentonite mixtures also showed consistent trends, but trends that were different than those observed for the pure polymer suspensions. Results suggest that polymer-bentonite interaction is an important factor in the rheological and hydraulic behavior of polymer-bentonite suspensions and that this behavior is systematically affected by anion type. Hydraulic conductivity of PMB-GCLs appears to be controlled by the bentonite fraction at the initial stage of permeation, then by polymer-bentonite interaction as permeation continues, and ultimately by polymer elution. Anion type influences all three factors, and thus is considered an essential factor in influencing the hydraulic conductivity of PMB-GCLs.

Chapter 7, titled “Effect of anion type on hydraulic conductivity of sodium bentonite geosynthetic clay liners,” is similar to Chapter 6, but with focus on conventional Na-B. Results show that Na-B exposed to sulfate rich solutions tends to retain Na^+ in the

interlayer space and exhibit sufficient osmotic swelling compared to conditions in chloride rich solutions. Corresponding hydraulic conductivity of Na-B GCLs in sulfate-rich solutions is lower than that in chloride-rich solutions.

1.5 TABLES

Table 1.1. Index Properties, Cation Exchange Capacity and Bound Cations of PMB and Na-B

Property	ASTM Standard	PMB-GCL Quantity	NaB-GCL Quantity	Unit
Dry Mass per Area	D5993	3.6	3.6	kg/m ²
GCL Thickness	US.EPA.2001	7.1-8.3	7.3-8.2	mm
GCL Moisture Content	D5993	4.4	4.8	%
Swell Index	D5890	27	28	mL/2 g
Polymer Content	-	5.1	0	% by mass
Montmorillonite Content	-	79	84	%
Cation Exchange Capacity (CEC)	D7503	89.6	71.3	cmol ⁺ /kg
Bound Na ⁺		0.14	0.45	mole fraction
Bound K ⁺		0.01	0.04	mole fraction
Bound Ca ²⁺		0.13	0.29	mole fraction
Bound Mg ²⁺		0.04	0.12	mole fraction
D ₁₀	D422	0.4	0.4	mm
D ₃₀		0.6	0.7	mm
D ₆₀		1.0	1.1	mm

Note: Polymer content calculated based on loss on ignition per ASTM D7348 after accounting for bentonite fraction. Bound cations and CEC measured on base bentonite in PMB prepared using LOI to remove all polymer prior to test.

1.6 REFERENCES

- Ashmawy, A., Darwish, E., Sotelo, N., and Muhammad, N. (2002). Hydraulic performance of untreated and polymer-treated bentonite in inorganic landfill leachates. *Clays and Clay Miner.*, 50(5), 546-552.
- Benson, C., Kucukkirca, E., and Scalia, J. (2010) Properties of geosynthetics exhumed from a final cover at a solid waste landfill. *Geotext. Geomembr.*, 28, 536-546.
- Benson, C., Chen, J., and Edil, T. (2013) Hydraulic conductivity of geosynthetic clay liners to coal combustion product leachates, *interim report*. Sustainability Report No. OS-13-07, Office of Sustainability, University of Wisconsin-Madison, Madison, WI.
- Bradshaw, S. and Benson, C. (2014). Effect of municipal solid waste leachate on hydraulic conductivity and exchange complex of geosynthetic clay liners. *J. Geotech. And Geoenvironmental Eng.*, 140(4), 04013038.
- Chen, J., Benson, C.H., and Edil, T.B. (2015). Hydraulic conductivity of geosynthetic clay liners to coal combustion product leachates. *Geosynthetics 2015*, Portland, OR.
- Di Emidio, G., Van Impe, W., and Flores, V. (2011). Advances in geosynthetic clay liners: polymer enhanced clays. *GeoFrontiers 2011. Advances in Geotechnical Engineering*, American Society of Civil Engineer, Reston, USA, 1931-1940.
- Jo, H., Katsumi, T., Benson, C., and Edil, T. (2001). Hydraulic conductivity and swelling of non-prehydrated GCLs permeated with single species salt solutions. *J. Geotech. Geoenviron. Eng.*, 127(7), 557-567.

- Jo, H., Benson, C., Shackelford, C., Lee, J., and Edil, T. (2005). Long-term hydraulic conductivity of a non-prehydrated geosynthetic clay liner permeated with inorganic salt solutions. *J. Geotech. Geoenviron. Eng.*, 131(4), 405-417.
- Kolstad, D., Benson, C., Edil, T., and Jo, H. (2004b). Hydraulic conductivity of dense prehydrated GCL permeated with aggressive inorganic solutions. *Geosynth. Int.*, 11(3).
- McRory, J., and Ashmawy, A. (2005). Polymer treatment of bentonite clay for contaminant resistant barriers. GSP 142 *Waste Containment and Remediation*, 1-11
- Katsumi, T., Ishimori, Ho, Onikata, M., and Fukagawa, R. (2008). Long-term barrier performance of modified bentonite materials against sodium and calcium permeant solutions. *Geotext. And Geomembranes* 26(1), 14-30.
- Lin, L., Katsunami, T., Kamon, M., Benson, C., Onikata, M., and Kondo, M. (2000). Evaluation of chemical-resistant bentonite for landfill barrier application. *Annuls of Disas. Prev. Res. Inst.*, Kyoto Univ., No. 43 B-2, 525-533.
- Shackelford, C., Benson, C., Katsumi, T., Edil, T., and Lin, L. (2000). Evaluating the Hydraulic Conductivity of GCLs Permeated with Non-standard Liquids. *Geotextiles and Geomembranes*, 18(2-4), 133-162.
- Scalia, J., and Benson, C. (2011). Hydraulic conductivity of geosynthetic clay liners exhumed from landfill final covers with composite barriers. *J. Geotech. Geoenviron. Eng.*, 137(1), 1-13.

- Scalia, J., Benson, C., Bohnhoff, G., Edil, T., and Shackelford, C. (2014). Long-term hydraulic conductivity of a bentonite-polymer composite permeated with aggressive inorganic solutions. *J. Geotech. Geoenviron. Eng.*, 140(3), 1-13.
- Scalia, J., and Benson, C. (2014). Barrier Performance of Bentonite-Polyacrylate Nanocomposite to Artificial Ocean Water. Proceedings, *Geo-Congress 2014 Geo-Characterization and Modeling for Sustainability*, GSP No. 234, ASCE, Reston, VA.
- Tian, K., Benson, C., and Likos, W. (2016). Hydraulic Conductivity of Geosynthetic Clay Liners to Low-Level Radioactive Waste Leachate. *J. Geotech. Geoenviron. Eng.*, 142(8).
- Trauger R., and Darlington J. (2000) Next-generation geosynthetic clay liners for improved durability and performance. TR-220. Colloid Environmental Technologies Company, Arlington Heights, 2-14.

CHAPTER TWO

MICROSTRUCTURE INVESTIGATION OF POLYMER-MODIFIED BENTONITE USING BET PORE SIZE ANALYSES

ABSTRACT

This chapter presents a quantitative study of the microstructure of polymer modified bentonites (PMBs) using nitrogen adsorption and BET (Brunauer-Emmett-Teller) analysis. Nitrogen sorption isotherms measured for a commercially available PMB show that polymer is present in the bentonite inter-aggregate voids. The presence of the polymer increases the mesopore fraction by decreasing the volume of macropores. Results from the sorption-based pore size analysis are combined with pore size distributions (PSD) available in the literature from mercury intrusion porosimetry (MIP) for conventional bentonite to propose a tri-modal PSD for dry-blended PMBs.

2.1 INTRODUCTION

Microstructure of soils has been intensively investigated at the particle/aggregate scale ($< 100 \mu\text{m}$) to understand the arrangement and distribution of soil particles and pores (Santamarina *et al.* 2002, Mitchell and Soga 2005, Romero *et al.* 2005). In the context of bentonite, measurements and observations were performed on the scale of clods and aggregations to obtain better insight into microstructural consequences on hydro-mechanical behavior (Tessier *et al.* 1992, Delage *et al.* 1996). Soil fabric was correlated to the hydraulic conductivity of both compacted and nature clays due to the changes in the pore voids (Lapierre *et al.* 1990, Benson and Daniel 1990).

Geosynthetic Clay Liners (GCLs) were developed as hydraulic barrier in landfills and are often used in lieu of compacted clay liner (CCL) for the advantages of easy installation and low cost. GCLs are primarily composed of a layer of sodium bentonite (Na-B) with a thickness of 7-10 mm, sandwiched between two geotextiles. Because of the pronounced swelling nature of sodium bentonite, GCLs have been used as effective barriers in some containment applications, especially with solutions of low ionic strength (I), as well as municipal solid waste leachate (Shackelford *et al.* 2000, Jo *et al.* 2004, Bradshaw and Benson 2014). However, GCLs are less effective when applied in aggressive leachates (e.g. high I, low RMD, extreme pH), as the chemical compatibility of Na-B is susceptible to change in these solutions. The demand of chemical resistant GCLs has led to development of polymer-modified GCLs, in which bentonite is amended with polymers physically or chemically using different procedures (Lin *et al.* 2000, Trauger and Darlington 2000, Ashmawy *et al.* 2002, Kolstad *et al.* 2004, McRory and Ashmawy 2005, Katsumi *et al.* 2008, Benson *et al.* 2010, Di Emidio *et al.* 2011, Scalia *et al.* 2011,

Benson *et al.* 2013, Scalia and Benson 2014, Scalia *et al.* 2014). Among all the existing PMB products, the dry blended (DB) product of polymer and bentonite is the most industrial favorable because of the relatively low cost. Tian *et al.* (2018) considered results from SEM imaging analysis to hypothesize that the low hydraulic conductivity of PMBs was attributed to the clogging of polymer hydrogel in bentonite pores. However, to date, there are no quantitative studies available to evaluate the pore size distribution of PMBs.

Since the PSD is an essential element correlated to macroscopic properties of soil, there is motivation to improve understanding of the microstructural properties of PMBs. The objective of this study, therefore, is to evaluate the meso-pore size distribution of a commercially available PMB-GCL. The BET surface area and pore size distribution (PSD) were assessed by gas adsorption using nitrogen. Results provide evidence on the location and characteristics of the polymer fraction in the bentonite matrix.

2.2 BACKGROUND

2.2.1. Pore Size Distribution of Bentonite

Pore size distribution (PSD) is an elemental parameter directly correlated to the engineering behavior of soils (Juang and Holtz 1986, Reed *et al.* 1979, Romero *et al.* 1999). A bimodal distribution including inter-aggregate ($\sim 10\mu\text{m}$ to $100\mu\text{m}$) pores and intra-aggregate pores ($\sim 0.1\mu\text{m}$ to $1\mu\text{m}$) in bentonite was probed by various techniques such as, mercury intrusion porosimetry (MIP), scanning electron microscopy (SEM), and multi-scale X-ray scattering measurements (Romero and Simms 2008, Likos and Wayllace, 2010, Gadikota *et al.*, 2017). Fig.2.1, for example, represents a PSD ranging from 10 nm

to 300,000 nm (solid line) for FEBEX bentonite (Romero and Simms, 2005). A pore size density function was defined as follows:

$$f_x(x) = \frac{-d(V_t - V)/dx}{V_t}$$

where $f_x(x)$ is the pore size density function that can be determined from the mercury intrusion data, V_t is the total volume of pores in soil, which is a constant, and $V_t - V$ is the volume of pores with pore sizes that are greater than or equal to x .

As observed from the PSD of FEBEX bentonite, two modes are generally detected for typical bentonites. The large pore size mode at a value of around 20 μm corresponds to a range of inter-aggregate pores, which are characterized between pore sizes of 2 μm and 25 μm . The other mode at pore size of around 20 nm corresponds to an intra-aggregate porosity characterized by pores smaller than 2 μm , as indicated by Romero *et al.* (2002). Within the intra-aggregate porosity, the pores that are smaller than 2 nm, between 2 nm and 50 nm, and greater than 50 nm are referred to as micropores, mesopores and macropores, respectively (Gregg and Sing, 1982). The lowest value, having pore size around 10 nm, is not detectable by MIP due to the limitation of mercury intrusion pressure. However, it is reasonable to hypothesize that there is another mode at the pore range smaller than 10 nm, which can be better investigated by gas adsorption techniques (Webband Orr, 1997). A conceptual multi-modal PSD including this range of pores is shown schematically by the dashed line in Fig.2.1.

2.2.2. Sodium Bentonite and Implication of Swelling on Bentonite Pores

Sodium-bentonite (Na-B) is used as a component of GCLs because of its unique properties (e.g. highly plastic and swelling) that result in low permeability to water ($\sim 10^{-11}$ m/s). Na-bentonite is primarily composed of montmorillonite, in the interlayer of which, osmotic swelling occurs when the cations (e.g. Na^+) bound to the surface hydrate (Norrish and Quirk 1954, van Olphen 1977). The degree of swelling affects the pore structure of bentonite and determines the overall bentonite particle and pore fabric (Mitchell and Soga, 2005).

There are two swelling mechanisms in Na-B, crystalline swelling and osmotic swelling. When dry Na-B is placed in a humid environment, water molecules first start to cluster around the bound Na. At higher humidity, the bentonite surfaces adsorb moisture and expand the interlayer space in a stepwise manner (Akin and Likos, 2016). The expansion of interlayer space reduces the macroporosity of bentonite. If the predominant bound cations are Ca^{2+} , crystalline swelling is limited, and results in larger macropore space (Likos, 2004). In environments characterized by a high water content, where osmotic adsorption occurs, the immobile water layer resulting from crystalline swelling reduces the size and frequency of pores (Mesri and Olson 1971). In the presence of divalent or polyvalent cations (e.g. Ca^{2+}), or high ionic strength (I) of the surrounding pore water, osmotic swell can be suppressed. Without osmotic swelling, bound water in the interlayers is insufficient, which will reopen the intergranular pores (Jo *et al.* 2001). However, the osmotic swelling only occurs when monovalent cation (e.g. Na^+) dominates the exchange complex (McBride, 1994), the replacement of Na in bentonite by multivalent cations is thermodynamically favorable (Sposito 1989, McBride 1994). Likos and Wayllace (2010) presented a bimodal porosity model of bentonite, which was

primarily composed of inter-aggregate pores ($\sim 10 \mu\text{m}$ to $100 \mu\text{m}$) and intra-aggregates ($\sim 0.1 \mu\text{m}$ to $1 \mu\text{m}$), as shown in Fig. 2.2. Pores that have direct effect on macro-engineering properties are considered to be those inter-aggregate voids (Fig. 2.2b) that form among the aggregates. Intra-aggregate voids are formed within the larger aggregates of clay particles (Fig. 2.2c) which are composed of quasicrystals. Reduced interlayer voids that are triggered by suppressed osmotic swelling in presence of divalent cation are comprised by oriented sub-stacks of mineral layers (Fig. 2.2d). Pores comprising the smaller-scale microstructure of compacted bentonites are designated as the result of interlayer separation (Fig.2.2e).

2.3 MATERIALS AND METHODS

2.3.1. Polymer Modified Bentonite (PMB) and PMB-GCLs

PMB for BET measurements and hydraulic conductivity tests was obtained from a commercially available GCL consisting of a dry blend of granular Na-B and a proprietary polymer. The polymer has a networked microstructure and is insoluble in water and most inorganic solutions. It exhibits over 90% similarity in the measured spectrum with a known commercially available anionic PAM (Polysciences Inc., Warrington, PA, USA, Cat.#. 04652) by Fourier transform infrared spectroscopy (FTIR), shown in Fig.2.3. The difference between the commercial PAM and the proprietary polymer primarily exists in their skeleton structure (linear vs. networked).

The PMB-GCL was formed by needle punching to sandwich the bentonite-polymer mixture with an upper woven and a lower nonwoven geotextile. Polymer loading was estimated at 5.1%, quantified by loss on ignition (LOI) conducted according to ASTM

D7348 accounting for loss of strongly bound water molecules, calcite, and organic matter associated with the bentonite fraction (Scalia *et al.* 2014; Tian *et al.* 2016). Montmorillonite (79%) is the primary component of the PMB by quantitative X-ray diffraction (XRD) analysis, along with measureable quantities of quartz, feldspar and mica (Chen *et al.* 2015). Other properties including mass per unit area, moisture content, thickness, cation exchange capacity (CEC), bound cations (Ca^{2+} , Na^+ , Mg^{2+} , K^+), and granule size distribution (D10, D30, D60) are summarized in Table 1.1. CEC and the initial distribution of bound cations (i.e., prior to permeation) were determined by ammonium acetate extraction (ASTM D7503).

2.3.2. Gas sorption, BET Surface Area, and BJH Pore Volume Measurements

Quantachrome Autosorb-1-C (Quantachrome Instruments, FL, USA, Part# 05061-C) was employed for gas adsorption, surface area, and pore size distribution measurements on the Na-B samples with and without polymers (Fig. 2.4). Prior to testing, the samples were ground by a pestle and mortar to pass a No.40 US sieve (0.425mm). Samples were heated overnight to 150°C in an oven to remove any water, and outgassed with Helium to avoid any drastic change due to surface modification. Gas sorption (adsorption/desorption) measurements were performed using nitrogen at a range of relative pressure ($P/P_0 \sim 0 - 0.90$). P_0 and P are the vapor pressures of the bulk liquid nitrogen and equilibrium pressure at liquid nitrogen pressure, respectively. Sorption isotherms were obtained by introducing successive amounts of nitrogen. At each stage the system was allowed sufficient time to attain equilibrium. BET specific surface area was estimated based on Brunauer-Emmett-Teller theory, where the BET monolayer capacity was derived from the best linear fit of adsorption isotherm. The pore size

distribution was calculated based on the method developed by Barrett, Joyner and Halenda (BJH) based on a pressure at which the adsorptive will spontaneously condense in a cylindrical pore of a given size. The pore size is calculated from the Kelvin equation and the selected statistical thickness equation.

2.4 RESULTS AND DISCUSSION

2.4.1. BET Specific Surface Area and Porosity

Fig. 2.5 shows a nitrogen sorption isotherm (adsorption-desorption at 77.3K) for Na-B and bentonite-polymer mixture (BP) at relative pressure up to $P/P_0 \sim 0.90$. The N_2 adsorption volume is higher with BP than with Na-B at a certain relative pressure over the entire range. This suggests that the bentonite-bearing polymer adsorbs more gas than bentonite per gram. A much higher surface area was measured with BP ($115.2 \text{ m}^2/\text{g}$) than with bentonite ($24.9 \text{ m}^2/\text{g}$), as shown in Fig. 2.6. The higher surface area of BP is consistent with the higher observed porosity of BP, indicating the polymer did not coat the bentonite surface but is present in bentonite pores without contacting the bentonite surface. The low measured specific surface area for bentonite can be attributed to that the N_2 gas did not cover the interlayer surface of bentonite (Fig.2.2e) which remains tightly bound under dry condition (Rutherford *et al.* 1997, Santamarina *et al.* 2002). The N_2 molecular has an area of adsorbate as low as 16.2 \AA^2 ; however, uncertainty exists on which layer of bentonite that can be reached by N_2 . Hayati (2012) pointed out that N_2 could not cover the interlamellar space as indicated in Fig.2.2c. Sample preparation may play an important role in determining the smallest spaces the N_2 can be reached. In this

study, reasonable comparison can be made between bentonite and BP since two samples are prepared using similar procedures.

Fig.2.7 presents the cumulative pore volume (a), and pore size distribution (b) in the mesopore region measured by BJH (Barrett and Joyner, 1951) for the desorption curve of the isotherm. The cumulative pore volumes in terms of liquid nitrogen were estimated from desorption data at the relative equilibrium pressure $\sim P/P_0$ of 0.90. The measured pores include micro- and meso-pores, and the cumulative volume of pores are generally larger with BP than with bentonite. The PSD of bentonite and BP are shown in Fig.2.7b, the pore size density function is the derivative of cumulative pore volume to logarithm diameter. The pore volume is larger with BP than with bentonite over the entire measurement range, with the maximum mesopore volume of 0.31 mL/g and 0.09 mL/g respectively at pore size of 4 nm. The results indicate that polymer does not exist in bentonite mesopores because a decreased mesopore volume would otherwise be observed. The presence of an increased BET surface area and increased mesopore volume of BP from N₂ porosimetry reveals the existence of polymer in bentonite pores, specifically, in the macro- or intra-aggregate pores. As a result, the mesopore volume increases due to decreasing macro/intra-aggregate pores in the presence of polymer.

2.4.2. Pore Size Distribution of PMBs

Since N₂ porosimetry provides the PSD in a lower range of pore size (~ 2 -10 nm), which often can't be detected by MIP, it is informative to integrate the PSD measured by N₂ porosimetry into PSD obtained by MIP. Fig.2.8 presents the evolution of multi-modal PSD in the presence of polymer combined by the two techniques (ranging from 1 nm to

1 mm). The PSDs of bentonite and BP in the range of 1 nm to 10 nm were measured by N₂ porosimetry, PSD of bentonite in the range of 10 nm to 1 mm was obtained from FEBEX bentonite (Romero and Simms, 2005). PSD of BP by MIP was not available due to polymer would be easily intruded out under pressure in dry condition; thus was conceptually sketched (red solid line). As observed, a third mode emerged at micro/meso pore size (~2-10 nm) along with the shifting of previous presented modes at intra-aggregates pore size and inter-aggregate pore size with BP. The occurrence of mode at micro/meso pore size is accompanied by a reduction of certain class of macropores due to the filling of polymer, leading towards a tri-modal or new bi-modal (in the case of complete disappear of macropore mode) distribution.

2.5 SUMMARY AND CONCLUSIONS

This chapter provides a quantitatively evaluation to characterize the pore size distribution (PSD) of bentonite and polymer modified bentonite, namely N₂ porosimetry. BET surface analysis and BET-BJH pore size analysis were conducted on bentonite and bentonite-polymer mixture respectively. An integrated PSD was presented by combining the PSD obtained from mercury intrusion porosimetry (MIP) from literature. This study yielded several key findings. Pore sizes in the range of ~1 nm to 10 nm were successfully determined using BET pore size analysis. These data complement the larger pore sizes obtained from MIP. Polymer bearing bentonite has a higher surface area and meso-scale porosity compared to bentonite. The results suggest that polymer does not block access to the micropores in bentonite, and that the polymer may exist in the pore space without necessarily contacting the bentonite surface. Given the larger meso-pore volume in BP

compared to bentonite, it can be inferred that the polymer exists in the larger macro-/inter-aggregate pores.

2.6 REFERENCES

- Akin, I. and Likos, W. (2016). Evaluation of isotherm models for water vapor sorption behavior of expansive clays. *J. Perform. Constr. Facil.*, 31(1).
- Ashmawy, A., Darwish, E., Sotelo, N., and Muhammad, N. (2002). Hydraulic performance of untreated and polymer-treated bentonite in inorganic landfill leachates. *Clays and Clay Miner.*, 50(5), 546-552.
- Benson, C. and Daniel, D. (1990). Influence of Clogs on hydraulic conductivity of compacted clay, *J. of Geotechnical Engineering*, 116(8).
- Benson, C., Kucukkirca, E., and Scalia, J. (2010b). Properties of geosynthetics exhumed from a final cover at a solid waste landfill. *Geotext. Geomembr.*, 28, 536-546.
- Bradshaw, S. and Benson, C. (2014). Effect of municipal solid waste leachate on hydraulic conductivity and exchange complex of geosynthetic clay liners, *J. Geotechnical and Geoenvironmental Engineering*, 140(4), 04013038.
- Delage P., Audiguier M., Cui, Y.J., Howatt, M.D. (1996). Microstructure of a compacted silt. *Can Geotech J.*, 33:150–158.
- Di Emidio, G., Van Impe, W., and Flores, V. (2011). Advances in geosynthetic clay liners: polymer enhanced clays. *GeoFrontiers 2011. Advances in Geotechnical Engineering*, American Society of Civil Engineer, Reston, USA, 1931-1940.
- Gadikota G, Zhang, F. & Allen, A. J. (2017). Angstrom-to-micrometer characterization of the structural and microstructural changes in kaolinite on heating using Ultra-Small-Angle, Small-Angle, and Wide-Angle X-ray Scattering

- (USAXS/SAXS/WAXS). *Industrial and Engineering Chemistry Research*, 56, 11791-11801.
- Gregg, S. and Sing, K. S. W. (1982). *Adsorption Surface Area and Porosity*, Academic Press, London.
- Hayati, M.A. (2012). Characterization of nano-porous bentonite (Montmorillonite) particles using FTIR and BET-BJH analyses. *Part. Part. Syst. Charact.*, 28, 71–76.
- Jo, H., Benson, C., Shackelford, C., Lee, J., and Edil, T. (2005). Long-term hydraulic conductivity of a non-prehydrated geosynthetic clay liner permeated with inorganic salt solutions. *J. of Geotech. and Geoenviron. Eng.*, 131(4), 405–417.
- Juang, C.H., Holtz, R.D. (1986a). Fabric, pore size distribution and permeability of sandy soils. *J Geotech Eng.*, ASCE 112(9): 855–868.
- Kolstad, D., Benson, C., Edil, T., and Jo, H. (2004b). Hydraulic conductivity of dense prehydrated GCL permeated with aggressive inorganic solutions. *Geosynth. Int.*, 11(3).
- Katsumi, T., Ishimori, Ho, Onikata, M., and Fukagawa, R. (2008). Long-term barrier performance of modified bentonite materials against sodium and calcium permeant solutions. *Geotext. And Geomembranes* 26(1), 14-30.
- Lapierre, C., Leroueil, S., Locat, J (1990). Mercury intrusion and permeability of Louisville clay. *Can Geotech J.*, 27:761–773.
- Likos, W. (2004). Measurement of crystalline swelling in expansive clay. *Geotechnical Testing Journal*, 27(6).

- Likos, W. and Wayllace, A. (2010). Porosity evolution of free and confined bentonites during interlayer hydration. *Clay and Clay Miner.*, 58(3), 399-414.
- Lin, L. and Benson, C. (2000). Effect of wet-dry cycling on swelling and hydraulic conductivity of geosynthetic clay liners. *J. of Geotech. and Geoenviron. Engr.*, 126(1), 40-49.
- McBride (1994). Environmental chemistry of soils, Oxford University Press, New York, 406.
- McRory, J., and Ashmawy, A. (2005). Polymer treatment of bentonite clay for contaminant resistant barriers. *GSP 142 Waste Containment and Remediation*, 1-11.
- Mesri, G. and Olson, R. (1971). Mechanisms controlling the permeability of clays. *Clays and Clay Miner.*, 19(3).
- Mitchell, J.K. and Soga, K. (2005). Fundamentals of soil behaviour, 3rd edn. John Wiley, Sons, Inc, New Jersey.
- Norrish, K., and Quirk, J. (1954). Crystalline swelling of montmorillonite, use of electrolytes to control swelling. *Nature*, 173, 255-257.
- Reed, M.A., Lovell, C.W., Altschaeffl, A.G., Wood, L.E. (1979). Frost heaving rate predicted from pore-size distribution. *Can Geotech J.*, 16:463–472.
- Romero, E., Gens, A., Lloret, A. (1999). Water permeability, water retention and microstructure of unsaturated Boom clay. *Eng Geol.*, 54:117–127.

- Romero, E., Castellanos, E., Alonso, E. E. (2002). Lead nitrate tests on compacted sand-bentonite buffer material GMT Emplacement Project. *Internal Report*, NAGRA, Switzerland.
- Romero, E., Hoffmann, C., Castellanos, E., Suriol, J., Lloret, A. (2005). Microstructural changes of compacted bentonite induced by hydro-mechanical actions. *Proceedings of International Symposium on Large Scale Field Tests in Granite*, Sitges, Spain. In: Alonso EE, Ledesma A (eds) *Advances in understanding engineered clay barriers*. Taylor, Francis Group, London, pp 193–202, 12–14th November 2003.
- Romero, E. and Simms, P.H. (2008). Microstructure investigation in unsaturated soils: A review with special attention to contribution of mercury intrusion porosimetry and environmental scanning electron microscopy. *Geotechnical and Geological Engineering*, 26, 705-727.
- Rutherford, D., Chiou, C.T., Eberl, D.D. (1997). Effects of exchanged cation on the microporosity of montmorillonite. *Clays and Clay Miner.*, 45, 534-543.
- Santamarina, J.C., Klein, K.A., Wang, Y.H., Prencke, E. (2002). Specific surface: determination and relevance. *Can Geotech J.*, 39:233-241.
- Scalia, J., and Benson, C. (2011). Hydraulic conductivity of geosynthetic clay liners exhumed from landfill final covers with composite barriers. *J. Geotech. Geoenviron. Eng.*, 137(1), 1-13.

- Scalia, J., Benson, C., Bohnhoff, G., Edil, T., and Shackelford, C. (2014). Long-term hydraulic conductivity of a bentonite-polymer composite permeated with aggressive inorganic solutions. *J. Geotech. Geoenviron. Eng.*, 140(3), 1-13.
- Scalia, J., and Benson, C. (2014). Barrier Performance of Bentonite-Polyacrylate Nanocomposite to Artificial Ocean Water. *Proceedings, Geo-Congress 2014 Geo-Characterization and Modeling for Sustainability*, GSP No. 234, ASCE, Reston, VA.
- Shackelford, C., Benson, C., Katsumi, T., Edil, T., and Lin, L. (2000). Evaluating the hydraulic conductivity of GCLs permeated with non-standard liquids. *Geotextiles and Geomembranes*, 18(23), 133–161.
- Sposito, G. (1989). *The chemistry of soils*, Oxford University Press, New York.
- Tessier, D., Lajudi, A., Petit, J.C. (1992). Relation between the macroscopic behaviour of clays and their microstructural properties. *Appl Geochem.*, 1(Suppl):151–161.
- Trauger R., and Darlington J. (2000). Next-generation geosynthetic clay liners for improved durability and performance. *TR-220*. Colloid Environmental Technologies Company, Arlington Heights, 2-14.
- Tian, K, Likos, W., and Benson, C. (2018). Polymer Elution and Hydraulic Conductivity of Bentonite-Polymer Composite Geosynthetic Clay Liners. *J. Geotech. Geoenviron. Eng.*, in review.
- Van Olphen, H, (1977). *An introduction to clay colloid chemistry*, 2nd Ed. John Wiley and Sons, Inc., New York
- Webb, P.A. and Orr, C. (1997). *Analytical methods in fine particle technology*. Micromeritics Instrument Corp, Norcross.

2.7. FIGURES

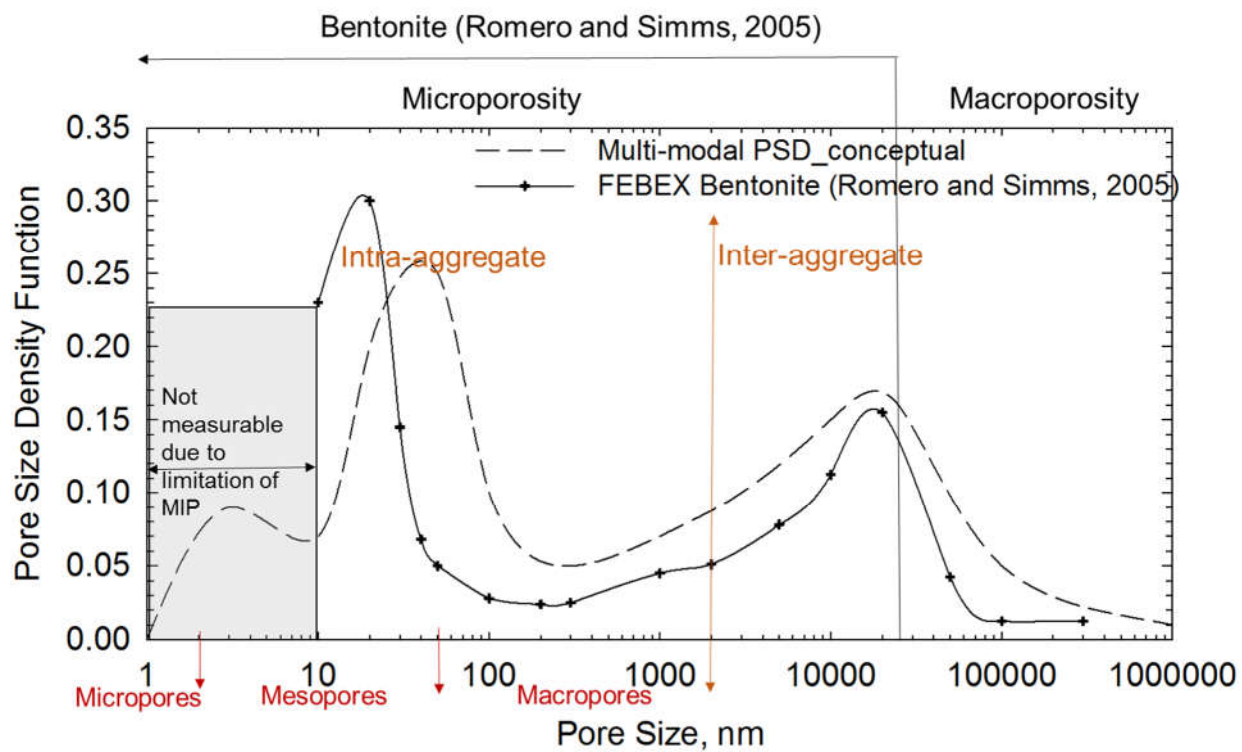


Figure 2.1. Evolution of pore size distribution (PSD) for FEBEX bentonite (from Romero et al. 2005) and a conceptual multi-modal PSD for a typical bentonite.

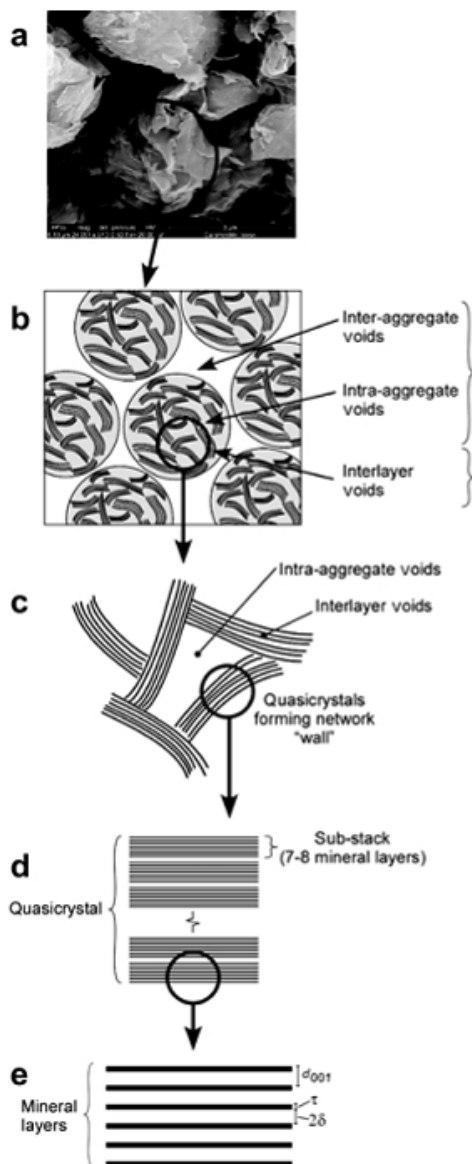


Figure 2.2. (a) SEM image of Wyoming bentonite. Parts b-e are conceptual diagrams of pore spaces on the (b) inter-aggregate scale, (c) intra-aggregate scale, (d) quasicrystal scale, and (e) interlayer scale. (From Likos and Wayllace, 2010).

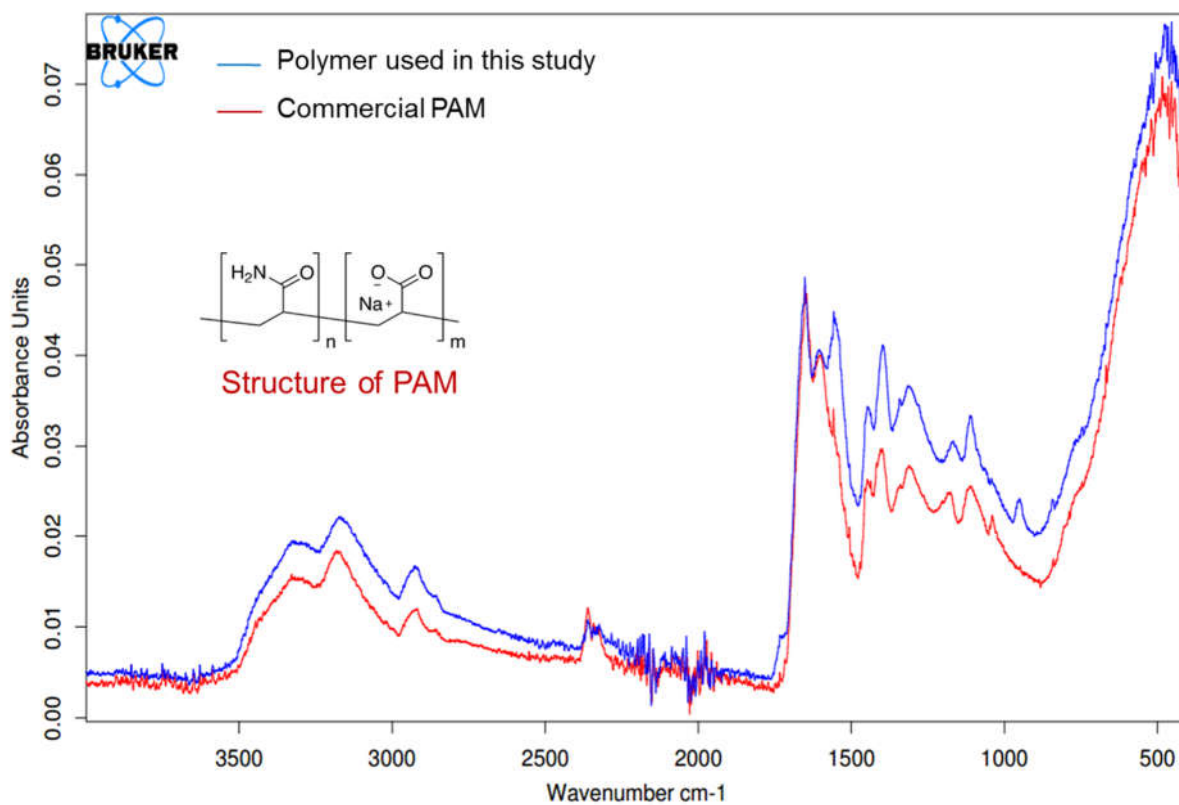


Figure 2.3. Fourier transform infrared spectroscopy (FTIR) of polymer used in this study and commercial PAM.

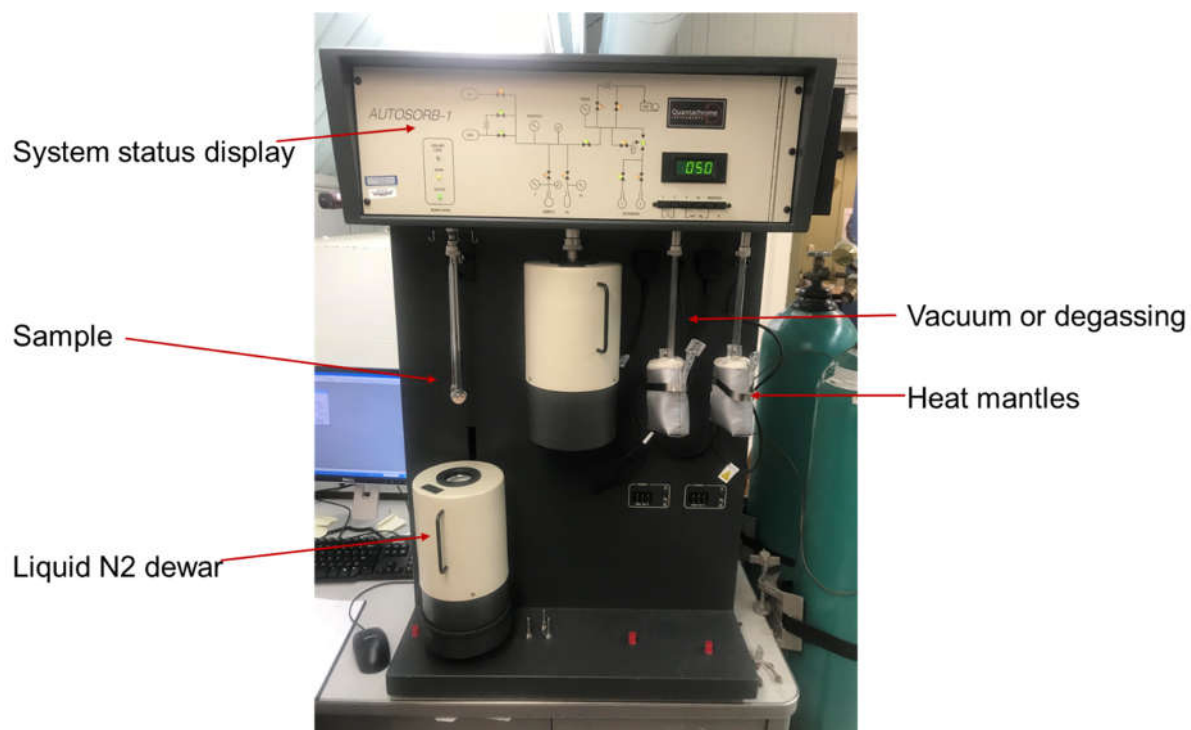


Figure 2.4. Photograph of Quantachrome Autosorb-1-C N₂ porosimetry.

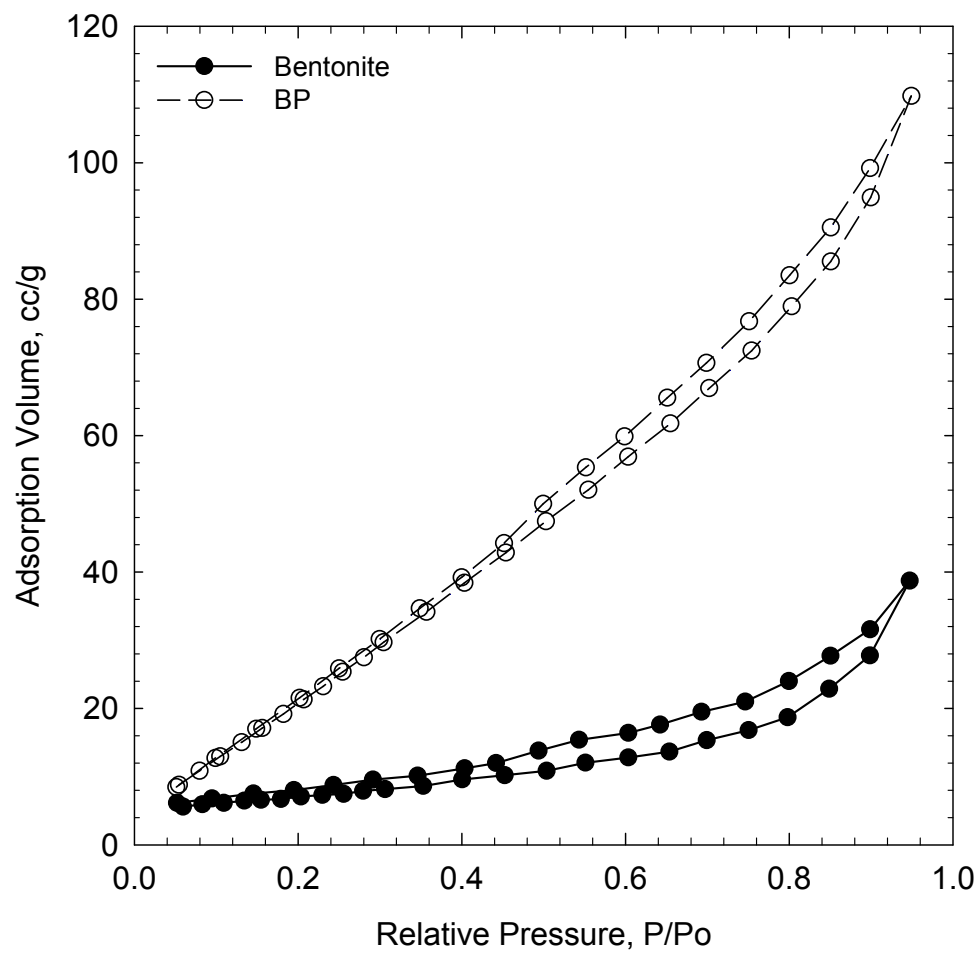


Figure 2.5. Measured N₂ isotherms for bentonite and polymer bentonite mixture.

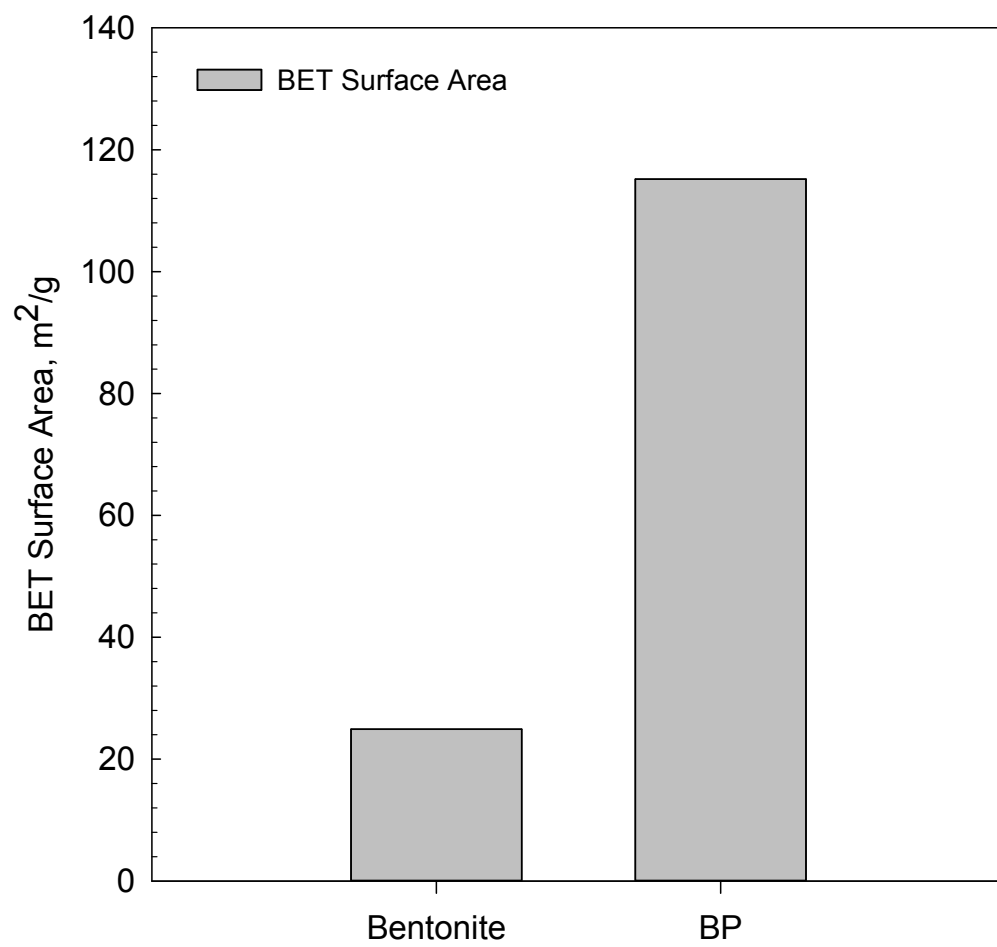


Figure 2.6. BET surface area for bentonite and polymer bentonite.

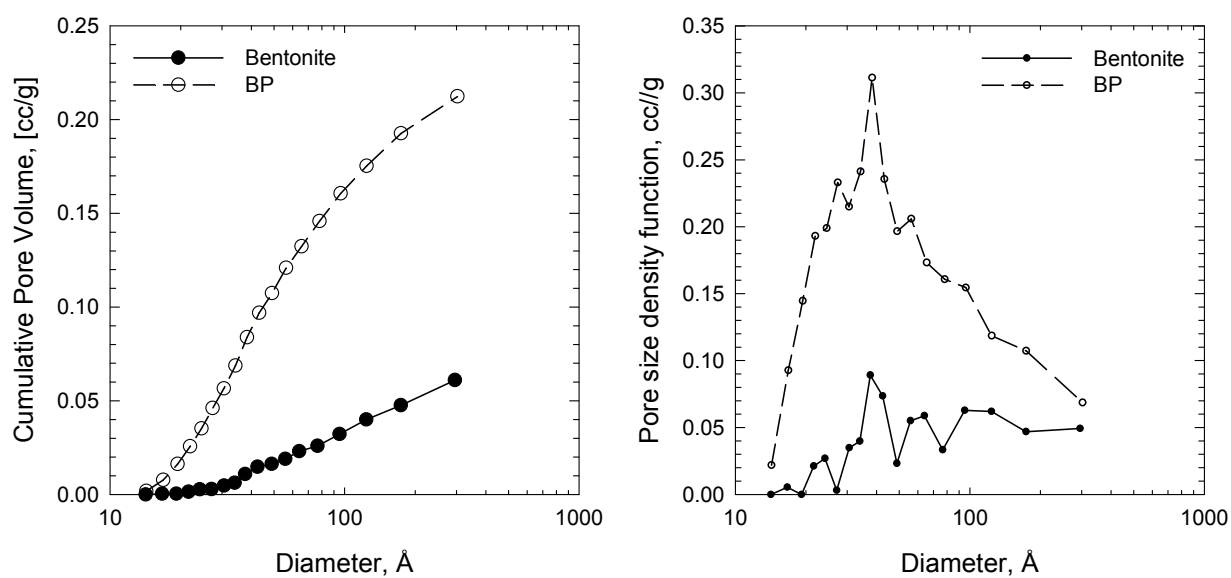


Figure 2.7. (a) Cumulative pore volume, and (b) pore size density function for bentonite and polymer bentonite mixture.

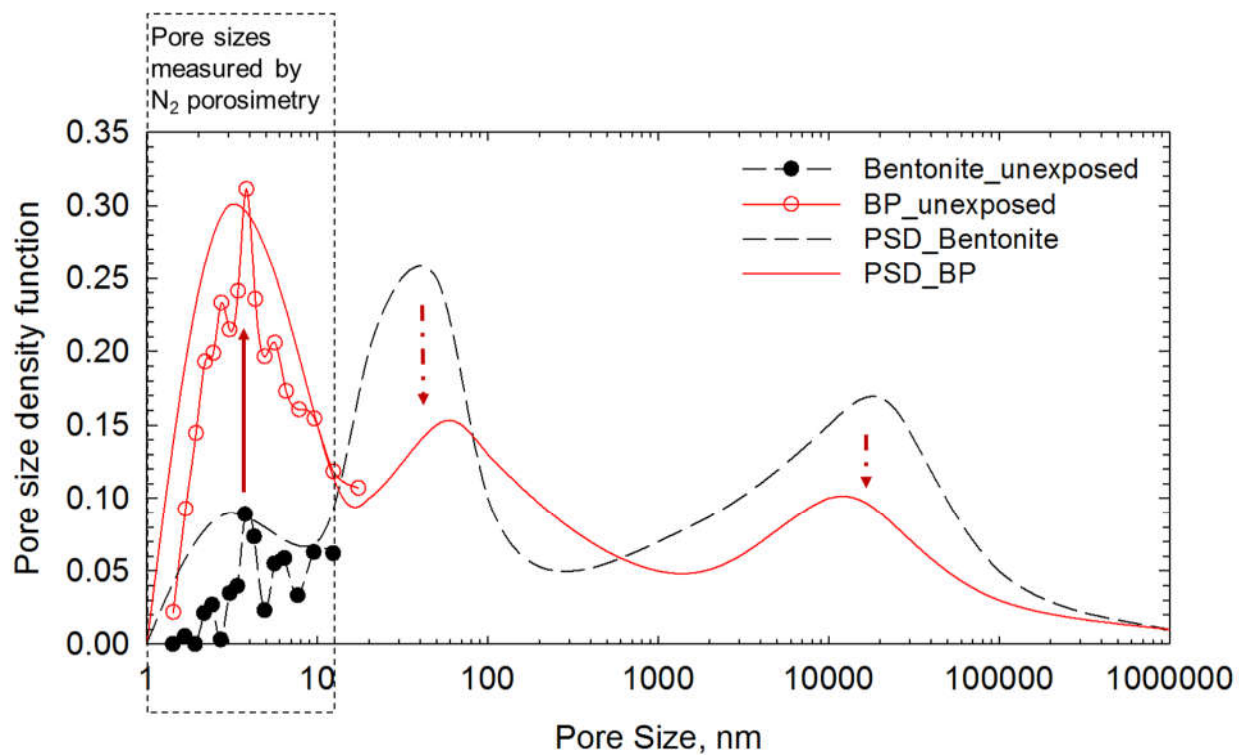


Figure 2.8. Evolution of PSDs combined by N₂ porosimetry and mercury intrusion porosimetry showing tri-modal PSD for bentonite and polymer bentonite mixture.

CHAPTER 3

VISCOSITY AS AN ALTERNATIVE INDEX TEST FOR POLYMER-MODIFIED GEOSYNTHETIC CLAY LINERS

ABSTRACT

Index tests including free swell, liquid limit, and fluid loss are accepted as surrogates for evaluating hydraulic conductivity and chemical compatibility of geosynthetic clay liners (GCLs) containing sodium bentonite (Na-B). Conventional indices are not reliable for application to GCLs containing enhanced bentonite (EB), including polymer modified bentonite (PMB). Experiments were conducted to evaluate viscosity as an alternative index test for screening hydraulic performance and chemical compatibility of PMB-GCLs. Viscosity of representative polymer and polymer-bentonite suspensions is influenced by polymer loading, ionic strength, and chemistry of the test solution. Viscosity systematically decreases with decreasing polymer loading and increasing ionic strength, and is lower in salt solutions having multivalent cations and increasing concentrations of chloride over sulfate. Higher viscosity of PMB in test solutions systematically corresponds to lower hydraulic conductivity of PMB-GCLs permeated with the same solutions. A threshold viscosity at 200 cP is required for achieving hydraulic conductivity lower than 10^{-10} m/s for the PMB-GCL evaluated in this study. A similar trend for Na-B GCLs is not evident. Elution of polymer from PMB-GCLs during permeation corresponds to lower viscosity of PMB in suspension with the same solution, indicating a more mobile polymer phase and high hydraulic conductivity resulting from formation of preferential flow paths. Viscosity can potentially be used as an effective index for evaluating hydraulic

conductivity and chemical compatibility of PMB-GCLs as an alternative to swell index, fluid loss, and liquid limit.

3.1 INTRODUCTION

Sodium bentonite (Na-B) is a highly swelling clay mineral commonly used as the functional component of engineered hydraulic barrier systems such as geosynthetic clay liners (GCLs). Conventional GCLs include a thin (7- to 10-mm) layer of granular or powdered Na-B sandwiched between two geotextiles and can replace thicker compacted clay liners in many environmental containment applications, including solid waste landfills, waste impoundments, lagoons, and tailings impoundments (*e.g.*, Ruhl and Daniel 1997, Petrov and Rowe 1997, Shackelford *et al.* 2000, Jo *et al.* 2001, 2005, Kolstad *et al.* 2004a, Scalia and Benson 2010, Tian *et al.* 2016.).

Fully hydrated Na-B GCLs can maintain low hydraulic conductivity ($k < 10^{-10}$ m/s) if osmotic swelling of the bentonite is not limited by contact with aggressive permeant solutions. In particular, solutions having high ionic strength (I), a prevalence of polyvalent cations, or extreme pH ($2 > \text{pH} > 12$) can inhibit osmotic swelling, alter the bentonite fabric by opening larger and less tortuous flow paths, and result in hydraulic conductivity as much as three to four orders of magnitude higher than required (Shackelford *et al.* 2000, Kolstad *et al.* 2004a, Jo *et al.* 2004, Katsumi *et al.* 2007, Benson *et al.* 2007, Meer and Benson 2007). Conventional Na-B GCLs are thus often less effective barriers to aggressive leachates that may exist in some containment scenarios, such as energy production and mining applications (Benson *et al.* 2010, Bouazza 2010, Gates and Bouazza 2010, Horsney *et al.* 2010, Bouazza and Gates 2014, Chen *et al.* 2014, 2018, Tian *et al.* 2016).

Enhanced bentonites (EB) have emerged in recent years to improve chemical compatibility and hydraulic performance of GCLs for a wider range of applications (*e.g.*, Lin *et al.* 2000, Trauger and Darlington 2000, Ashmawy *et al.* 2002, Kolstad *et al.* 2004, McRory and Ashmawy 2005, Katsumi *et al.* 2008, Benson *et al.* 2010, Di Emidio *et al.* 2011, Scalia *et al.* 2011, Benson *et al.* 2013, Scalia and Benson 2014, Scalia *et al.* 2014). EBs include those where the bentonite is chemically modified, blended, or intercalated with organic molecules or polymers, and increasingly are being adopted in practice to contain aggressive leachates (Scalia *et al.* 2018). Hydraulic conductivity of EB GCLs permeated with aggressive solutions have been measured up to four orders of magnitude lower than GCLs containing unmodified Na-B and permeated with the same solutions.

Chemical compatibility between a particular permeant solution and GCL specimen is directly evaluated by conducting flow-through hydraulic conductivity tests using actual or synthesized leachate (*e.g.*, ASTM D6766). Hydraulic conductivity tests must be conducted until hydraulic and chemical equilibrium are reached to account for ion exchange and corresponding fabric changes that occur when bentonite is contacted with an aggressive solution (Shackelford *et al.* 2000; Jo *et al.* 2005). The practical consequence of this requirement is that direct permeation tests can have very long durations, often on the order of months to years (Jo *et al.* 2005, 2006).

Relatively simple index tests are treated as a surrogate measures to initially screen bentonite quality and to evaluate chemical compatibility of a GCL with a given permeant solution. Three index properties are commonly used, including swell index (ASTM D5890; ASTM 2011b), fluid loss (ASTM D5891; ASTM 2016), and liquid limit (ASTM D4318; ASTM 2010). For screening purposes, for example, the Geosynthetic Research Institute

(GRI) standard GRI-GCL3 (Geosynthetics Institute 2016, Rosin-Paumier *et al.* 2010) requires a minimum swell index in deionized (DI) water of 24 mL/2 g and a maximum fluid loss of 18 mL (Scalia *et al.*, 2018). Hydraulic incompatibility (*i.e.*, potential for $k \gg 5 \times 10^{-11}$ m/s) for GCLs permeated with specific solutions is evaluated by measuring index properties with that solution instead of DI water (Jo *et al.* 2001, Lee *et al.* 2005, Chung and Daniel 2008, Guyonnet *et al.* 2009, Liu *et al.* 2013). Index properties thus provide an indication of hydraulic conductivity and potential for incompatibility between the GCL and the permeant liquid, but do not capture all factors that can affect hydraulic conductivity, including pore structure, void ratio, and any effects of amendments or enhancements that do not directly affect swelling behavior of the bentonite (Lee *et al.* 2005; Katsumi *et al.* 2008, Guyonnet *et al.* 2009, Benson *et al.* 2010, Scalia *et al.* 2014).

A number of studies have shown that swell index (SI), fluid loss (FL), and liquid limit (LL) may not be reliable indicator parameters for enhanced bentonites. Scalia *et al.* (2018) presented a historical overview of GCLs containing EBs and specifically evaluated applicability of SI, FL, and LL as surrogate indices for hydraulic conductivity. Except for EB GCLs where swelling of the bentonite likely remains the primary mechanism responsible for low hydraulic conductivity [*e.g.*, multi-swellable bentonite (Onikata *et al.* 1996), HYPER-clay (Di Emidio *et al.* 2010, 2011)], SI, FL, and LL were shown to be ineffective indicator parameters for hydraulic conductivity of many common types of EB GCLs.

The emphasis of the study described herein is on EB GCLs containing polymer modified bentonite (PMB). Mechanisms hypothesized to control the hydraulic conductivity of GCLs containing PMB include increased swelling capacity (Onikata *et al.*, 1996, 1999,

Katsumi *et al.* 2008), prevention of cation exchange (Trauger and Darlington 2000, Ashmawy *et al.* 2002, Deng *et al.* 2006), and pore clogging (Scalia *et al.* 2014, Tian *et al.* 2016). Recent studies involving analysis of total organic carbon (TOC) to quantify elution of polymer in effluent solution from hydraulic conductivity tests and scanning electron microscopy (SEM) to observe pore-scale interactions between bentonite and polymer suggest that clogging of macropores by polymer hydrogel is a predominant mechanism for maintaining low hydraulic conductivity of PMBs (*e.g.*, Tian *et al.*, 2018). Polymer conformation (structure) and physical and chemical interactions between polymer and bentonite (bonding, pore clogging, polymer elution) thus appear to be important factors governing hydraulic conductivity and chemical compatibility of PMB GCLs. Changes to polymer conformation and polymer-bentonite interaction that occur in contact with aggressive solutions are potentially important measures of chemical compatibility.

There is motivation to develop alternative index measurements for screening and chemical compatibility of PMB GCLs that may more effectively account for these mechanisms. In this paper, viscosity of PMB in suspension with aggressive solution is evaluated as an indirect measure of polymer conformation and polymer-bentonite interaction. Procedures for conducting viscosity tests using a representative polyacrylamide (PAM) polymer, PAM-bentonite mixtures, and PMB sampled from a commercially available PMB-GCL are described. Viscosity measurements are evaluated for correlation to hydraulic conductivity measured for the PMB-GCL permeated with the same solutions and with polymer elution measured using TOC analysis. Test solutions are selected to represent a wide range of aggressive chemistries and actual leachates from coal combustion product (CCP) disposal facilities throughout the USA.

3.2 BACKGROUND

3.2.1. Polymers, Polymer Conformation, and Bentonite-Polymer Interaction

Polymers are long-chain molecules composed of unit cells (monomers) linked in either straight or branched chains to form macromolecules (Painter and Coleman 1997). A single macromolecule may contain thousands of monomers. Depending on the monomer forming the macromolecule, polymers can have positively charged functional groups (cationic), negative charge groups (anionic) or have electrical neutrality (nonionic). In solution some polymers form a hydrogel comprising a web of polymer strands and associated water molecules with a gelatinous structure. Polymers used in PMB-GCLs generally form hydrogels when hydrated (Tian *et al.* 2016, Chen *et al.* 2018b).

The conformation (shape and structure) of polymer chains in solution is sensitive to environmental conditions such as pH, ionic strength, temperature, electrical potential, and photo-irradiation (Park and Hoffman 1992, Gudeman and Peppas 1995, Swann 2010, Kim and Palomino 2011). Low pH and/or high ionic strength generally result in a coiled polymer conformation, whereas high pH and/or low ionic strength generally result in an extended polymer conformation that forms a well-developed polymer gel upon swelling. In low ionic strength solutions, the charged functional groups along an anionic polymer chain such as PAM repel, extending the polymer chain and forming a three-dimensional networked structure. In high ionic strength solutions, cations in solution neutralize the negatively charged carbonyl groups along the polymer chain, causing the polymer chain to contract or coil (Klenina and Lebedeva 1983, Kurenkov 1997, Schweins *et al.* 2003).

Polymers can associate with clay minerals through ion-dipole interaction and electrostatic forces (Theng *et al.* 2012). Cationic polymers bind to montmorillonite via electrostatic interaction, whereas anionic polymers bind to montmorillonite surfaces through cation bridging (Deng *et al.* 2006). Anionic polymers also bind to positively-charged edge surfaces of montmorillonite and other clay minerals (Black *et al.* 1965, Heller and Keren 2003). Interactions between montmorillonite and polymers can have three forms (Kim and Palomino 2011): (i) phase-separated interaction (Fig. 3.1a) where intact clay particles or aggregates of particles are dispersed with a polymer; (ii) intercalated interaction (Fig. 3.1b) where polymer molecules are inserted into the interlayer space of clay minerals, but individual unit layers of the mineral maintain a well-defined and coherent layered structure; and (iii) exfoliated interaction (Fig. 3.1c) where clay mineral interlayers are disassociated and dispersed in the polymer (Giannelis *et al.* 1999, Alexandre and Dubois 2000; Ray and Okamoto 2003, Ruiz-Hitzky and van Meerbeek 2006). Composites having phase-separated and intercalated forms have been used for hydraulic barriers (*e.g.*, Onikata and Kondo 1996, Trauger and Darlington 2000, Di Emidio *et al.* 2011, Kim and Palomino 2011, Bohnhoff and Shackelford 2014, Scalia *et al.* 2014, Tian *et al.* 2016, Chen. *et al.* 2018b).

3.2.2. Limitations of Conventional Index Parameters

Limitations in the application of traditional index parameters to EBs are illustrated in Figure 3.2. Scalia *et al.* (2018) compiled relations between SI and k (Fig. 3.2a), LL and k (Fig. 3.2b), and FL and k (Fig. 3.2c) for Na-B and several EBs reported in the literature for use, or potential use, in GCLs. Trends for Na-B (open symbols) show generally decreasing k with increasing SI and LL and generally increasing k with increasing FL. For

Na-B GCLs, $k > 10^{-10}$ m/s generally corresponds to $SI < 20$ mL/2 g (Fig. 3.2a), whereas lower $k (< 5 \times 10^{-11}$ m/s) generally corresponds to $SI > 20$ mL/2 g, illustrating that SI is a reasonable indicator of k for Na-B-GCLs, particularly at low effective stress and without prehydration (Jo *et al.*, 2001; Kolstad *et al.*, 2004; Lee *et al.*, 2005; Katsumi *et al.*, 2008; Chen *et al.*, 2018).

Similar trends are evident in the relations compiled between LL and k (with the exception of MSB) and FL and k . Results for the EBs (closed symbols), however, are less systematic and SI, LL, and FL are effectively decoupled from hydraulic conductivity. Low hydraulic conductivity values are evident even at very low SI, low LL, and high FL, indicating that these traditional index properties may not be reliable to assess whether many types of EB GCLs will have low hydraulic conductivity. Based on these observations, Scalia *et al.* (2018) recommend that direct hydraulic compatibility tests are necessary to assess whether EBs will have low k to a given permeant solution.

Figure 3.3 illustrates an additional limitation in the use of free swell tests for PMB. Free swell tests shown here were conducted according to ASTM D5890 using PMB sampled from a commercially available GCL in solutions (from left to right) of 300 mM NaCl, 150 mM Na₂SO₄, 300 mM KCl, and 150 mM K₂SO₄. Swell indices determined from observation of the equilibrium location of the bentonite fraction and k of intact the PMB-GCLs permeated with the same solutions are not correlated. Rhodamine WT dye (pink color) added to the test solutions was observed to diffuse to a steady state location marked by a clear boundary located several mL above the top of the bentonite surface. This boundary is interpreted to indicate location of polymer in solution and suggests that substantial separation of the polymer from the bentonite confounds interpretation of how

the composite system swells. This introduces uncertainty into how SI is determined for PMB following traditional procedures.

3.2.3. Viscosity as an Alternative Index Test

Differences in polymer conformation affect macroscopic properties of a polymer hydrogel (Kim and Palomino 2011) and have been conceptually correlated to the hydraulic conductivity of PMB GCLs (Tian *et al.*, 2018). Upon permeation of PMB with DI water, osmotic swelling of the Na-B fraction closes intergranular pores and forces water to flow through small and tortuous pores within the granules, resulting in low hydraulic conductivity. In contrast, it is hypothesized that permeation of PMB with a high ionic strength solution inhibits osmotic swelling of the Na-B fraction, compromises hydrogel formation by producing a coiled polymer conformation, precludes bonding between the polymer and bentonite surfaces, and promotes elution of polymer that would otherwise clog the bentonite's intergranular pores and maintain low hydraulic conductivity.

Since viscosity is a direct measurement of the resistance of a fluid or a fluid suspension to shear, it is hypothesized that viscosity of a PMB suspension is an indirect measure of polymer conformation and polymer-bentonite interaction, and therefore can potentially be used as a surrogate for the hydraulic conductivity of a PMB-GCL. Specifically, a polymer-bentonite suspension with well-developed hydrogel and strong polymer-bentonite interaction is expected to have higher viscosity than a polymer-bentonite suspension with contracted polymer coils and weak polymer-bentonite interaction (illustrated conceptually in Figure 3.4). Corresponding hydraulic conductivity of a hydrated PMB-GCL is expected to be relatively low and relatively high in each

respective case, creating a potential link between the viscosity of a PMB in suspension with a particular solution and the hydraulic conductivity of a PMB-GCL permeated with that solution.

3.3 MATERIALS AND METHODS

3.3.1. Test Solutions

Table 3.1 summarizes test solution properties including pH, electrical conductivity (EC), ionic strength (I), and ratio of monovalent to divalent cations (RMD) for all of the test solutions used for viscosity and hydraulic conductivity testing. Inorganic salt solutions were prepared at various ionic strengths by dissolving monovalent and divalent cation salts (of CO_3 , OH , NO_3 , F , I , Cl , and SO_4) in DI water. A second suite of NaCl , Na_2SO_4 , KCl , and K_2SO_4 solutions was prepared at 300 mM Na and 300 mM K concentrations but to different molar ratios of Cl to SO_4 (denoted anion ratio, R) to evaluate effects of anion ratio ranging from 0 (SO_4 -rich) to 100 (Cl -rich). Five coal combustion product (CCP) leachates were selected from a database established by Benson *et al.* (2015) through analysis of a CCP leachate database compiled by the Electric Power Research Institute (EPRI) to represent a range of conditions encountered in CCP disposal facilities throughout the USA (EPRI 2006 and 2009). Synthetic leachates representing these chemistries (denoted EPRI on Table 1) were created by dissolving reagent-grade CaSO_4 , Na_2SO_4 , MgSO_4 , K_2SO_4 , NaCl , and CaCl_2 in DI water. These five leachates are referred to as typical CCP leachate, predominantly divalent cation ash leachate (low RMD), flue gas desulfurization residual (FGD) leachate, high ionic strength leachate, and trona ash leachate. Chemical characteristics of five additional CCP leachates (CCP 1, CCP 2 and

CCP 3), MSW-I leachate and gold PLS leachate were obtained from coal combustion, municipal solid waste combustion (MSW) and heap leach facilities impoundments around the U.S. and used to produce corresponding synthetic leachates in the laboratory (referred to as site-specific leachates in Table 3.1). Predominance of monovalent and polyvalent cations summarized in Table 1 was characterized by the parameter RMD, defined as (Kolstad *et al.* 2004):

$$\text{RMD} = \frac{M_M}{\sqrt{M_D}}$$

where M_M is the total molarity of monovalent cations and M_D is the total molarity of polyvalent cations.

3.3.2. Polymer Modified Bentonite (PMB) Geosynthetic Clay Liner

PMB for viscosity and hydraulic conductivity tests was sampled from a commercially available GCL containing a phase-separated (see Fig.3.1) blend of granular Na-B and a proprietary polymer. The bentonite-polymer mixture was encapsulated between a woven and a nonwoven geotextile by needle punching to form a PMB-GCL. Mass per unit area, moisture content, thickness, cation exchange capacity (CEC), bound cations (Ca^{2+} , Na^+ , Mg^{2+} , K^+), granule size distribution (D_{10} , D_{30} , D_{60}), and polymer content of the PMB-GCL are summarized in Table 1.1 CEC and the initial distribution of bound cations (i.e., prior to permeation) were determined by ammonium acetate extraction (ASTM D7503). Polymer content of the PMB was quantified by loss on ignition (LOI) conducted according to ASTM D7348 accounting for loss of strongly bound water molecules, calcite, and organic matter associated with the bentonite fraction (Scalia *et*

al., 2014; Tian *et al.*, 2016). Quantitative X-ray diffraction (XRD) analysis showed that the PMB contained 79% montmorillonite, along with measureable quantities of quartz, feldspar and mica (Chen *et al.* 2015). Polymer type was estimated by comparing Fourier transform infrared (FTIR) spectra measured for a sample of polymer with a library of known materials (Tian *et al.*, 2018). That analysis indicated that 80% of the measured spectrum for the polymer is consistent with anionic polyacrylamide (PAM). FTIR spectra obtained for a commercially available anionic PAM (Polysciences Inc., Warrington, PA, USA, Cat. No. 04652) were also comparable (Fig.2.3).

3.3.3. Polyacrylamide (PAM) Polymer

Preliminary tests were conducted to measure the viscosity of commercially available anionic polyacrylamide (PAM) (Polysciences, Inc., Warrington, PA; Cat. #04652) in NaCl and CaCl₂ solutions having ionic strength ranging from 0 (DI water) to 1000 mM. Polymer suspensions for these tests were prepared with polymer concentrations (dry mass of polymer to mass of solution) of 2%, 3%, 4%, and 5%. While the polymer in the PMB-GCL cannot be defined precisely by FTIR analysis, PAM is believed to be a major fraction (Tian *et al.*, 2018). The commercial PAM selected here is thus considered representative of the general polymer type in the PMB-GCL used for concurrent testing.

3.3.4. Mixtures of PAM Polymer and Na-B

A suite of tests was conducted to measure viscosity of PAM and Na-B prepared by dry mixing at polymer-to-bentonite (P/B) ratios of 0%, 0.5%, 5.0%, and 10% by dry mass in NaCl solutions ranging from I = 150 mM to I = 1000 mM. Bentonite used for this

series of tests was a GCL-grade natural sodium bentonite (Na-B) from Wyoming, USA available under the name Volclay CG-50 (CETCO, Hoffman Estates, IL). Index properties of the Na-B and of a Na-B GCL used for hydraulic conductivity testing are included in Table 1.1. Polymer-bentonite mixtures were prepared to a total solid-liquid ratio of 10% in the salt solutions for viscosity testing.

3.3.5. Viscosity Testing

Viscosity of PAM, PAM-NaB mixtures, and PMB sampled from the GCL in the test solutions was measured using a Brookfield DV-I PRIME Viscometer (Middleboro, MA). This bench-scale viscometer (Figure 3.5) measures fluid viscosity at a given shear rate by driving a rotating spindle through a calibrated spring. Different spindles may be selected for various ranges of viscosity. For the tests reported here, shear rate was controlled at a torque speed of 100 RPM and for a maximum measured time of 20 minutes. All tests were conducted at room temperature (15 °C - 25 °C).

Two mixing methods were used to prepare the polymer-bentonite suspensions. For suspensions in high-ionic-strength solutions (i.e., corresponding to relatively low viscosity), the polymer-bentonite mixture was placed in a beaker with the corresponding solution, continuously stirred using a magnetic bar stirrer at approximately 720 rpm for no less than 120 min, and for at least another 15 minutes prior to viscosity testing. Suspensions in low-ionic-strength solutions (i.e., corresponding to relatively high viscosity) were prepared in a similar manner, but stirred using a blunt-bladed mixing paddle powered by an external motor. The purpose of the blunt paddle was to minimize local shear forces that may otherwise break down polymer chains. Mixing time following

this procedure varied with solution type and ionic strength, and was considered complete when uniform suspensions were achieved by manual observation. Viscosity tests in all cases were conducted immediately after mixing.

3.3.6. Hydraulic Conductivity Testing

Hydraulic conductivity tests for intact GCLs were conducted according to ASTM D6766 in flexible-wall permeameters using the falling headwater-constant tailwater method. Influent permeant solution was contained in 50-mL graduated glass pipettes. Effluent was collected in 60-mL polyethylene bottles. Electrical conductivity (EC), pH, and cation concentration of the effluent were measured periodically to assess chemical equilibrium. The burettes and bottles were covered with parafilm to minimize evaporation and atmospheric interaction. GCL specimens were prepared by cutting a circular sample directly from a roll provided by the manufacturer using a razor knife and steel ring following the procedures in Jo *et al.* (2001). Paste prepared with bentonite-polymer mixture and permeant solution was placed around the perimeter of the specimen to prevent loss of the mixture during handling and preferential flow along the edge during permeation. Initial thickness of each GCL specimen was measured with calipers at six equidistant points. Effective confining stress was maintained at 20 kPa during permeation. Permeation was conducted using an average hydraulic gradient of 130 and continued until the hydraulic and chemical termination criteria in ASTM D6766 were met. Hydraulic equilibrium was defined as steady hydraulic conductivity for three consecutive measurements with ratio of incremental volumetric outflow to inflow (flow ratio) within 1.00 ± 0.25 . Chemical equilibrium was assumed when the ratio of effluent to influent electrical

conductivity (EC_{out}/EC_{in}) and effluent to influent pH (pH_{out}/pH_{in}) were steady and within 1.0 ± 0.1 .

3.4 RESULTS AND DISCUSSION

3.4.1. Viscosity of PAM Polymer

Figure 3.6 is a plot of viscosity (cP) for PAM polymer suspensions at solid-liquid concentrations ranging from 2% to 5% by mass in NaCl and CaCl₂ solutions ($0 \leq I \leq 1000$). Viscosity is relatively low at low polymer concentrations and increases systematically with increasing polymer concentration. This is attributed to the presence of more polymer chains and more intensive hydrogel formation. With more polymer in solution, more water molecules are absorbed onto the polymer chains, the polymer chains provide connectivity among the water molecules, and there are less free water molecules. Strong interaction among the polymer and water molecules results in more shear resistance and corresponding higher viscosity.

Increasing ionic strength results in a general decrease in viscosity, most notably at relatively low ionic strength. This initial decrease is attributed to an ion-screening effect (Brown *et al.*, 1992), where negative charges on functional groups of the anionic polymer chains are effectively shielded by cations in solution. Ion-screening minimizes repulsive forces arising from like charges along the polymer macromolecule, promoting collapse or coiling of the chains. Coiling of the polymer chain decreases its hydrodynamic radius and results in lower viscosity of the suspension (see Fig. 3.4). As ionic strength increases to ~200 mM, the initial decrease in viscosity ceases because the charge groups on the polymer chains have been neutralized by cations in solution and capacity for the polymer

to absorb solvent (water) molecules is reduced (Rashidi *et al.*, 2009). Viscosity is also lower in solutions with divalent cations (CaCl_2) than in solutions with monovalent cations (NaCl) across a wide range of ionic strength. Solutions rich in divalent cations are poor solvents for anionic polymers (and thus promote coiled conformation) because the strong bonding between divalent cations and negatively-charged carboxylate groups along the polymer chain more effectively prevent the polymer chains from extending in solution (Taylor *et al.*, 1995; Maradi *et al.*, 1995; Levitt *et al.*, 2008).

Viscosity trends toward higher values very high ionic strengths, most notably for the suspensions in CaCl_2 and at higher polymer concentrations. This is interpreted to indicate that that Ca^{2+} behaves like a cross-linker among the polymer molecules. Zhang *et al.* (2008) found a similar result by quantifying the molecular dimension of polymer in CaCl_2 solution by static laser light scattering, and concluded that crosslinking mechanisms may dominate polymer behavior at high salt concentrations. For higher polymer concentrations, the increase in viscosity is higher because entanglements of polymer chains increase and thus extend the shear thinning region (Ait-Kadi *et al.*, 1987). An apparent peak in viscosity at moderate ionic strength (~ 50 mM) may also be observed for each of the polymer suspensions in NaCl. This phenomenon may be caused by hydrolysis of the PAM polymer molecule and conversion to hydrolyzed polyacrylamide (HPAM), which has been reported to have a peak viscosity at some threshold salt concentration in NaCl (Rashidi *et al.*, 2009; Dautzenberg, 1999). While this effect has been extensively studied, the sensitive range of HPAM has not been reported.

3.4.2. Viscosity of PAM Polymer and Na-B Mixtures

Viscosity of PAM polymer and Na-B mixtures having polymer-bentonite (P/B) ratios of 0%, 0.5%, 5%, and 10% and a total solid-liquid ratio of 10% in NaCl solutions are shown in Figure 7a. Viscosity of the end-member bentonite (P/B = 0) and of each polymer-bentonite mixture decreases with increasing ionic strength. The trend in the relation between viscosity and ionic strength is essentially the same at lower polymer concentrations (0%, 0.5%, 5%), but is steeper for the suspension having the highest polymer content (10%). With the exception of one data point at the highest polymer ratio (P/B = 10%) and highest ionic strength ($I = 1000$ mM), viscosity systematically increases with increasing polymer fraction, regardless of ionic strength. Viscosity of the end member bentonite and the polymer-bentonite mixture at the lowest polymer fraction (P/B = 0.5%) are essentially the same, indicating that polymer-to-bentonite ratio does not significantly influence viscosity behavior for polymer fractions less than about 5% and that, within this range, the bentonite fraction controls the rheological behavior of the mixtures. Increased sensitivity of viscosity to ionic strength at higher polymer loading (P/B = 10%) and the very low viscosity measured for this mixture at $I = 1000$ mM suggests that the polymer has a stronger influence on the rheology of the mixture and that the viscosity of the polymer is more sensitive to ionic strength than the bentonite.

Figure 3.7b is a plot of results from tests to measure viscosity of PAM and Na-B mixtures at a polymer-to-bentonite ratio of 5% in a wider range of solutions (NaCl, CaCl₂, KCl, K₂SO₄, N₂SO₄, MgSO₄). A polymer-bentonite ratio of 5% was selected to be representative of the commercial PMB-GCL evaluated in this study (polymer loading of 5.1%). Viscosity generally decreases with increasing ionic strength for each solution. At any ionic strength, viscosity decreases according to the following approximate trend (from

high to low viscosity): $\text{Na}_2\text{SO}_4 > \text{K}_2\text{SO}_4 > \text{NaCl} > \text{KCl} > \text{MgSO}_4 > \text{CaCl}_2$. Polymer-bentonite suspensions in solutions with monovalent cations generally have higher viscosity than solutions with divalent cations. This is consistent with results for the end member PAM polymer (Fig. 3.6) and is attributed to the fact that divalent cation solutions are relatively poor solvents for anionic polymers.

The viscosity trend in Figure 3.7b also indicates that viscosity is higher in SO_4^{2-} solutions than in Cl^- solutions, suggesting that SO_4^{2-} tends to expand the polymer chains or promote more polymer-bentonite interaction. This is further illustrated in Figure 3.8, which is a plot of viscosity measured for suspensions of polymer isolated from the PMB-GCL and mixed with Na-B at a polymer-to-bentonite ratio of 5% and a total solids content of 10%. Solutions for these tests included monovalent cation (Na^+ or K^+) or divalent cation (Mg^{2+}) salts with either Cl^- or SO_4^{2-} . The molar concentration ratio of Cl^- to SO_4^{2-} is defined as the anion ratio (R). Solutions were prepared with a fixed cation concentration (e.g., 300 mM Na^+ , 300 mM K^+ , and 50 mM Mg^{2+}) and $R = 0$ (pure SO_4^{2-}), 0.2, 1, 5, 20, and ∞ (pure Cl^-). Anion ratio of 0 and ∞ are plotted on the far left ($R = 10^{-2}$) and right ($R = 10^2$) hand side of Figure 3.8, respectively. For the 300 mM Na^+ and K^+ , the viscosity of the polymer-bentonite mixture decreased as R increased (shifts to Cl^- rich condition) regardless of a corresponding decrease in ionic strength from 450 mM to 300 mM. This illustrates that anion species has a more profound effect on the viscosity behavior of the polymer-bentonite mixture than ionic strength. The change of viscosity suggests that bonding between the polymer and bentonite degrades as the anionic species become Cl^- rich. The viscosity in 50 mM Mg^{2+} solutions falls in a much lower range and is essentially independent of, or slightly increases, with ionic strength. This is attributed to enhanced

cation screening, where the divalent cations attract two anionic function groups of polymer, resulting in collapsing of polymer structures and weak polymer bentonite interaction. Combine these results show that for polymer-bentonite mixtures, extended polymer chains in monovalent, low ionic strength, and sulfate rich solutions may lead to more effective bridging among clay particles or aggregates, more effective hydrogel formation, and corresponding higher viscosity of the suspension. Coiled polymer chains in polyvalent, high ionic strength, and chloride-rich solutions, on the other hand, may bridge clay units and form hydrogel less effectively, resulting in lower viscosity of the suspension.

3.4.3. Viscosity and Hydraulic Conductivity of PMB-GCL

Results from viscosity tests conducted on polymer-bentonite mixtures obtained directly from the PMB-GCL at a solid-to-liquid ratio of 10% (by dry mass) and hydraulic conductivity tests conducted for intact PMB-GCLs to the same permeant solutions are plotted on Figure 3.9a. Solutions used for viscosity and hydraulic conductivity tests included the salt solutions and synthetic leachates summarized in Table 3.1. While there is scatter in the relation, there is a clear trend toward decreasing hydraulic conductivity with increasing viscosity. A trendline fit through the data set is in the form:

$$k = 0.0001\eta^{-2.607}$$

where k is hydraulic conductivity (m/s) and η is viscosity (cP). A sharp decrease in hydraulic conductivity for the PMB-GCLs was observed as viscosity increases beyond around 200 cP. The PMB-GCLs maintain low hydraulic conductivities ($< 10^{-10}$ m/s) with the when viscosity is greater than the threshold value of 200 cP, and high hydraulic

conductivities correspond to the suspensions with the viscosities below the threshold point. The threshold point is interpreted to reflect the change in the PMB system from a contracted coil structure to a well-developed polymer gel structure. A similar trend in the relation between viscosity for Na-B sampled from conventional GCLs and hydraulic conductivity of those GCLs is not evident (Figure 3.9b).

3.4.4. Viscosity and Polymer Elution

Effluent from hydraulic conductivity tests for the PMB-GCLs with higher hydraulic conductivity was visibly more viscous than the influent, as also reported by Scalia *et al.* (2014) and Tian *et al.* (2016) for PMB-GCLs. The polymer hydrogel in the pore space of a PMB-GCL is a viscous liquid that can be mobile under a hydraulic gradient. Mobility of the polymer likely is affected by polymer loading, changes in conformation of the polymer due to interactions with the permeant solution, and potentially the hydraulic gradient. When the hydrogel becomes mobile, polymer elution can occur, thus reducing the volume and effectiveness of polymer blocking the flow paths in the pore space.

Effluent samples for PMB-GCL were analyzed for TOC to evaluate polymer elution during permeation with various solutions, including [Na] of 300mM single species salt solutions, 50 mM CaCl₂, Trona leachate and permeant solutions with various anion ratios. The cumulative mass of polymer elution (calculated from TOC) increased with pore volumes of flow (PVF) over the entire permeation period (Fig. 3.10a), indicating continuous polymer elution from the GCL. The shape of elution curve is differed for each permeant solution under same testing conditions (effective stress, hydraulic gradient, etc.). These differences are attributed to differences in polymer confirmation and polymer-

bentonite interaction. With some solutions (e.g., Trona, [Mg] at R of 20), the cumulative polymer elution curve levels off at early PVF (~5-10), indicating less polymer elution. This is hypothesized to result from the formation of preferential flow paths as polymer is eluted from localized zones and a corresponding increase in hydraulic conductivity.

Figure 3.10b is a plot of cumulative polymer elution measured at hydraulic equilibrium versus viscosity. In general, greater polymer elution during hydraulic conductivity testing corresponds to lower viscosity. This supports the notion that viscosity is a function of polymer conformation and polymer bentonite interaction. High viscosity is observed in suspensions with well-developed polymer gel and more effective polymer bentonite interaction and, as a result, the polymer is tightly held within bentonite pores and less prone to elution. On the other hand, significant polymer elution observed in solutions with lower viscosity indicates a suspension with contracted polymer coils and poor polymer bentonite interaction. Preferential flow paths may form during permeation, resulting in a relatively rapid spike in polymer elution at low PVF that levels off as flow continues.

3.5 SUMMARY AND CONCLUSIONS

This study evaluated viscosity as an indirect measure of polymer conformation and polymer-bentonite interaction for polymer-modified bentonite in suspension with solutions selected to represent a wide range of aggressive chemistries. Viscosity of PAM polymer in suspension increases systematically with increasing polymer concentration. Viscosity generally decreases rapidly at low ionic strength ($0 \text{ mM} < I < \sim 200 \text{ mM}$), plateaus at moderate ionic strength ($200 \text{ mM} < I < \sim 600 \text{ mM}$), and in CaCl_2 solution appears to

increase at high ionic strength ($600 \text{ mM} < I < 1000 \text{ mM}$). Viscosity of polymer suspensions is generally lower in divalent solution (CaCl_2) than in monovalent solution (NaCl) across a wide range of ionic strength due to the cross-linking effects of divalent cations.

Viscosity of polymer-bentonite suspensions is influenced by polymer loading, ionic strength, and chemistry of the test solution. Viscosity generally decreases with increasing ionic strength. The influence of ionic strength is relatively weak and essentially independent of polymer-to-bentonite ratio at low polymer concentrations ($P/B \leq 5\%$), but is more pronounced at higher polymer concentration ($P/B = 10\%$). These results suggest that the bentonite fraction controls rheological behavior of the mixtures at low polymer concentration, and that there is some threshold polymer fraction between about $P/B = 5\%$ and $P/B = 10\%$ where the polymer fraction begins to control the mixture rheology.

Viscosity of polymer-bentonite suspensions in a range of different salt solutions indicates that solutions with monovalent cations generally produce higher viscosities than solutions with divalent cations. Solutions of Cl^- salts generally result in lower viscosity than solutions of SO_4^{2-} salts for cations of the same valence.

A link is established between the viscosity of PMB suspensions and the hydraulic conductivity of a PMB-GCL permeated with the same solutions. A threshold value of viscosity at 200 cP was required for achieving a hydraulic conductivity lower than 10^{-10} m/s for the PMB-GCL evaluated in this study. A similar trend for Na-B GCLs is not evident. Polymer elution generally increases with decreasing viscosity, indicating a more mobile polymer phase and corresponding potential for high hydraulic conductivity resulting from preferential flow paths. These results indicate that viscosity can potentially be used as an

effective index indicator for PMB-GCLs and may potentially replace commonly adopted, but ineffective indices such as swell index, fluid loss, and liquid limit.

3.6 REFERENCES

- Ait-Kadi, A., Carreau, P.J., and Chauveteau, G. (1987). Rheological properties of partially hydrolyzed polyacrylamide solutions, *J. Rheology*, 31: 537.
- Alexandre, M., and Dubois, P. (2000). Polymer-layered silicate nanocomposites: preparation, properties and uses of a new class of materials. *Materials Science and Eng.*, 28, 1-63.
- Ashmawy, A., Darwish, E., Sotelo, N., and Muhammad, N. (2002) Hydraulic performance of untreated and polymer-treated bentonite in inorganic landfill leachates. *Clays and Clay Miner.*, 50(5), 546-552.
- ASTM. (2006). *Standard test method for swell index of clay mineral component of geosynthetic clay liner*. D5890, West Conshohocken, PA.
- ASTM (2010). *Standard test methods for liquid limit, plastic limit, and plasticity index of soils*. D4318, West Conshohocken, PA.
- ASTM (2012). *Standard Test Method for Evaluation of Hydraulic Properties of Geosynthetic Clay Liners Permeated with Potentially Incompatible Aqueous Solutions*, D6766, West Conshohocken, PA.
- ASTM (2013). *Standard Test Methods for Loss on Ignition (LOI) of Solid Combustion Residues*, D7348, West Conshohocken, PA.
- ASTM. (2016). *Standard Test Methods for Measurement of Hydraulic Conductivity of Saturated Porous Materials Using a Flexible Wall Permeameter*. D5084, West Conshohocken, PA.
- ASTM. (2016). *Standard test method for fluid loss of clay component of geosynthetic clay liners*. D5891, West Conshohocken, PA.

- Athanassopoulos, C., Benson, C., Donovan, M., and Chen, J. (2015). Hydraulic conductivity of a polymer-modified GCL permeated with high-pH solutions. *Proceedings, Geosynthetics Conference 2015*, Portland, Oregon, 181-186.
- Benson, C., Thorstad, P., Jo, H., Rock, S. (2007). Hydraulic performance of geosynthetic clay liners in a landfill final cover, *J. Geotech. Geoenviron. Eng.*, 133(7): 814-827.
- Benson, C., Kucukkirca, E., and Scalia, J. (2010b) Properties of geosynthetics exhumed from a final cover at a solid waste landfill. *Geotext. Geomembr.*, 28, 536-546.
- Benson, C., Chen, J., and Edil, T. (2014). Engineering prosperities of geosynthetic clay liners Permeated with Coal Combustion Product Leachates, Report No. 3002003770, Electric Power Research Institute (EPRI), Palo Alto, CA.
- Black, A., Birkner, F., and Morgan, J. (1965). Destabilization of dilute clay suspensions with labeled polymers. *Journal of the American Water Works Association*, 57, 1547–1560.
- Bohnhoff, G. and Shackelford, C. (2014). Hydraulic conductivity of polymerized bentonite-amended backfills. *J. Geotech. Geoenviron. Eng.*, 140(3).
- Bouazza, A. (2010). Geosynthetics lining in mining applications. *Proceedings of Sixth International Conference on Environmental Geotechnics*, International Society for Soil Mechanics and Geotechnical Engineers, New Delhi, India, Nov. 8-12, 2010, 221-259.
- Bouazza, A, and Gates W.P. (2014). Overview of performance compatibility issues of GCLs with respect to leachates of extreme chemistry. *Geosynthetics International*, Vol. 21(2).

- Brown, W., Fundin, J, and Miguel, M. G. (1992). Poly (ethylene oxide)-sodium dodecyl sulfate interactions studies using static and dynamic light scattering, *Macromolecules*, 25, 7192-7198.
- Chen, J., Bradshaw, S., Likos, W., Benson, C., and Edil, T. (2014). Hydraulic Conductivity of Geosynthetic Clay Liners to Synthetic Coal Combustion Product Leachates. *Geo-Characterization and Modeling for Sustainability*, Geotechnical Special Publication No. 234, ASCE, Reston, VA, 334-342.
- Chen, J., Benson, C.H., and Edil, T.B. (2015). Hydraulic conductivity of geosynthetic clay liners to coal combustion product leachates. *Geosynthetics 2015*, Portland, OR.
- Chen, J., Benson, C.H., and Edil, T.B. (2018). Hydraulic Conductivity of Geosynthetic Clay Liners with Sodium Bentonite to Coal Combustion Product Leachates. *J. Geotech. Geoenviron. Eng.*, 144 (4).
- Chu, B., Ying, Q., and Grosberg, Y. (1995). Two-stage kinetics of single chain collapse, *Macromolecules*, 28(1), 180–189.
- Chung, J., and Daniel D. (2008). Modified fluid loss test as an improved measure of hydraulic conductivity for bentonite. *Geotech. Test. J.*, 31(3).
- Dautzenberg, H., and Karibyants, N. (1999). Polyelectrolyte complex formation in highly aggregating systems. Effect of salt: response to subsequent addition of NaCl, *J. Macromol Chem Phys*, 200 (1):118–125.
- Deng, Y., B., D. J., White, N. G., Loeppert, R. H., and Juo, A. S. (2006). Bonding between polyacrylamide and smectite. *Colloids and Surfaces*, 281(1), 82-91.
- Di Emidio, G., Van Impe, W., and Mazzieri, F. (2010). A polymer enhanced clay for impermeable geosynthetic clay liners. *Proceedings of Sixth International*

Conference on Environmental Geotechnics, International Society for Soil Mechanics and Geotechnical Engineers, New Delhi, India, 963-967.

Di Emidio, G., Van Impe, W., and Flores, V. (2011). Advances in geosynthetic clay liners: polymer enhanced clays. *GeoFrontiers 2011. Advances in Geotechnical Engineering*, American Society of Civil Engineer, Reston, USA, 1931-1940.

EPRI (2006). Characterization of field leachates at coal combustion product management sites, Electric Power Research Institute, Palo Alto, CA.1012578.

EPRI (2009). Coal ash: characteristics, management, and environmental issues. Electric Power Research Institute, Palo Alto, CA.1019022.

Gates. WP, and Bouazza, A (2010). Bentonite transformations in strongly alkaline solutions. *Geotext. Geomembranes*, 28(2), 219-225.

Geosynthetic Institute. (2016). GRI test method GCL3: Test Methods, Required Properties, and Testing Frequencies of Geosynthetic Clay Liners (GCLs). Geosynthetic Institute, Folsom, PA.

Giannelis E P, Krishnamoorti R K and Manias E (1999). Polymer-Silicate Nanocomposites: Model Systems for Confined Polymers and Polymer Brushes, *Adv. Polym. Sci.* 138, 108-147.

Gudeman, L. F., and Peppas, N. A. (1995). Preparation and characterization of pH-sensitive, interpenetrating networks of poly(vinyl alcohol) and poly(acrylic acid), *Appl. Polym. Sci.* 55(6), 919-928.

Guyonnet, D., Cazaux, D., Vigier-Gailhanou, H., and Chevrier, B. (2009). Effect of cation exchange on hydraulic conductivity in a sand-bentonite-polymer-mixture.

Proceedings, Sardinia 2009, 12th International Waste Management and Landfill Symposium, Environmental Sanitary Engineering Centre (CISA), Cagliari, Italy.

- Heller, H, and Keren, R., (2003). Anionic polyacrylamide polymer adsorption by pyrophyllite and montmorillonite. *Clays and Clay Minerals*, 51(3):334-339.
- Hornsey, W., Schers, J., Gates, W., and Bouazza, A. (2010). The impact of mining solutions/liquors on geosynthetics. *Geotext. Geomembranes*, 28(2), 191-198.
- Jo, H., Katsumi, T., Benson, C., and Edil, T. (2001). Hydraulic conductivity and swelling of non-prehydrated GCLs permeated with single species salt solutions. *J. Geotech. Geoenviron. Eng.*, 127(7), 557-567.
- Jo, H., Benson, C., Shackelford, C., Lee, J., and Edil, T. (2005). Long-term hydraulic conductivity of a non-prehydrated geosynthetic clay liner permeated with inorganic salt solutions. *J. Geotech. Geoenviron. Eng.*, 131(4), 405-417.
- Jo, H., Benson, C., and Edil, T. (2006). Rate-limited cation exchange in thin bentonitic barrier layers. *Can. Geotech. J.*, 43(4), 370-391.
- Jo, H., Benson, C., Shackelford, C., Lee, J., and Edil, T. (2005). Long-term hydraulic conductivity of a non-prehydrated geosynthetic clay liner permeated with inorganic salt solutions. *J. Geotech. Geoenviron. Eng.*, 131(4), 405-417.
- Kolstad, D., Benson, C., and Edil, T. (2004a). Hydraulic conductivity and swell of nonprehydrated GCLs permeated with multi-species inorganic solutions. *J. Geotech. Geoenviron. Eng.*, 130(12), 1236-1249.
- Kolstad, D., Benson, C., Edil, T., and Jo, H. (2004b). Hydraulic conductivity of dense prehydrated GCL permeated with aggressive inorganic solutions. *Geosynth. Int.*, 11(3).

- Katsumi, T., Ishimori, Ho, Onikata, M., and Fukagawa, R. (2008). Long-term barrier performance of modified bentonite materials against sodium and calcium permeant solutions. *Geotext. And Geomembranes* 26(1), 14-30.
- Klenina, O., and Lebedeva, L., (1983). Viscometric properties of dilute solutions of hydrolyzed polyacrylamide. *Polymer Science U.S.S.R.*, Vol. 25 (10): 2380–2389.
- Kim, S., and Palomino, A.M. (2011). Factors influencing the synthesis of tunable clay-polymer nanocomposites using bentonite and polyacrylamide. *Applied Clay Science*, 51: 491-498.
- Kurenkov, V. (1997). Acrylamide Polymers. In: N. P. Cheremisinoff ed. *Handbook of engineering polymeric materials*, Marcel Dekker, New York: 61–72.
- Lee, J., and Shackelford, C. (2005). Impact of bentonite quality on hydraulic conductivity of geosynthetic clay liners. *J. Geotech. Geoenviron. Eng.*, 131(1), 64-77.
- Lage, S., Lindner, P., Sinha, P., Kiriy, A., Stamm, M., and Huber, K. (2009). *Macromolecules*, 42, 4288-4299.
- Levitt, D. B., and Pope, G. A. (2008). In Proceeding of SPE/DOE Symposium on Improved Oil Recovery, Tulsa, Oklahoma, USA, April 20–23.
- Liu, Y., Gates, W., Bouazza, A., and Rowe, K. (2013). Fluid loss as a quick method to evaluate hydraulic conductivity of geosynthetic clay liners under acidic conditions. *Can. Geotech. J.*, 51, 158-163.
- McRory, J., and Ashmawy, A. (2005). Polymer treatment of bentonite clay for contaminant resistant barriers. *GSP 142 Waste Containment and Remediation*, 1-11.

- Moradi, A. A., Cleveland, D. J., Jones, W. W., and Westerman, I. J. (1995). Proceeding of SPE International Symposium on Oilfield Chemistry, San Antonio, Texas, USA, Feb., 14–17.
- Meer, S., and Benson, C. (2007). Hydraulic conductivity of geosynthetic clay liners exhumed from landfill final covers, *J. Geotech. Geoenviron. Eng.*, 133(5): 550-563.
- Onikata, M., Kondo, M., and Kamon, M. (1996). Development and characterization of a multishwellable bentonite. *Environmental Geotechnics*. Taylor and Francis, Rotterdam, 587-590.
- Onikata, M., Kondo, M., Hayashi, N., and Yamanaka, S. (1999). Complex formation of cation-exchanged montmorillonites with propylene carbonate: Osmotic swelling in aqueous electrolyte solutions. *Clays and Clay Miner.* 47(5), 672-677.
- Painter, PC and Coleman, MM. (1997). *Fundamentals of Polymer Science: An Introductory Text*. CRC Press.
- Park, T. G., and Hoffman, A. S. (1992). Synthesis and characterization of pH- and/or temperature-sensitive hydrogels, *Appl. Polym. Sci.*, 46(4), 659-671.
- Petrov, R. J., & Rowe, R. K. (1997). Geosynthetic clay liner (GCL) - chemical compatibility by hydraulic conductivity testing and factors impacting its performance. *Canadian Geotechnical Journal*, 34, 863-885.
- Rashidi, M., Blokhus, A. M., and Skauge, A. (2010). Viscosity study of salt tolerant polymers, *J. Applied Polym. Science*, 117(3), 1551-1557.
- Ray, S. and Okamoto, M. (2003). Polymer/layered silicate nanocomposites: a review from preparation to processing. *Progress in Polymer Science*, Vol. 28, 1539–1641.

- Ruhl, J.L., and Daniel, D.E. (1997). Geosynthetic clay liners permeated with chemical solutions and leachates. *J. Geotech. Geoenviron. Eng.*, Vol. 123(4): 369-381.
- Ruiz-Hitzky, E. and Van Meerbeek, A. (2006). Clay mineral- and organoclay-polymer nanocomposite. In: Bergaya, F., Theng, B.K.G., Lagaly, G. (Eds.), *Handbook of Clay Science*, Developments in Clay Science, Elsevier, Amsterdam, 583–621.
- Rosin-Paumier, S., Touze-Foltz, N., Pantet, A., Monnet, P., Didier, G., Guyonnet D., and Norotte, V. (2010). Swell index, oedopermeametric, filter press and rheometric tests for identifying the qualification of bentonites used in GCLs. *Geosynth. Int.*, 17(1), 1-11.
- Scalia, J., and Benson, C. (2011). Hydraulic conductivity of geosynthetic clay liners exhumed from landfill final covers with composite barriers. *J. Geotech. Geoenviron. Eng.*, 137(1), 1-13.
- Scalia, J., Benson, C., Bohnhoff, G., Edil, T., and Shackelford, C. (2014). Long-term hydraulic conductivity of a bentonite-polymer composite permeated with aggressive inorganic solutions. *J. Geotech. Geoenviron. Eng.*, 140(3), 1-13.
- Scalia, J., and Benson, C. (2014). Barrier Performance of Bentonite-Polyacrylate Nanocomposite to Artificial Ocean Water. *Proceedings, Geo-Congress 2014 Geo-Characterization and Modeling for Sustainability*, GSP No. 234, ASCE, Reston, VA.
- Scalia, J., Bohnhoff, G., Shackelford, C., Benson, C., Sample-Lord, K., Malusis, M., and Likos, W. (2018). Enhanced Bentonites for Containment of Inorganic Waste Leachates by GCLs. In review.

- Schweins, R., Lindner, P., and Huber, K. (2003). Calcium Induced Shrinking of Napa Chains: A SANS Investigation of Single Chain Behavior. *Macromolecules*, Vol. 36 (25).
- Shackelford, C., Benson, C., Katsumi, T., Edil, T., and Lin, L. (2000). Evaluating the Hydraulic Conductivity of GCLs Permeated with Non-standard Liquids. *Geotextiles and Geomembranes*, 18(2-4), 133-162.
- Swann, J., Bras, W., Topham, P., Howse, J. and Ryan, A. (2010). Effect of the Hofmeister anions upon the swelling of a self-assembled pH-responsive hydrogel. *Langmuir*, 26(12).
- Taylor, K. C., and Nasr-El-Din, H. A. (1995). *In Proceeding of SPE International Symposium on Oilfield Chemistry*, San Antonio, Texas, USA, Feb 14–17.
- Theng, B. (2012). *Formation and properties of clay-polymer complexes*. Elsevier.
- Trauger R., and Darlington J. (2000). Next-generation geosynthetic clay liners for improved durability and performance. *TR-220*. Colloid Environmental Technologies Company, Arlington Heights, 2-14.
- Tian, K., Benson, C., and Likos, W. (2016). Hydraulic Conductivity of Geosynthetic Clay Liners to Low-Level Radioactive Waste Leachate, *J J. Geotech. Geoenviron. Eng.*, 142(8).
- Tian, K, Likos, W., and Benson, C. (2018). Polymer Elution and Hydraulic Conductivity of Bentonite-Polymer Composite Geosynthetic Clay Liners. *J. Geotech. Geoenviron. Eng.*, in review.

Zhang, Q., Zhou, J., Zhai, Y., Liu, F., and Gao, G. (2008). Effect of salt solutions on chain structure of partially hydrolyzed polyacrylamide, *J. Cent. South Univ. Technol.*, 15(s1): 080–083.

3.7 TABLES

Table 3.1. Properties of chemical solutions used in the study

Type of Solution		Concentration [mM]	I [mM]	RMD [$M^{1/2}$]	pH [-]	EC [S/m]	
Deionized water		0	0	0	7	0	
Single-species salt	Na ₂ CO ₃	150	450	-	11.41	18.6	
	NaOH	300	300	-	13.16	55.4	
	NaNO ₃	300	300	-	7.27	24.2	
	NaF	300	300	-	7.45	20	
	NaI	300	300	-	6.27	26.4	
	NaCl	150	150	-	-	-	
		300	300	-	5.67	-	
		1000	1000	-	-	-	
	KCl	150	150	-	-	-	
		300	300	-	5.51	-	
	Na ₂ SO ₄	50	150	-	-	-	
		100	300	-	-	-	
		150	450	-	6.57	-	
	K ₂ SO ₄	50	150	-	-	-	
		100	300	-	-	-	
		150	450	-	5.90	-	
	CaCl ₂	300	900	-	-	-	
		20	60	-	-	-	
		50	150	-	6.85	8.85	
		100	300	-	-	-	
200		600	-	-	-		
MgSO ₄	300	900	-	-	-		
	500	1500	-	-	-		
	100	400	-	-	-		
Multi-Species Salt, (Anion Ratio)	[Na]=300 mM, Cl ⁻ /SO ₄ ²⁻	0.01	-	450	-	6.57	20.2
		1	-	400	-	6.43	22.1
		5	-	343	-	6.14	24.4
		20	-	313.6	-	5.85	25.5
	[K]=300 mM, Cl ⁻ /SO ₄ ²⁻	100	-	300	-	5.67	-
		0.01	-	450	-	5.90	25.4
		1	-	400	-	5.68	27.5
		5	-	343	-	5.71	30.2
	20	-	313.6	-	5.45	30.8	
	100	-	300	-	5.51	32.7	
EPRI leachates	Typ CCP	-	40	0.16	8.0	2.10	
	Low RMD	-	48	0.01	8.0	2.15	
	High Str	-	178	1.00	8.0	-	
	FGD	-	97	0.39	8.0	4.87	
	Trona	-	755	4.40	11.0	41.3	
Site specific leachates	Gold PLS	-	13	0.21	7.9	0.29	
	MSW I	-	1042	0.87	6.6	17.0	
	CCP-1	-	179	0.26	8.2	11.1	
	CCP-2	-	370	0.12	5.7	2.59	
	CCP-3	-	975	1.86	7.9	15.3	

2.8 FIGURES

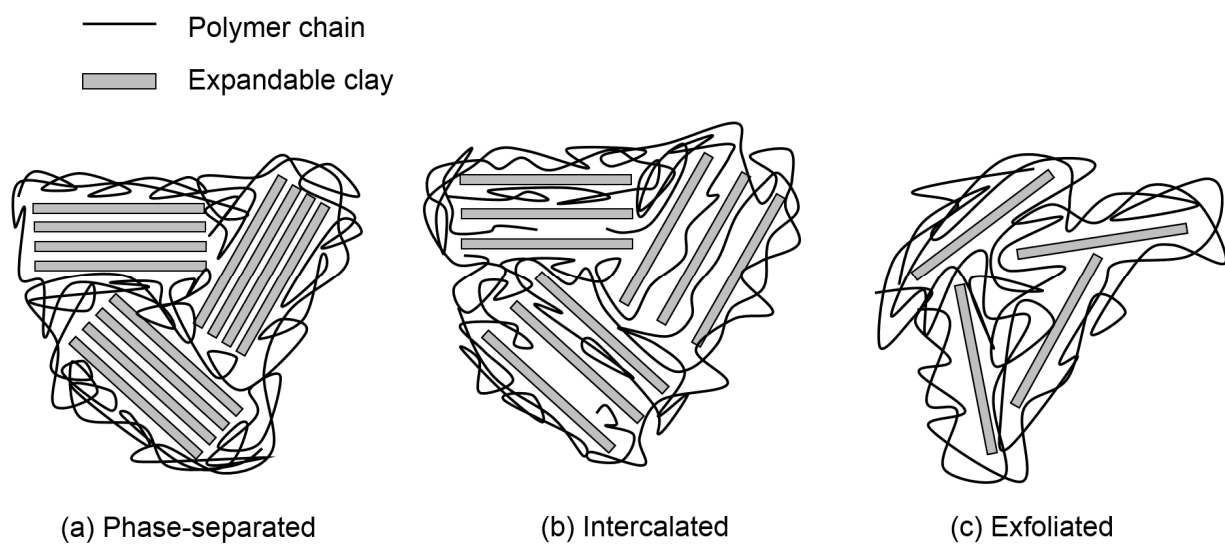


Figure 3.1. Conceptual illustration of polymer-clay interactions in composite forms (adapted from Kim and Palomino 2011).

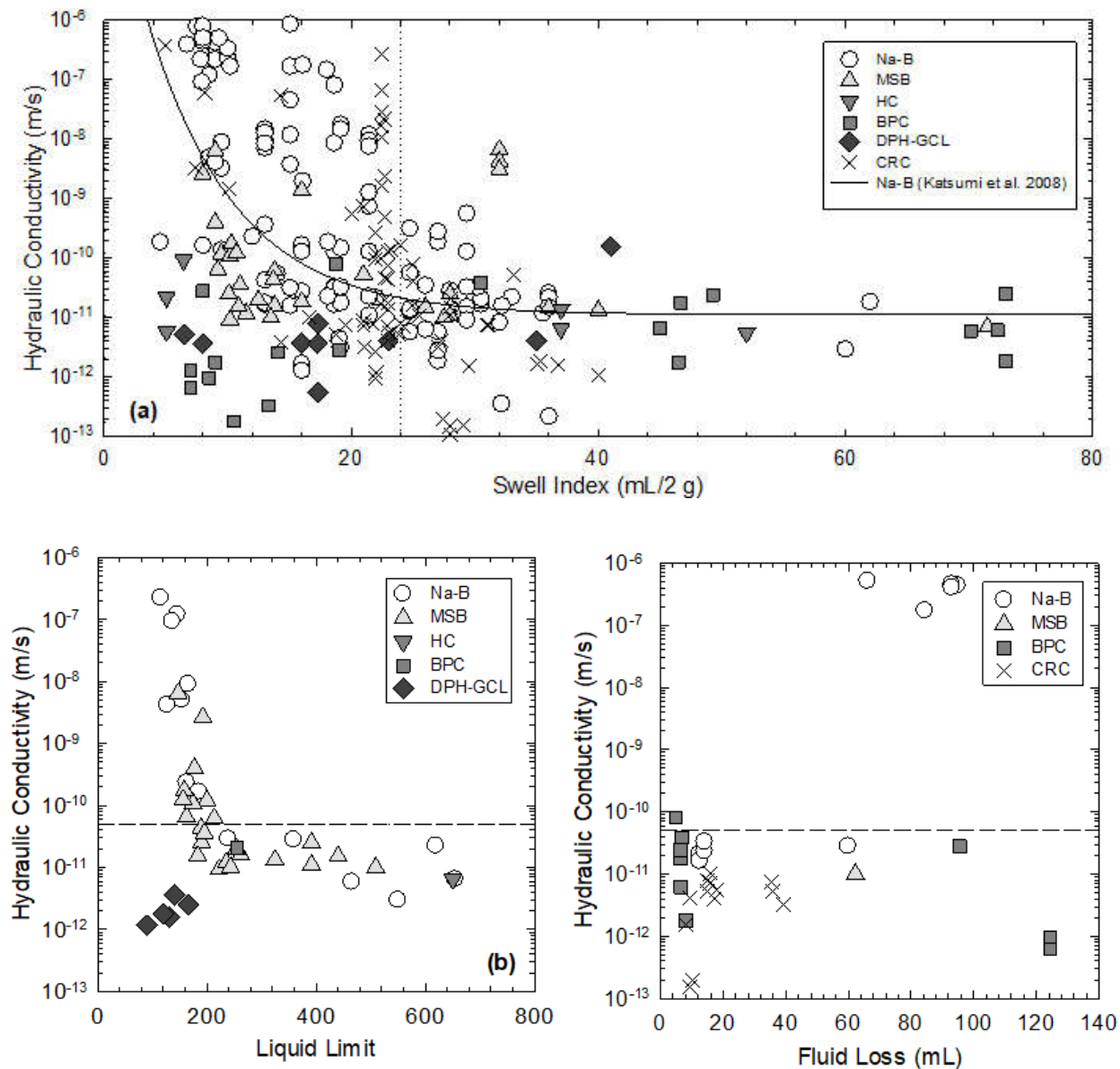


Figure 3.2. Relations between hydraulic conductivity and (a) swell index, (b) liquid limit, and (c) fluid loss compiled for enhanced bentonites and sodium bentonite (Na-B) from the literature. Enhanced bentonites include Multiswellable Bentonite (MSB) (Onikata et al. 1996), Hyper Clay (HC) (Di Emidio et al. 2010, 2011), Bentonite-polyacrylic-acid composite (BPC) (Scalia et al. 2014), dense prehydrated GCL (DPH-GCL) (Kolstad et al. 2004), and contaminant resistant clay (CRC) as defined and compiled by Scalia et al. (2018).

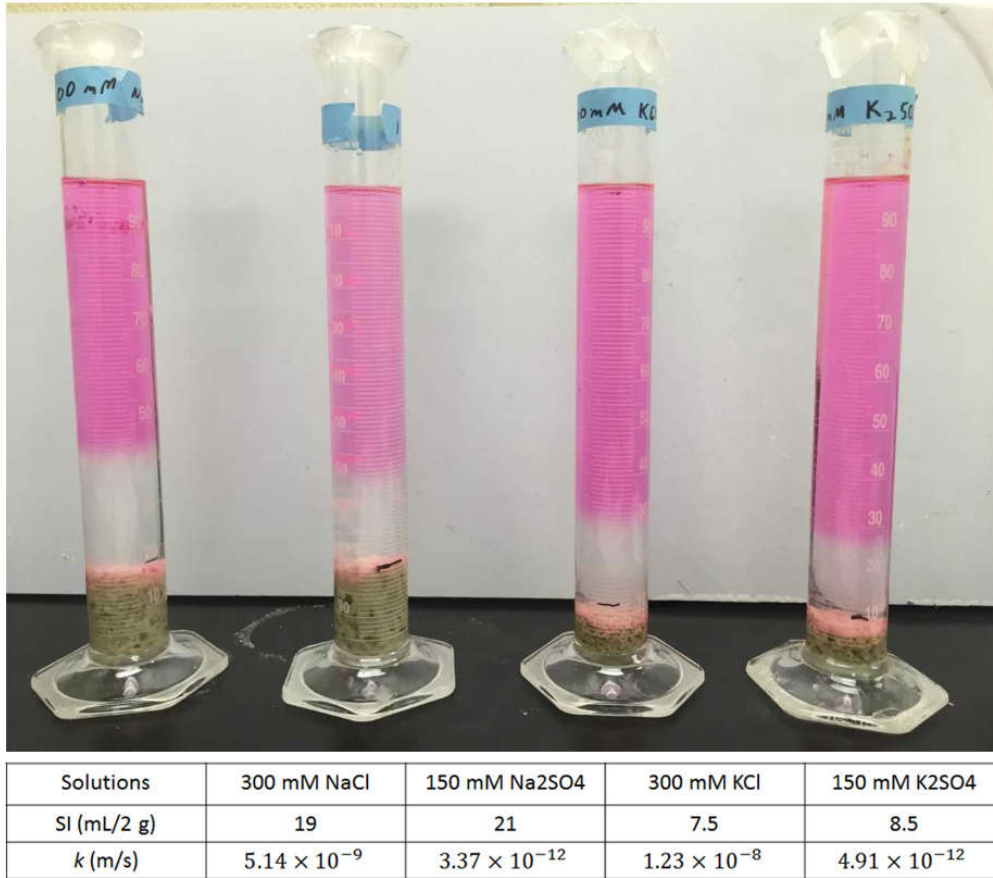


Figure 3.3. Swell index tests for polymer modified bentonite in salt solutions. Rhodamine WT dye (pink color) indicates a boundary between free solution and solution containing polymer dissociated from the bentonite.

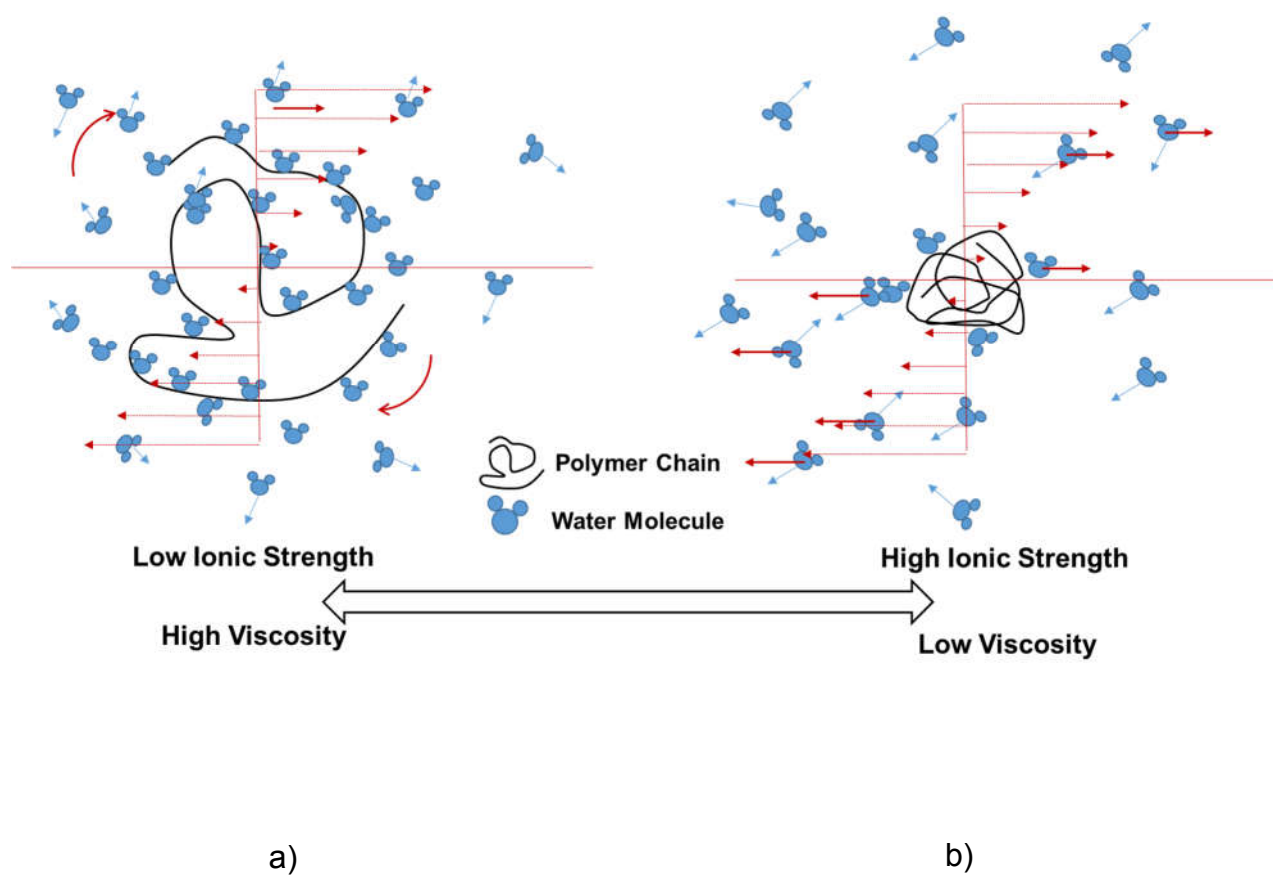


Figure 3.4. Conceptual illustrations of (a) extended polymer conformation resulting in high viscosity and (b) coiled polymer conformation resulting in low viscosity.

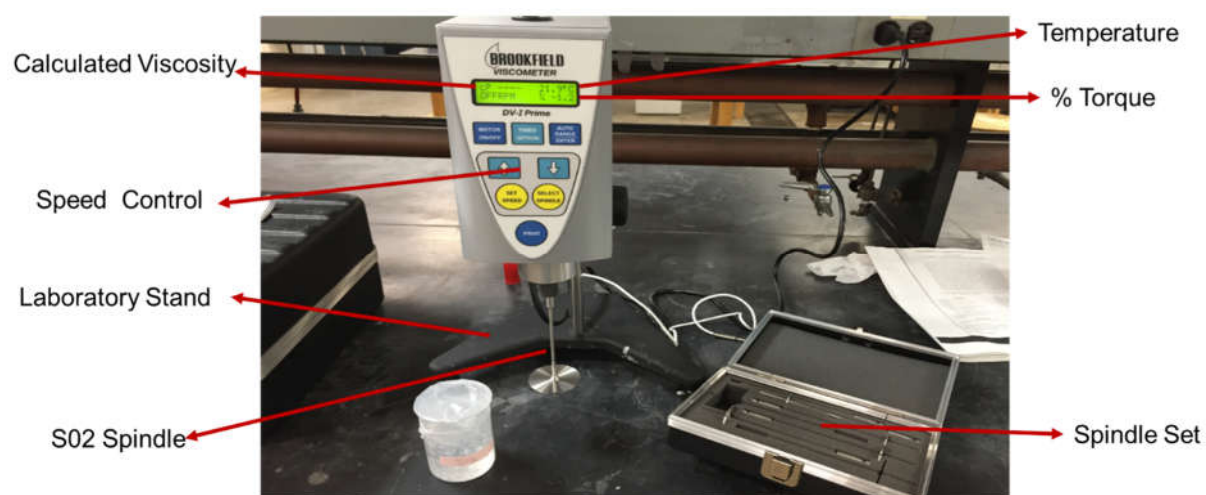


Figure 3.5. Brookfield DV-I PRIME Viscometer (Middleboro, MA) and spindle set.

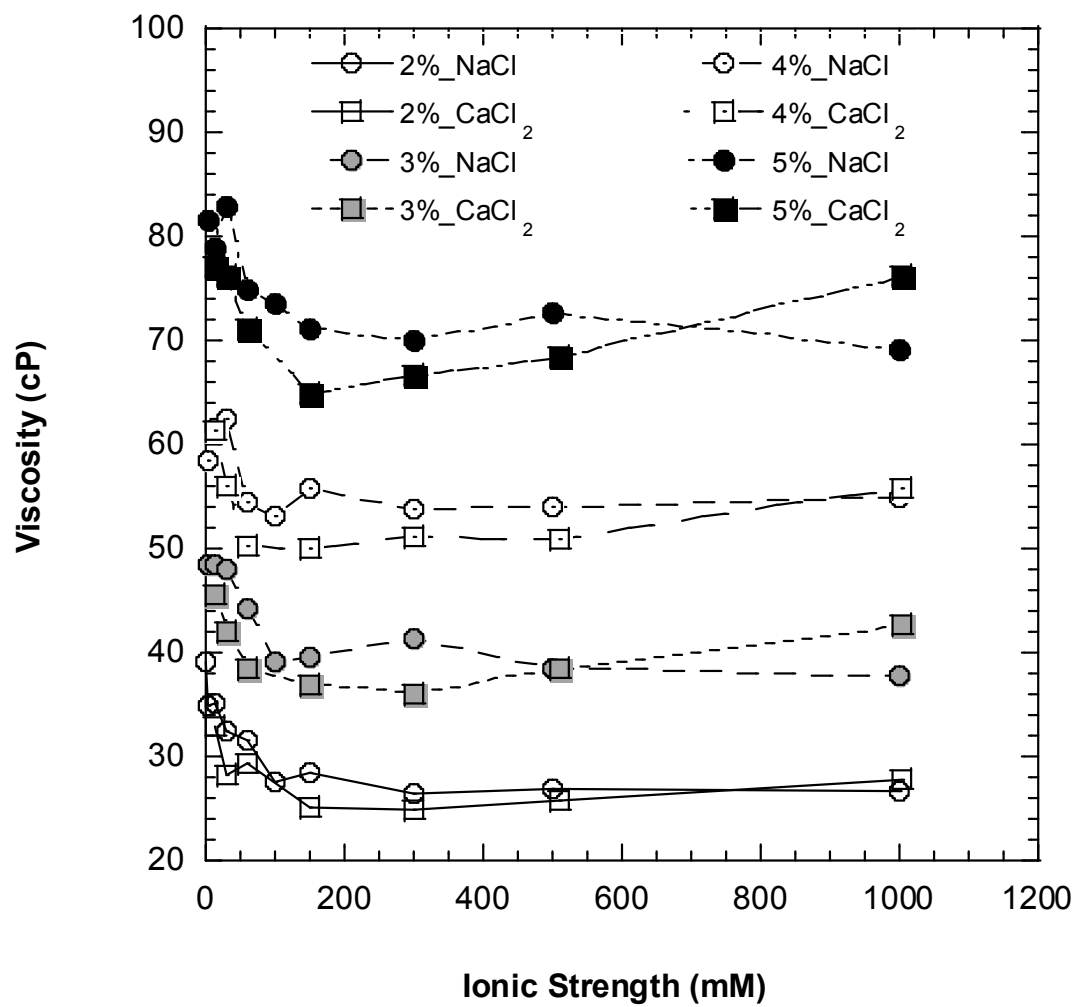


Figure 3.6. Viscosity versus ionic strength for polymer suspensions in NaCl and CaCl₂. Polymer concentrations vary from 2% to 5% by mass.

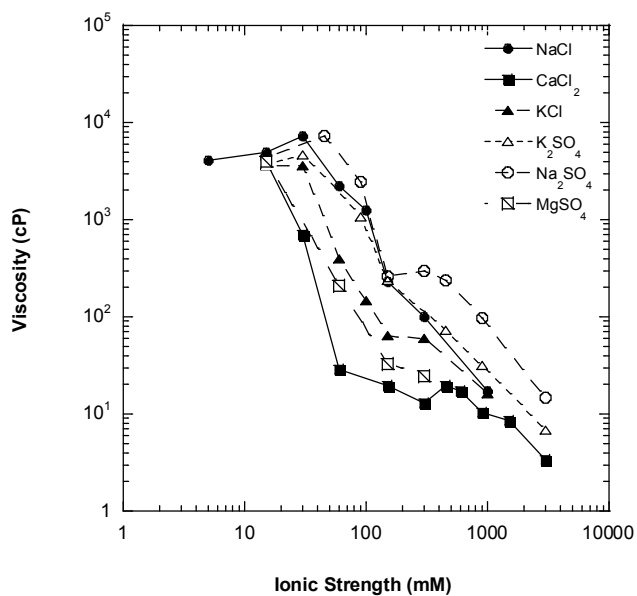
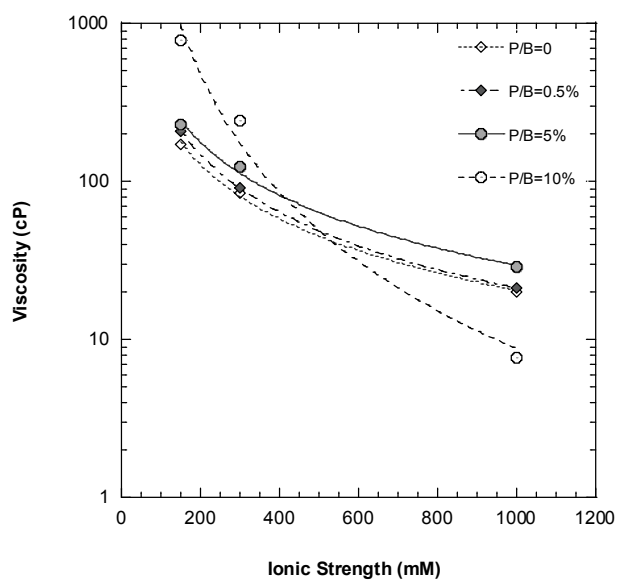


Figure 3.7. Viscosity of polymer (PAM)-bentonite suspensions (total solid-liquid ratio of 10%), in (a) NaCl at P/B (polymer-to-bentonite ratio) ranging from 0 to 10%, (b) in various salt solutions at P/B = 5%.

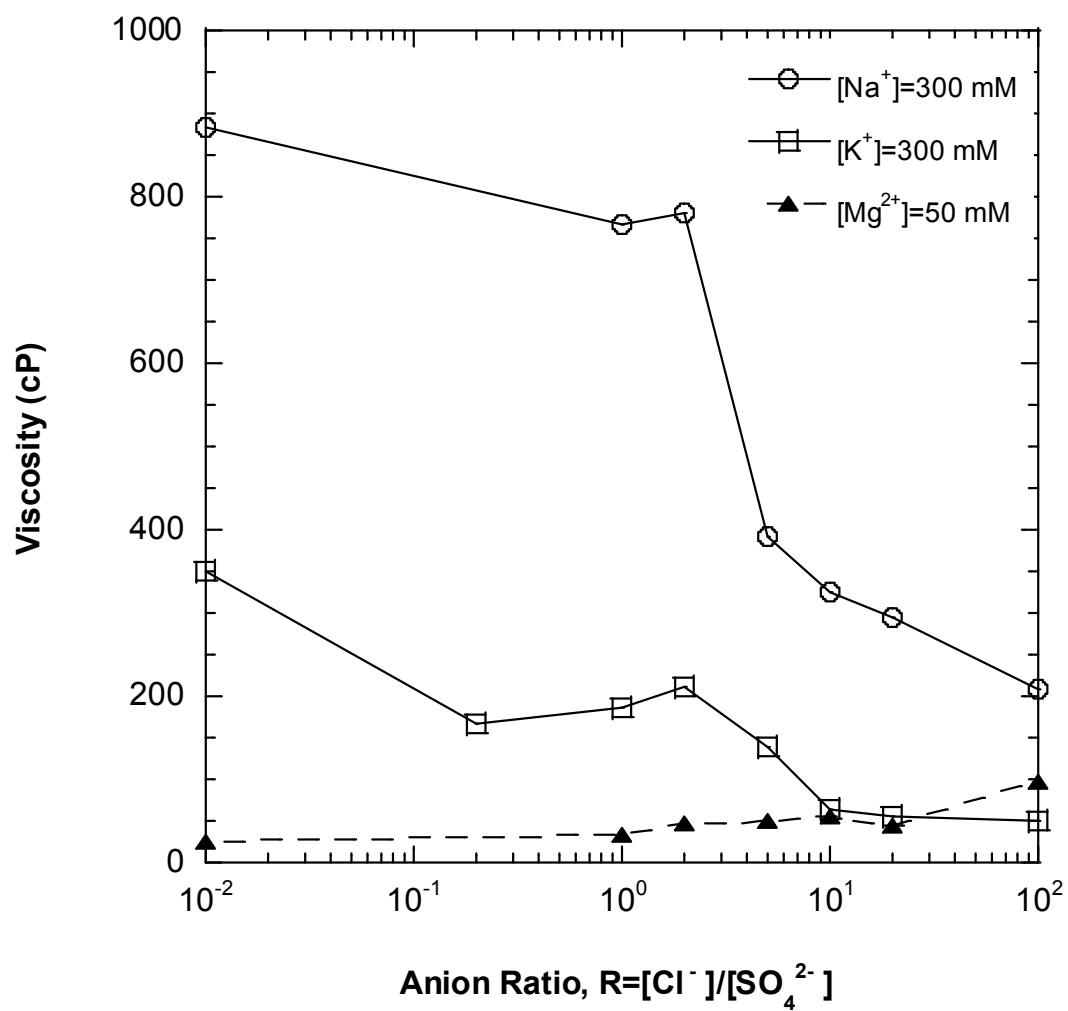


Figure 3.8. Viscosity of polymer-bentonite mixture in 300 mM K⁺ and Na⁺ solutions, and 50 mM Mg²⁺ solutions as a function of anion ratio ($R = \text{molar concentration ratio of Cl}^- \text{ to SO}_4^{2-}$).

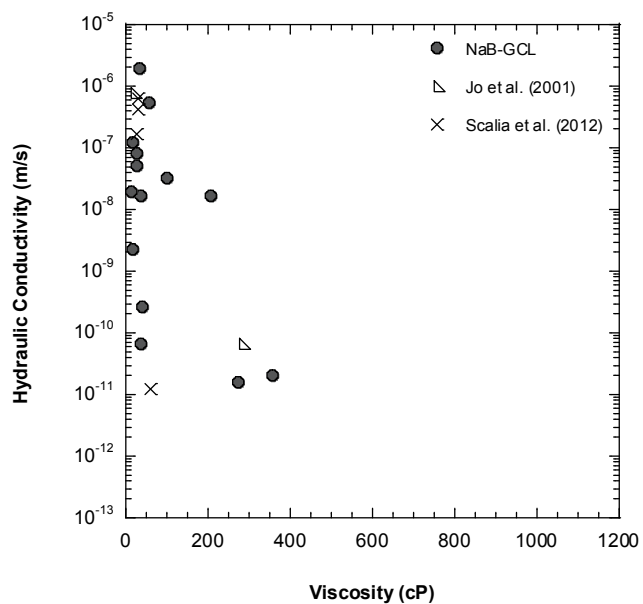
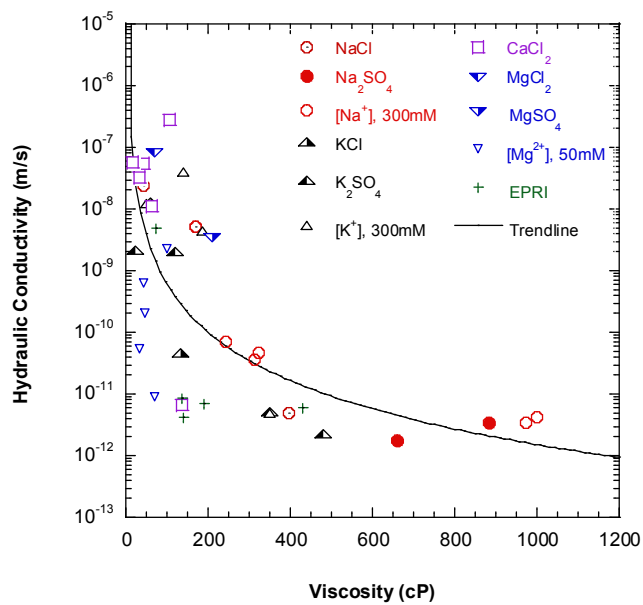


Figure 3.9. Hydraulic conductivity versus viscosity: (a) PMB-GCLa and PMB suspensions, (b) NaB-GCLs and NaB suspensions.

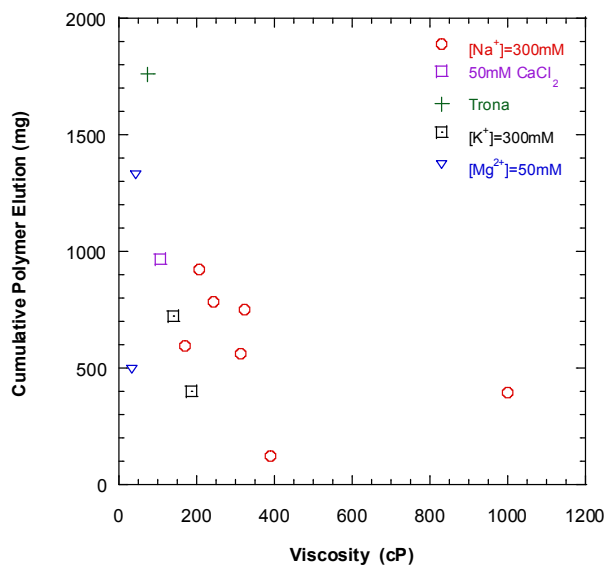
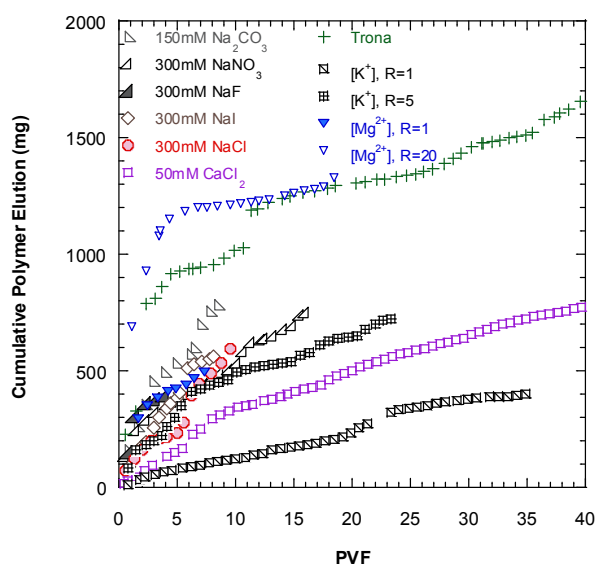


Figure 3.10. (a) Cumulative polymer elution as function of pore volumes of flow (PVF) for PMB-GCLs, and (b) Steady state polymer elution versus viscosity of PMB suspensions.

CHAPTER 4

TURBIDITY AND MODIFIED WATER CONTENT OF POLYMER-MODIFIED BENTONITE

ABSTRACT

The conformation (shape and structure) of polymer chains in solution is sensitive to environmental conditions such as pH, ionic strength, temperature, electrical potential, and photo-irradiation. Low pH and/or high ionic strength generally result in a coiled polymer conformation, whereas high pH and/or low ionic strength generally result in an extended polymer conformation that forms a well-developed polymer gel upon swelling. Polymer in PMBs ideally forms a hydrogel upon exposure to aqueous solution, clogs bentonite macropores, and results in low hydraulic conductivity of PMB GCLs. Turbidity measurements were conducted to qualitatively evaluate polymer conformation and hydrogel formation in aqueous solutions. Turbidity of polymer suspensions is influenced by solution chemistry and generally decreases with increasing ionic strength. Solutions rich in SO_4^{2-} rather than Cl^- have a thickening effect by forming strong polymer gels and increase the turbidity of polymer suspensions through more polymer-solvent interaction. A modified water content test developed to quantify the water-holding capacity for PMBs is correlated to the turbidity in solutions where Na-B exhibits comparable swelling. High modified water content of PMB in test solutions systematically correlates to lower hydraulic conductivity of PMB-GCLs permeated with the same solutions. A threshold modified water content value of 230% is required for achieving hydraulic conductivity lower than 10^{-10} m/s for the PMB-GCL evaluated in this study.

4.1 INTRODUCTION

Geosynthetic Clay Liners (GCLs) are comprised of a layer of sodium bentonite (Na-B) with a thickness of 7-10 mm, sandwiched between two geotextiles. Because of the pronounced swelling nature of sodium bentonite, GCLs have been used as effective barriers in some containment applications, especially with solutions of low ionic strength (I) (Shackelford et al. 2000, Jo et al. 2004, Bradshaw and Benson 2014) but are less effective in aggressive leachates (e.g. high I , low RMD, extreme pH). Demand for chemically resistant GCLs has promoted development of a variety of enhanced bentonite (EB) GCLs (Lin et al. 2000, Trauger and Darlington 2000, Ashmawy et al. 2002, Kolstad et al. 2004, McRory and Ashmawy 2005, Katsumi et al. 2008, Benson et al. 2010, Di Emidio et al. 2011, Scalia et al. 2011, Benson et al. 2013, Scalia and Benson 2014, Scalia et al. 2014), where the bentonite is chemically modified, blended, or intercalated with organic molecules or polymers. EB-GCLs, notably including GCLs containing polymer modified bentonite (PMB), increasingly are being adopted in practice to contain aggressive leachates (Scalia et al. 2018).

A primary difference among various types of PMB is in the polymer-bentonite phase form, as illustrated in chapter 3 (Fig.3.1). The phase-separated (e.g., dry blended) form is advantageous in many regards because of the relatively low cost. Previous studies involving analysis of total organic carbon (TOC) to quantify elution of polymer in effluent solution from hydraulic conductivity tests and scanning electron microscopy (SEM) to observe pore-scale interactions between bentonite and polymer suggest that clogging of macropores by polymer hydrogel is a predominant mechanism for maintaining low hydraulic conductivity of phase-separated PMB (e.g., Tian et al., 2018). Polymer

conformation, the quality of polymer hydrogel developed in the bentonite pores, and bonding or interaction between the polymer and bentonite fractions are hypothesized to be essential factors that influence corresponding hydraulic behavior.

This study provides a qualitative evaluation of polymer conformation and the quality of polymer hydrogel formation via measurements of turbidity of polymers and polymer-bentonite mixtures in suspension. A modified water content test is developed for evaluating the water-holding capacity of PMB and potential correlation to the hydraulic conductivity of PMB-GCLs.

4.2 BACKGROUND

4.2.1. Polymer Conformation and Polymer Swelling

Polymers are formed by linking together monomer molecules through chemical reactions (polymerization) and results in different types of skeletal structures. The variations in skeletal structure give rise to major differences in polymer properties. Fig.4.1 shows three common polymer skeletal structures (Young and Lovell, 2011). Fig.4.1a represents a linear skeletal structure as a chain with two ends. Fig.4.1b represents a branched polymer with side chains bonded to the main chain by junction points. Networked polymers (Fig.4.1c) are similar to branched polymers but have three dimensional structure characterized by crosslink density defined as the number of junction points per unit volume.

Polymerization alters the variations in skeletal structure and creates distinctive properties because of the polymer conformation. For example, a linear type polymer has two conformations upon swelling under the different environmental conditions (extended

vs. coiled), where an extended polymer chain indicates more polymer-solvent interaction and a coiled polymer chain indicates more polymer-polymer interaction (Fig.4.1-a-2 and Fig.4.1-a-3). Similar to a linear polymer, a branched polymer swells in good solvent (e.g. low I) and shrinks in poor solvent (e.g. high I), as shown in Fig.4.1-b-2 and Fig.4.1-b-3. Unlike linear and branched polymers, networked polymers will not dissolve in inorganic solvent, although they may have considerable swelling in compatible solvents. Networked polymers tend to bond water and swell to form a thick polymer gel in good solvents (Fig.4.1-c-2) and forms a globule structure because of the collapsed structure in poor solvent (Fig.4.1-c-3). Differences in polymer conformation determine macroscopic behaviors of polymer suspensions and potentially affect the macro-engineering behavior of PMB.

4.2.2. Precipitation and Turbidity of Polymer Suspensions

Since networked polymer cannot dissolve in inorganic solution, polymer aggregates will form in suspension. The degree of polymer collapse depends on the chemistry of the inorganic solution. The stability of a polymer suspension is related to polymer-solvent interaction, which is also a function of solvent chemistry. Fig.4.2, for example, shows a series of photographs for a 0.5% networked polymer suspension in deionized (DI) water and 50 mM CaCl_2 at different moments time points after initial agitation to produce a homogeneous polymer suspension. In DI water, the suspended polymers distribute homogeneously in clear solution, and do not precipitate (by observation) over time (for $t = 24\text{hr}$). Suspended polymer coils may be observed as an opaque solution in 50 mM CaCl_2 , indicating that a significant amount of precipitation

occurs within 30 mins. The former solvent (DI water) is considered an example of a good solvent, while the latter (CaCl_2) is considered a poor solvent for this type of polymer.

Turbidity measures the relative clarity of a solution or suspension. Turbidity is an optical characteristic of a liquid since it reflects the amount of light that is scattered by suspended material in liquid. In this study, turbidity is adopted to qualitatively measure the conformation and quality of polymer gel. The conceptual illustration shown as Fig. 4.3 (based on the observations on Fig.4.2) relates turbidity to these properties by hypothesizing that polymer forms aggregates with relatively large hydrodynamic radius due to strong polymer-solvent interaction in good solvent and maintains an effective network connection over time. High turbidity is expected to be measured over time due to the stable polymer structure in this case. In contrast, broken polymer chains containing small coils and contracted globules would be presented in poor solvent, resulting a weak network connection. Turbidity in this case may be initially high, but decreases over time as the polymer globules settle to bottom of the containment vessel. In a suspension where precipitation occurs, the difference in turbidity at different times can be related to the degree of polymer precipitation.

4.2.3. Modified Water Content (Rationale)

A water content measurement that quantifies that amount of water contained in PMB is hypothesized to be related to the hydraulic conductivity of PMB-GCLs. Specifically, a polymer-bentonite mixture with well-developed polymer hydrogel and significant bentonite swelling is expected to have high water content relative to a polymer-bentonite mixture with contracted polymer coils and limited bentonite swelling. Therefore,

a potential link between hydraulic conductivity of PMB-GCL permeated with a particular solution and a systematically measured water content of PMB in that solution can potentially be established, as the corresponding hydraulic conductivity of PMB-GCL is expected to be relatively low and relatively high in the former and latter case, respectively.

4.3 MATERIALS AND METHODS

4.3.1. Polymer and Polymer Modified Bentonite

The polymer used in this study is a proprietary networked polymer (Fig. 4.1 c). It was estimated by comparing Fourier transform infrared (FTIR) spectra with a commercial available PAM (Polysciences Inc., Warrington, PA, USA, Cat. No. 04652), shown in Fig.2.3, and is believed belongs to a PAM-based network polymer due to the exhibition of high similarity in spectroscopy.

The PMB used in this study is extracted from the PMB-GCL (Table 1.1) containing a blend of granular Na-B and this proprietary network polymer. Polymer loading was quantified to be 5.1% by loss on ignition (LOI) conducted according to ASTM D7348 accounting for loss of strongly bound water molecules, calcite, and organic matter associated with the bentonite fraction (Scalia et al., 2014; Tian et al., 2016). Quantitative X-ray diffraction (XRD) analysis showed that the PMB contained 79% montmorillonite, along with measureable quantities of quartz, feldspar and mica (Chen et al. 2015).

4.3.2. Turbidity Measurement

Turbidity of networked polymer and polymer-bentonite suspensions were measured using a Hach 2100N Laboratory Turbidity Meter (Cole-Parmer), as shown in

Fig.4.5. This benchtop turbidity meter provides results over a range from 0 to 4000 nephelometric turbidity units (NTU) in accordance with EPA method 180.1. Turbidity readings were taken at different increments in time ($t= 0$ to 15 mins) after initial mixing. Polymer suspensions were prepared with solution in a centrifuge tube placed on an end-over-end shaker (Fig.4.5) for mixing at polymer-to-liquid concentration of 0.5% without any physical forces (e.g. stirring) exerted. The suspensions were generally mixed for 48 hours and mixing was considered complete when uniform suspensions were achieved by visual observation. Turbidity measurements were performed immediately after removal from the end-over-end shaker at room temperature.

4.3.3. Modified Water Content Measurement

Modified water content tests were conducted on PMB extracted from the PMB-GCL. The mixture was mixed with permeant solutions at solid-to-liquid ratio of 10%. The polymer bentonite slurries were centrifuged at 10,000 rpm for 20 min to separate the solid from the liquid after being mixed in an end-over-end shaker for 48 hrs. Dye was then added to the centrifuged solution from the top surface of the containment vessel and allowed to rest for another 48 hrs such that the dye could freely penetrate the solution. As shown in Fig.4.6a, the bentonite and the polymer would partially separate and settle in the bottle of the centrifuge tube as 'solid' part, in the form of a layer of strongly bonded polymers adsorbed on top of the 'solid'. If presence of polymer in the liquid inhibits diffusion of the dye, then additional polymer in the form of weak polymer gels may be assumed to exist as the 'clear liquid-like' part, whereas the 'dyed liquid' may be assumed to primarily contain test solution with minimal polymer present. To obtain a modified water content value, therefore, the dyed part was decanted and the centrifuge tube was set

upside down on a filter paper for 2 hrs to remove the 'clear liquid-like' part, as shown in Fig. 4.6b. The remaining material was removed from the centrifuge tube and its water content was measured following ASTM D2216.

4.3.4. Hydraulic Conductivity Measurement

Hydraulic conductivity tests were conducted for 15.24-centimeter-diameter GCL specimens according to ASTM D6766 using falling headwater flexible-wall permeameters. Effective confining stress was maintained at 20 kPa during permeation. An average hydraulic gradient of 190 was applied for all tests. Influent permeant solution was contained in 50-mL graduated glass pipettes. Effluent was collected in 60-mL polyethylene bottles. Electrical conductivity (EC), pH, and cation concentration of the effluent were measured periodically to assess chemical equilibrium. The burettes and bottles were covered with parafilm to minimize evaporation and atmospheric interaction. GCL specimens were prepared by cutting a circular sample directly from a roll provided by the manufacturer using a razor knife and steel ring following the procedures in Jo *et al.* (2001). Paste prepared with PMB and permeant solution was placed around the perimeter of the specimen to prevent loss of the mixture during handling and preferential flow along the edge during permeation. Initial thickness of each GCL specimen was measured with calipers at six equidistant points. Hydraulic equilibrium was defined as steady hydraulic conductivity for three consecutive measurements with ratio of incremental volumetric outflow to inflow (flow ratio) within 1.00 ± 0.25 . Chemical equilibrium was assumed when the ratio of effluent to influent electrical conductivity (EC_{out}/EC_{in}) and effluent to influent pH (pH_{out}/pH_{in}) were steady and within 1.0 ± 0.1 .

4.4 RESULTS AND DISCUSSION

4.4.1. Turbidity of Polymer Suspensions

Fig.4.7 is a plot of turbidity results recorded over time ($t = 0$ min to $t = 15$ min) for this networked polymer suspensions in DI water and 50mM CaCl_2 . For DI water, turbidity gradually increases within the initial 3 mins from 250 NTU to 350 NTU and levels off. This is interpreted to indicate formation of a stable network structure. The initial formation of polymer hydrogel contributes to the initial change in turbidity and becomes stable over time. The polymer suspension in 50 mM CaCl_2 has high measured turbidity within the first 3 mins, which is interpreted to indicate that polymer coils and globules are distributed evenly in the solution. The turbidity then decreases rapidly within the next 3 mins as polymer globules precipitate and settle, and continues to decrease over the time.

Fig.4.8 plots average turbidity (average value over time) for polymer suspensions versus ionic strength in four single-species salt solutions (NaCl , Na_2SO_4 , CaCl_2 , and MgSO_4) that are common components in industrial leachates. A general decrease of average turbidity is observed with increasing ionic strength. High turbidity in dilute solution indicates the formation of a thick polymer gel (strong polymer-solvent interaction), where the polymer swells and exhibits a well-developed network structure. The decrease in turbidity with increasing ionic strength suggests the polymer gel becomes thinner and more intramolecular interaction (polymer-polymer) occurs. At given I , average turbidity follows a trend (turbidity from high to low): $\text{Na}_2\text{SO}_4 > \text{MgSO}_4 \approx \text{NaCl} > \text{CaCl}_2$ (little difference was observed for suspensions with NaCl and with MgSO_4). Results indicate that solutions containing divalent cations promote coiled conformation and that solutions

containing SO_4^{2-} have a thickening effect in forming strong polymer gels in comparison to solutions containing Cl^- .

Turbidity was measured for networked polymer suspensions in solutions containing a range of relative SO_4^{2-} and Cl^- concentrations (Table 3.1). Anion ratio (R) was defined as the molar ratio of Cl^- to SO_4^{2-} for a consistent cation concentration. Fig. 4.9 plots turbidity of polymer suspensions for the range of anion ratios and three cation solutions ($[\text{Na}] = 300\text{mM}$, $[\text{K}] = 300\text{ mM}$ and $[\text{Mg}] = 50\text{ mM}$) and five synthesized EPRI leachates. The EPRI solutions are synthesized coal combustion product (CCP) leachates selected from a CCP leachate database to represent a range of conditions encountered in CCP disposal facilities throughout the USA (EPRI 2006 and 2009). Error bars in Fig. 4.9 represent the standard deviation of measured turbidity at different time points, and is treated as an indicator of the degree of polymer precipitation (i.e., larger error bars indicate more change in turbidity with time and corresponding higher degree of polymer precipitation). In monovalent cation solutions (Na and K), turbidity decreases as anion ratio increases with minimal error bars. This indicates that SO_4^{2-} rich solutions promote more polymer hydrogel formation relative to Cl^- rich solutions. Polymer precipitation is limited in monovalent cation solutions regardless of anion type, suggesting a stable network structure for the monovalent cation solutions relative to the divalent cation solutions. Overall turbidity is higher in the Mg solutions than in monovalent cation solutions and exhibits relatively large error bars, suggesting that the divalent cation tends to promote polymer aggregation (and corresponding time-dependent settling). Average turbidity generally increases with increasing anion ratio. This trend can be interpreted to indicate that the coiling effect caused by Mg overwhelms the 'thinning' effect caused by

Cl⁻. Although the Cl⁻ tends to make the polymer gel thinner, the Mg has a more pronounced effect toward polymer conformation and dominate the overall quality of the polymer gel. No clear trend was observed in the turbidity of polymer suspensions with the EPRI leachates. This may attributed to the non homoionic composition as multiple cations and anions are presented in these leachates.

4.4.2. Turbidity of Polymer Suspensions and Modified Water Content of PMB

Modified water content of PMB versus average turbidity of polymer suspension is plotted in Fig.4.10. Modified water content generally increases with increasing turbidity. The rate of increase is the highest with Na and less so with K and divalent cations. This is interpreted to reflect osmotic swelling of the bentonite, which occurs in the Na solutions, such that the bentonite fraction of the PMB retains significant water. Since the modified water content includes the water-holding capacity of both the bentonite and polymer fraction, its value would be affected either by polymer swelling, which can be indicated by average turbidity as Na does not precipitate polymers, or by bentonite swelling. In K and divalent cation solutions, constrained swelling of bentonite reduces the water-holding capacity of bentonite. Thus, when the polymer suspension exhibits a similar average turbidity value, where the amount of polymer swelling is considered comparable, the modified water content is smaller than that in Na solution. The scattered points can be attributed to the polymer precipitation effect caused by divalent cations. The trend is more scattered with the EPRI leachates due to the more complex ion composition.

4.4.3. Modified Water Content and Hydraulic Conductivity of PMB-GCL

Modified water content results for PMB obtained directly from the PMB GCL at a solid-to-liquid ratio of 10% (by dry mass) and hydraulic conductivity tests conducted for intact PMB-GCLs to the same permeant solutions are plotted on Fig.4.11. While there is scatter in the relation, a trend line fits the data set in the following form:

$$k = 0.2855w^{-4}$$

where k is hydraulic conductivity (m/s) and w is modified water content (%). A threshold value of 230% corresponds to nominally “low” hydraulic conductivity ($< 10^{-10}$ cm/s). That is, to maintain a low hydraulic conductivity of PMB-GCL, the modified water content of PMB needs to be greater than 230%. Duplicate tests yielded values consistent with this threshold, shown as the standard deviation in the error bar. For PMB exhibiting high modified water content, as conceptually illustrated in Fig.4.4, both the bentonite and polymer fraction swell and maintain a well-developed network structure with stronger water holding capacity. The polymer is likely to remain in the system rather than being eluted out during permeation, forcing fluid flow to follow a more tortuous path and resulting in low hydraulic conductivity. For PMBs that exhibit low modified water content, the bentonite has limited swelling and the polymer forms contracted globules in poor solution. The polymer is likely more mobile under flowing conditions and the corresponding hydraulic conductivity of the GCL is nominally high.

4.5 SUMMARY AND CONCLUSIONS

This study employed turbidity measurements to evaluate polymer suspensions for a networked polymer in aqueous solutions. A modified water content method was developed as an index test for assessing the hydraulic conductivity of PMB-GCL

containing this networked polymer. The following conclusions can be drawn based on the findings of this study:

- Turbidity can potentially be used to evaluate polymer conformation and the quality of polymer hydrogel formation. A high and time-independent turbidity value is obtained for a polymer suspension in good solution. A low and time-dependent turbidity value is obtained for a polymer suspension in poor solution.
- Divalent cations tend to promote a coiled polymer conformation and precipitate polymers.
- Solutions rich in SO_4^{2-} anions have a thickening effect by forming strong polymer hydrogels. Solutions rich in Cl^- anions have a thinning effect.
- The effects of cation valence on polymer hydrogel formation supersede the effects of anion ratio.
- A modified water content test methods can be used to quantitatively asses the water-holding capacity of both polymer and bentonite.
- A link is established between the modified water content of PMB and the hydraulic conductivity of PMB-GCL permeated with the same solution. A threshold value of 230% of PMB corresponds to nominally low hydraulic conductivity ($<10^{-10}$ m/s).

4.6 REFERENCES

- Ashmawy, A., Darwish, E., Sotelo, N., and Muhammad, N. (2002). Hydraulic performance of untreated and polymer-treated bentonite in inorganic landfill leachates. *Clays and Clay Miner.*, 50(5), 546-552.
- Benson, C., Kucukkirca, E., and Scalia, J. (2010b). Properties of geosynthetics exhumed from a final cover at a solid waste landfill. *Geotext. Geomembr.*, 28, 536-546.
- Benson, C., Chen, J., and Edil, T. (2013). Hydraulic conductivity of geosynthetic clay liners to coal combustion product leachates, *interim report*. Sustainability Report No. OS-13-07, Office of Sustainability, University of Wisconsin-Madison, Madison, WI.
- Bradshaw, S., and Benson, C. (2014). Effect of Municipal Solid Waste Leachate on Hydraulic Conductivity and Exchange Complex of Geosynthetic Clay Liners. *J. Geotech. and Geoenviron. Eng.*, 140(4), 04013038.
- Di Emedio, G., Van Impe, W., and Flores, V. (2011). Advances in geosynthetic clay liners: polymer enhanced clays. *GeoFrontiers 2011. Advances in Geotechnical Engineering*, American Society of Civil Engineers, Reston, USA, 1931-1940.
- Dunn, J. R., & Mitchell, J. K. (1984). Fluid Conductivity Testing of Fine-Grained Soils. *Journal of Geotechnical Engineering*, 110(11), 1648-1665.
- EPA (1993). Determination of Turbidity by Nephelometry, Method 180.1. Cincinnati, OH.
- Jo, H., Benson, C., and Edil, T. (2004). Hydraulic conductivity and cation exchange in non-prehydrated and prehydrated bentonite permeated with weak inorganic salt solutions. *Clays and Clay Miner.*, 52(6), 661-679.

- Katsumi, T., Ishimori, Ho, Onikata, M., and Fukagawa, R. (2008). Long-term barrier performance of modified bentonite materials against sodium and calcium permeant solutions. *Geotext. and Geomembranes*, 26(1), 14-30.
- Kolstad, D., Benson, C., Edil, T., and Jo, H. (2004b). Hydraulic conductivity of dense prehydrated GCL permeated with aggressive inorganic solutions. *Geosynth. Int.*, 11(3).
- Lin, L., Katsunami, T., Kamon, M., Benson, C., Onikata, M., and Kondo, M. (2000). Evaluation of chemical-resistant bentonite for landfill barrier application. *Annals of Disas. Prev. Res. Inst.*, Kyoto Univ., No. 43 B-2, 525-533.
- McRory, J., and Ashmawy, A. (2005). Polymer treatment of bentonite clay for contaminant resistant barriers. *GSP 142 Waste Containment and Remediation*, 1-11.
- Scalia, J., and Benson, C. (2011). Hydraulic conductivity of geosynthetic clay liners exhumed from landfill final covers with composite barriers. *J. Geotech. Geoenviron. Eng.*, 137(1), 1-13.
- Scalia, J., Benson, C., Bohnhoff, G., Edil, T., and Shackelford, C. (2014). Long-term hydraulic conductivity of a bentonite-polymer composite permeated with aggressive inorganic solutions. *J. Geotech. Geoenviron. Eng.*, 140(3), 1-13.
- Scalia, J., and Benson, C. (2014). Barrier Performance of Bentonite-Polyacrylate Nanocomposite to Artificial Ocean Water. *Proceedings, Geo-Congress 2014 Geo-Characterization and Modeling for Sustainability*, GSP No. 234, ASCE, Reston, VA.

- Scalia, J., Bohnhoff, G., Shackelford, C., Benson, C., Sample-Lord, K., Malusis, M., and Likos, W. (2018). Enhanced Bentonites for Containment of Inorganic Waste Leachates by GCLs. In review.
- Shackelford, C., Benson, C., Katsumi, T., Edil, T., and Lin, L. (2000). Evaluating the hydraulic conductivity of GCLs permeated with non-standard liquids. *Geotext. and Geomembranes*, 18(2-3), 133-161.
- Trauger R., and Darlington J. (2000). Next-generation geosynthetic clay liners for improved durability and performance. TR-220. Colloid Environmental Technologies Company, Arlington Heights, 2-14.
- Tian, K, Likos, W., and Benson, C. (2018). Polymer Elution and Hydraulic Conductivity of Bentonite-Polymer Composite Geosynthetic Clay Liners. *J. Geotech. Geoenviron. Eng.*, in review.
- Young R., and Lovell P. (2011). Introduction to Polymers, 3rd Ed. *CRC press*, Boca Raton, FL, 668 p.

4.7 FIGURES

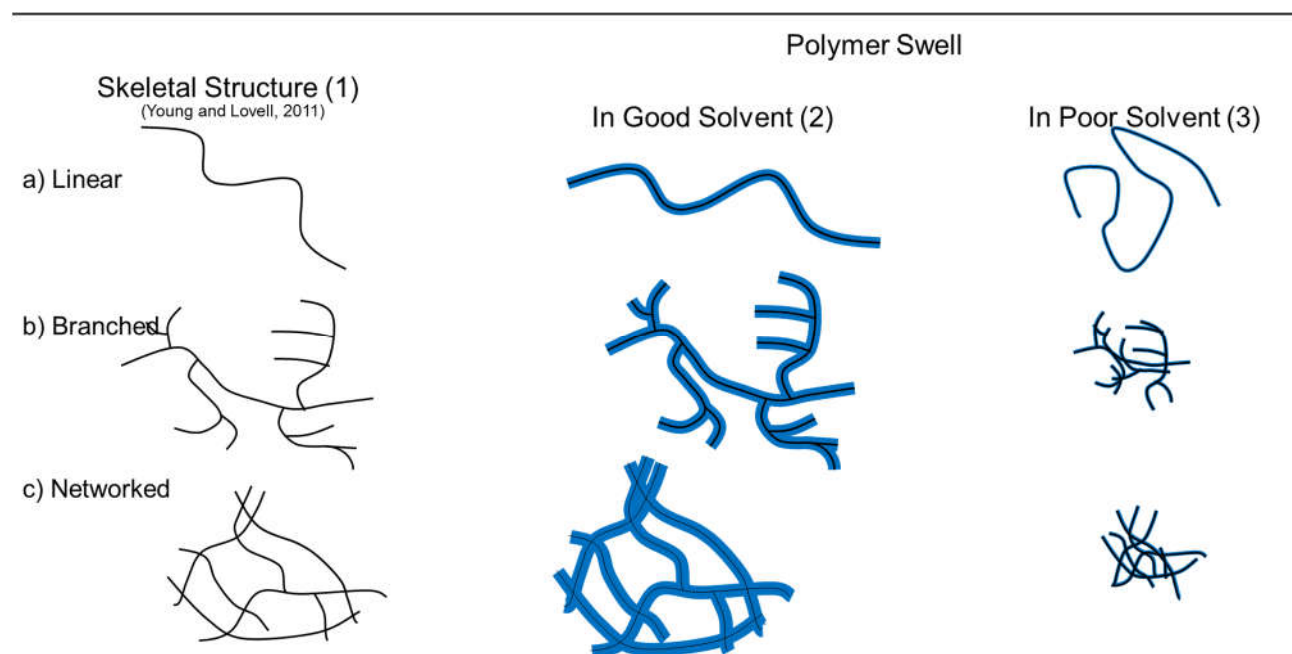


Figure 4.1. Schematic representation of polymers used in PMB GCLs (1) skeletal structure, (2) polymer swelling in good solvent, (3) polymer collapse in poor solvent for (a) linear, (b) branched and (c) network polymers.

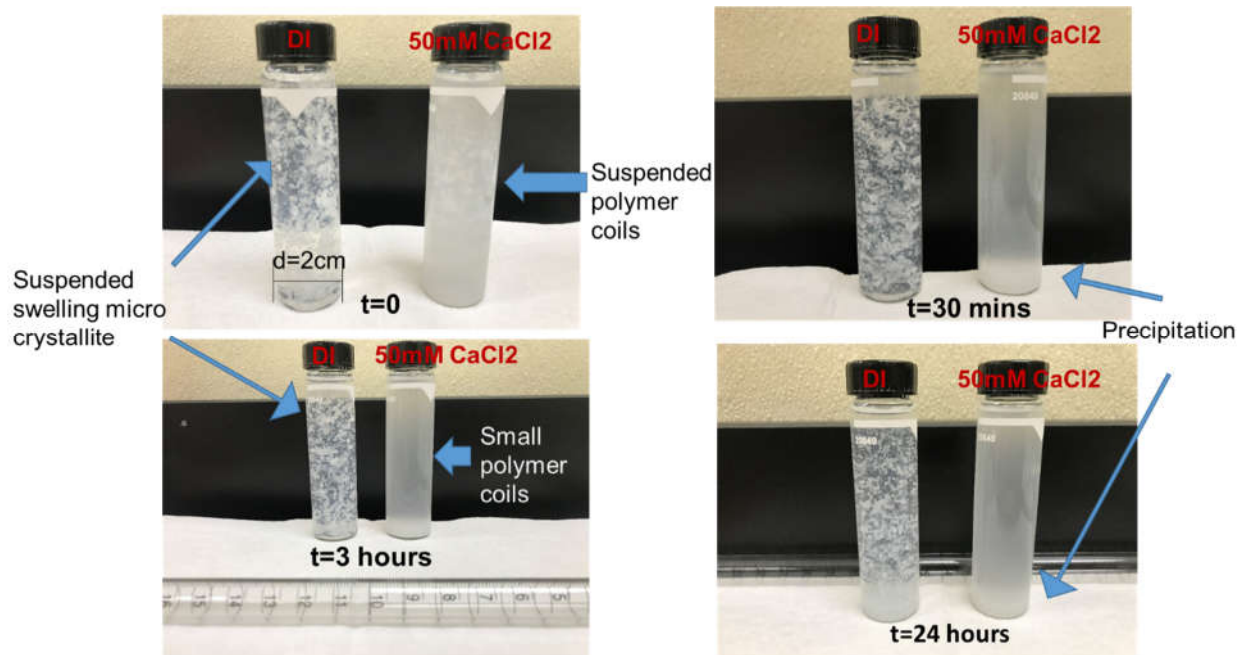


Figure 4.2. Photograph of networked polymer suspension for a networked polymer (at solid-to-liquid ratio of 0.5%) in DI water and 50 mM CaCl₂.

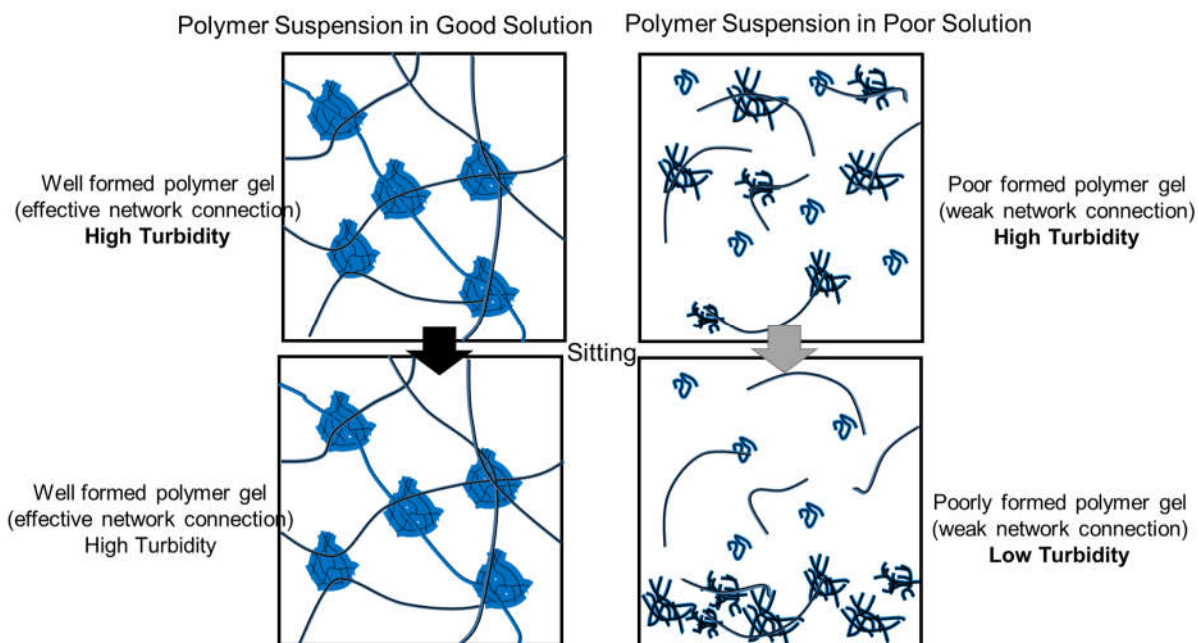


Figure 4.3. Conceptual illustration of polymer suspension in good and poor solution upon mixing and after sitting.

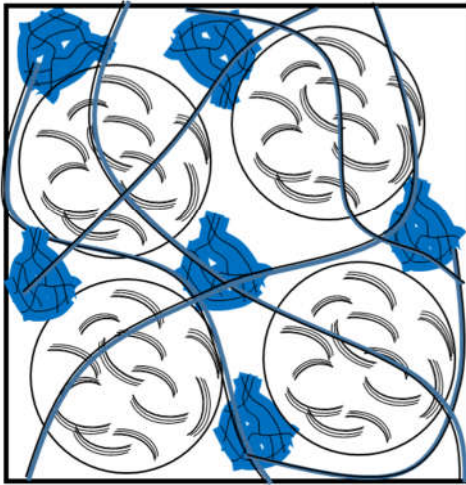
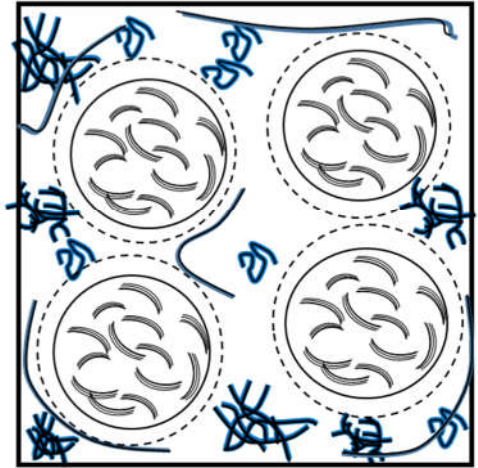
PMB Suspension in Good Solution**PMB Suspension in Poor Solution**

Figure 4.4. Conceptual illustration of polymer-bentonite suspension in good solution and poor solution.

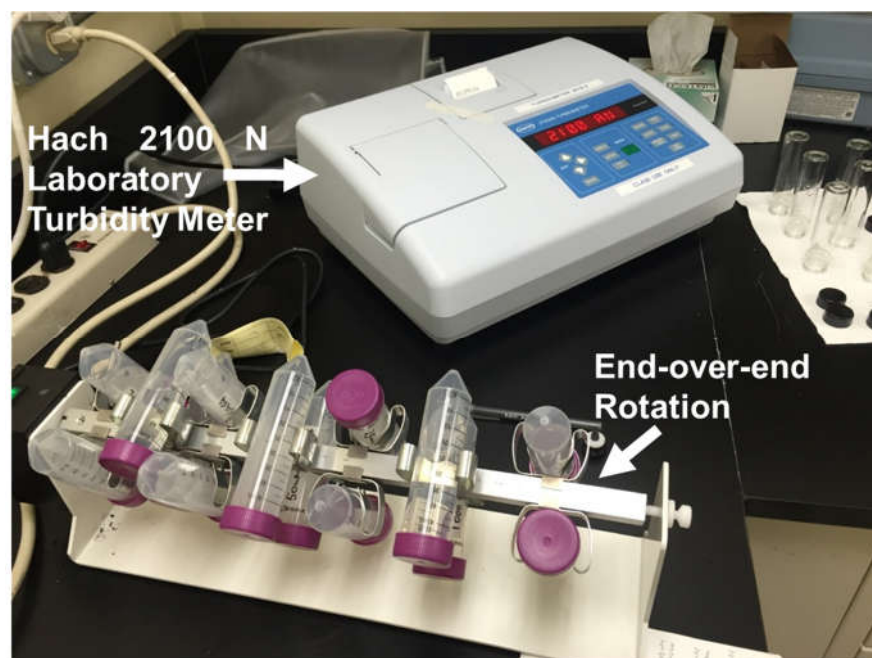


Figure 4.5. Photographs of Hach 2100N Laboratory Turbidity Meter and end-over-end rotation for preparing polymer suspension.

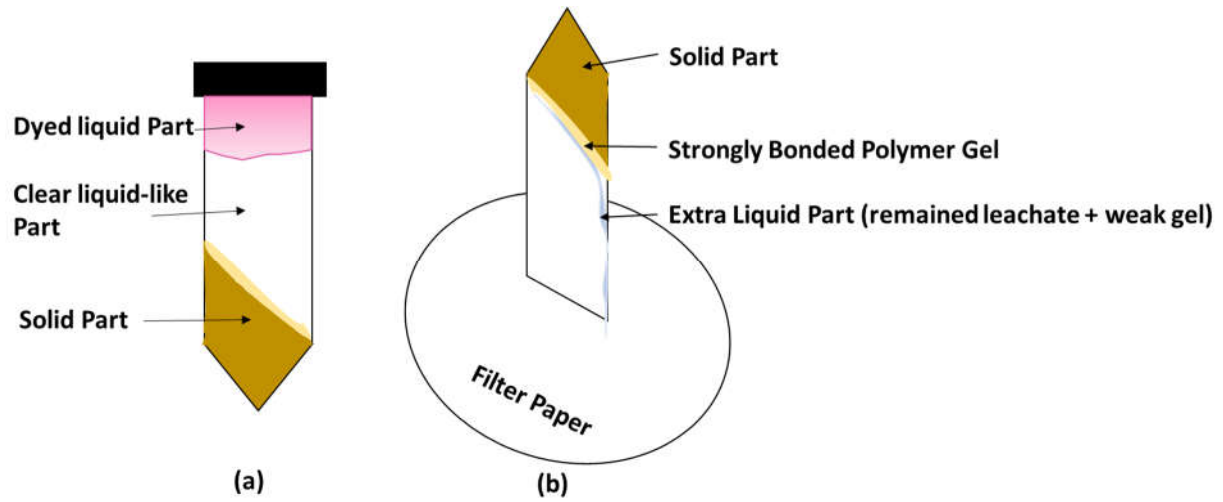


Figure 4.6. Schematic illustration of modified water content test procedures.

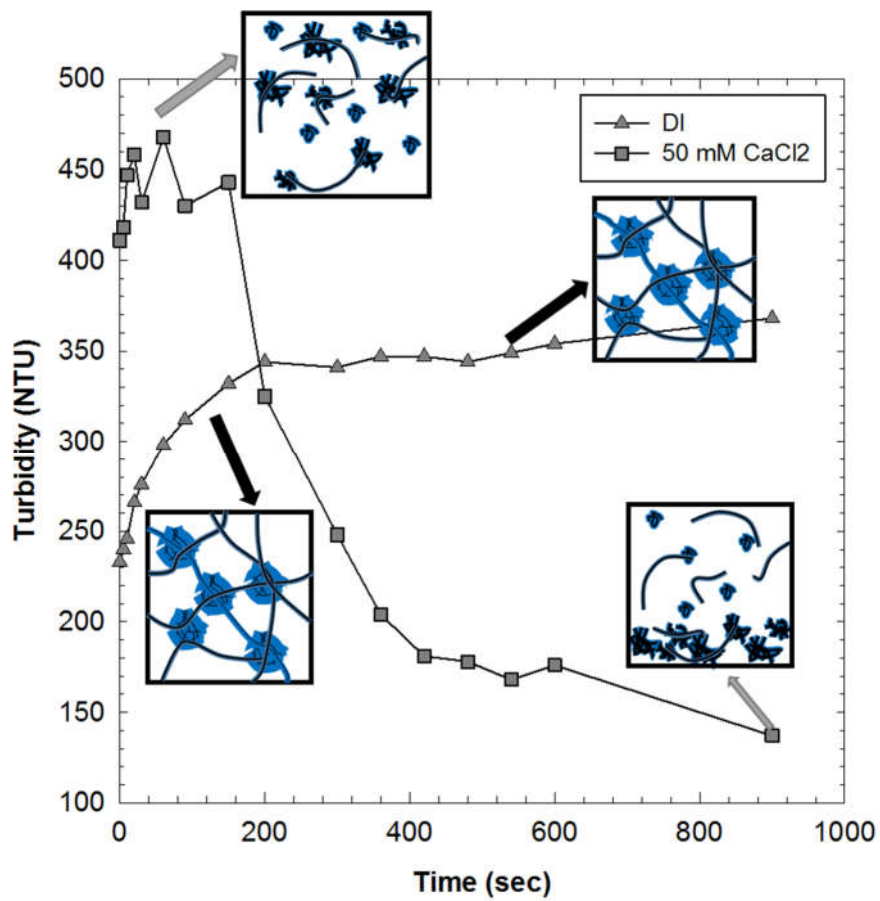


Figure 4.7. Turbidity of networked polymer suspension in DI water and 50 mM CaCl₂ with time.

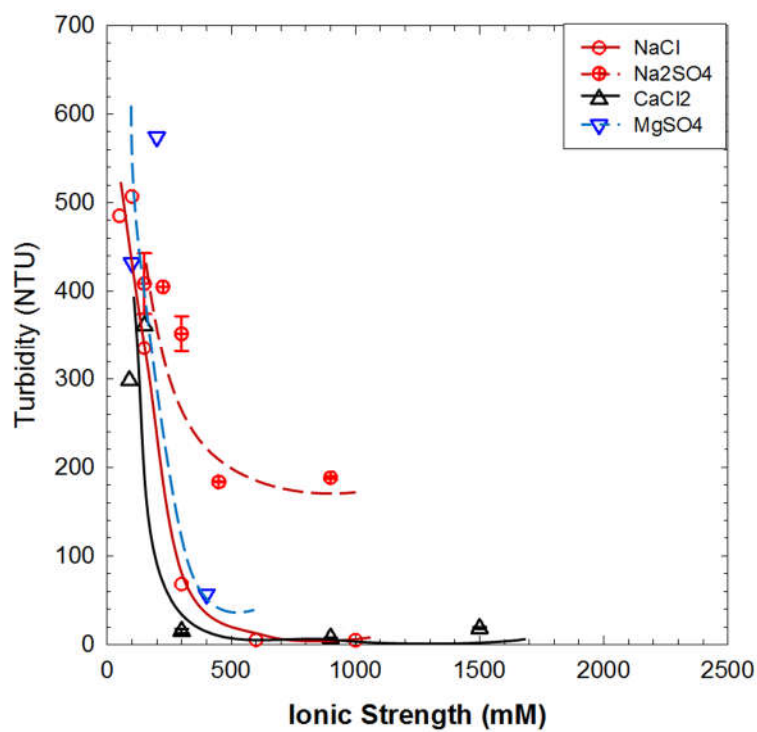


Figure 4.8. Turbidity of networked polymer suspensions in various single species salt solutions.

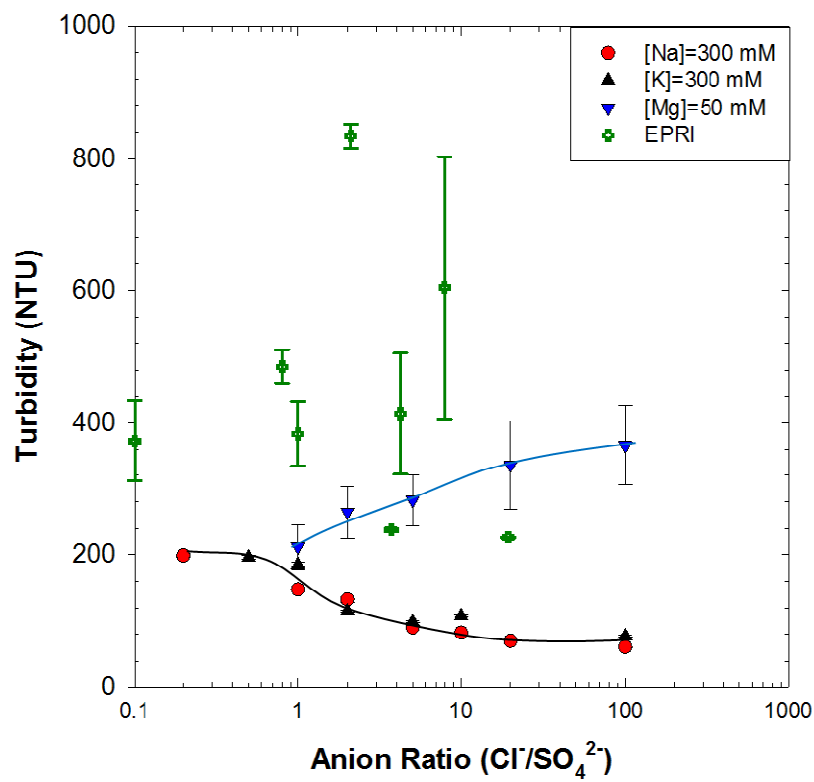


Figure 4.9. Turbidity of networked polymer suspension in 300 mM K^+ , 300 mM Na^+ , 50 mM Mg^{2+} solutions and EPRI leachates as a function of anion ratio (R =molar concentration ratio of Cl^- to SO_4^{2-}).

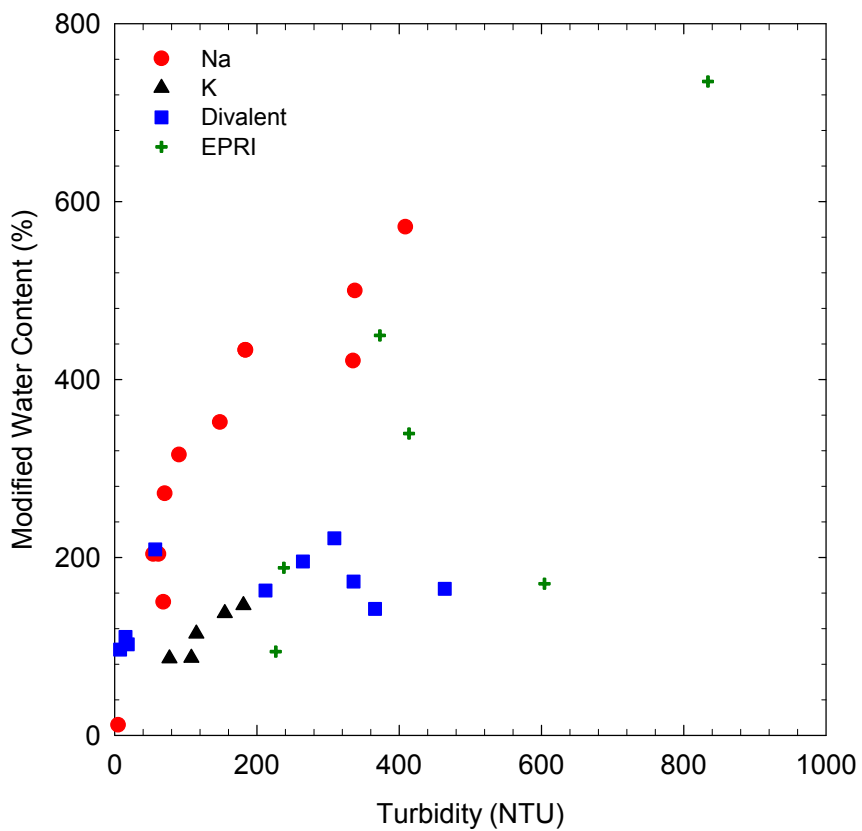


Figure 4.10. Modified water content of PMB suspensions versus average turbidity of polymer suspensions.

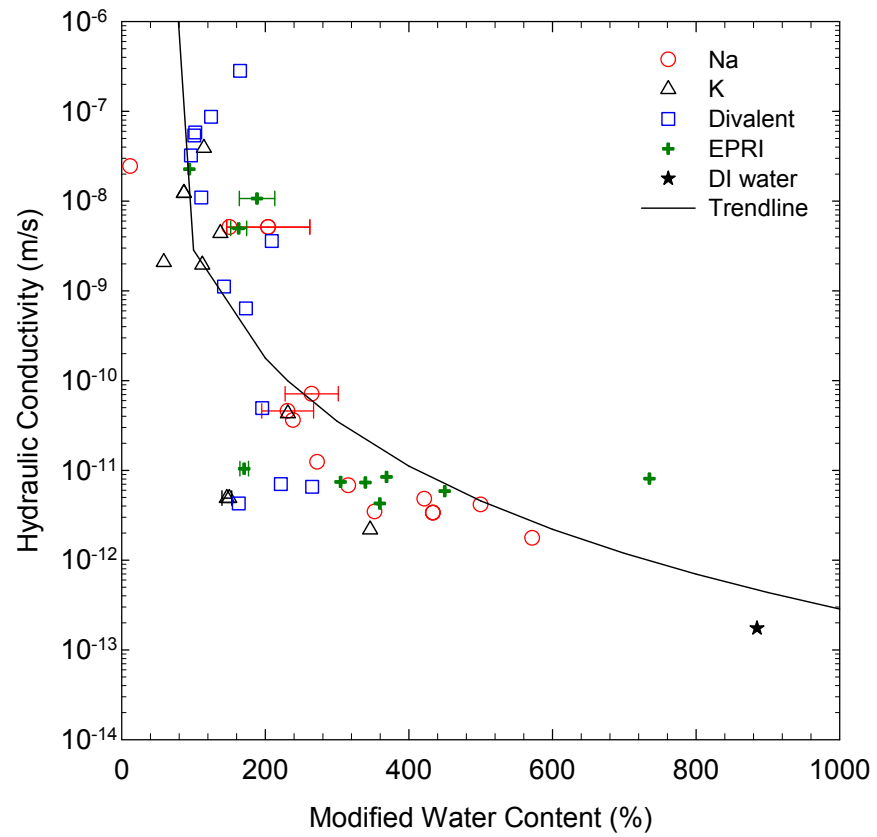


Figure 4.11. Hydraulic conductivity of PMB-GCL versus modified water content of PMB suspensions.

CHAPTER FIVE

EFFECT OF HYDRAULIC GRADIENT ON HYDRAULIC CONDUCTIVITY OF POLYMER MODIFIED GEOSYNTHETIC CLAY LINERS

ABSTRACT

Previous studies have shown that the magnitude of hydraulic gradient (i) used in laboratory permeation tests does not have a significant effect on measured hydraulic conductivity (k) of conventional Na-B GCLs. However, there is a potential effect on hydraulic conductivity of PMB GCLs due to mobilization and elution of polymer. Two sets of hydraulic conductivity tests were performed for PMB GCLs permeated with (1) pure divalent cation-chloride solution (50 mM CaCl_2), and (2) high sodic-sulfate synthetic leachate (Trona) using various hydraulic gradients ($10 \leq i \leq 380$) and at comparable effective stress. Uniformity of post-test polymer distribution within the GCLs was quantified by loss on ignition (LOI) testing to assess polymer elution and preferential flow path development. Results indicate that high hydraulic gradient promotes polymer elution and formation of preferential flow paths. Higher hydraulic gradient tends to elute polymer from PMB GCLs and increases hydraulic conductivity. Results support the hypothesis that polymer clogging in the bentonite macropores is a primary mechanism for low hydraulic conductivity of PMB GCLs.

5.1 INTRODUCTION

Geosynthetic Clay Liners (GCLs) are manufactured materials comprised of a thin layer (~7-10 mm) of bentonite sandwiched between two geotextiles layers. GCLs are commonly used in constructed hydraulic barrier systems, i.e. landfill liners, where in-service hydraulic gradients are typically around 10-20 in most cases (Dunn and Mitchell, 1984). To assess the hydraulic performance of GCLs, hydraulic gradients ($i = \Delta h/L$) that correspond to field conditions are ideally applied to obtain representative measurements of hydraulic conductivity (k) in the laboratory.

ASTM D5084 suggests application of hydraulic gradient similar that expected to occur in the field, but larger hydraulic gradient may be applied if higher hydraulic gradient can be shown not to change the hydraulic conductivity. Recommend hydraulic gradients include a maximum of 10 for $10^{-7} \text{ m/s} < k < 10^{-8} \text{ m/s}$, 20 for $10^{-8} \text{ m/s} < k < 10^{-9} \text{ m/s}$, and 30 for $k < 10^{-9} \text{ m/s}$.

Review of the literature shows that previous laboratory studies have used hydraulic gradients ranging from 50 to 550 for measuring hydraulic conductivity of conventional Na-B GCLs (Shan and Daniel, 1991; Daniel *et al.* 1993; Didier and Comeaga, 1997; Petrov and Rowe, 1997; Petrov *et al.* 1997a,b; Quaranta *et al.* 1997; Ruhl and Daniel, 1997; Lin, 1998). Hydraulic gradient typically ranging from 150-200 are commonly applied in lab tests in consideration of timing and budget. The objective of this testing series is to evaluate how hydraulic gradient, in particular elevated hydraulic gradient, might affect polymer elution and corresponding hydraulic conductivity of PMB GCLs. Two types of permeant solutions were selected to represent typical industrial leachate chemistries. Tests were conducted with hydraulic gradients ranging from 10 to 380 at comparable

effective stress. Loss on ignition (LOI) tests were conducted on the post-permeation GCLs to evaluate polymer distribution after long-term hydraulic conductivity tests. An elution index is introduced to quantify the potential of polymer elution from PMB GCLs.

5.2 BACKGROUND

5.2.1. Hydraulic Gradient Employed in Previous Hydraulic Conductivity Tests

Hydraulic gradients that are higher than expected in the field are often used in laboratory permeation tests for materials with low hydraulic conductivity due to timing and budget constraints. Previous studies have found that high gradient may result in artificially low measured hydraulic conductivity for compacted clay soil due to mobilization and migration of finer particles and clogging of pore spaces (Dunn & Mitchell, 1984) or by consolidation associated with high seepage force (ASTM D5084). Dunn and Mitchell (1984) tested the effect of hydraulic gradient on two clays, a predominantly kaolinite clay and a predominantly bentonite clay. In tests started with a hydraulic gradient of 20 and increased in increments to 200 the hydraulic conductivity of both soils decreased and was irreversible.

Fig. 5.1 summarizes results from a comprehensive literature survey to summarize hydraulic gradients used in previous hydraulic conductivity tests for conventional Na-B GCLs and PMB GCLs (frequency indicates number of tests). While hydraulic gradients ranging from 50 to 550 have been used, hydraulic gradient can have negligible effect on hydraulic conductivity of conventional Na-B GCLs. For example, Petrov *et al.* (1997a) concluded that the effect of hydraulic gradient was less than a factor of 2 by conducting hydraulic conductivity tests with hydraulic gradient ranging from 17 to 546. Rad *et al.*

(1994) showed that hydraulic gradient can be as high as 2800 without major effects on hydraulic conductivity measurements using a Claymax GCL. Shackelford *et al.* (2000) attributed the apparent insensitivity of hydraulic gradient on hydraulic conductivity testing of GCLs to the relationship between hydraulic gradient and effective stress. It was illustrated that the effective stress is far less sensitive to hydraulic gradient of GCLs because of they are very thin. For a GCL of 9 mm in thickness, that analysis showed that a hydraulic gradient of 380 would have to be applied to produce a difference in 34 kPa in stress between the inflow and outflow sides of the specimen (stress difference caused by using maximum hydraulic gradient of 30 by ASTM D5084 with a typical Proctor mold). Consequently, hydraulic gradient more than ten times larger than those typically applied to compacted clay soils could be applied without having significant change in hydraulic conductivity.

5.2.2. Implications of Hydraulic Gradient on PMB GCLs

GCLs containing enhanced bentonite (EB) are being adopted to improve chemical compatibility and hydraulic performance of GCLs in applications with aggressive leachates (Scalia *et al.* 2018). Recent studies have focused on EB GCLs containing polymer modified bentonite (PMB). Pore clogging of bentonite by polymer hydrogel has been hypothesized to be the primary mechanism that dominates hydraulic conductivity of PMBs (Scalia *et al.* 2014, Tian *et al.* 2016). Tian *et al.* (2018) indicated that clogging of bentonite macropores by polymer hydrogel was a predominant mechanism for maintaining low hydraulic conductivity of PMBs by observing pore-scale interaction between bentonite and polymer via SEM imaging. Salihoglu (2015) found that effluents from hydraulic conductivity tests on PMB GCLs was more viscous than the influent,

suggesting that polymer may elute from PMB GCLs during permeation. Further, hydraulic conductivity was found to be positively correlated with the amount of polymer elution; the higher the polymer elution, the higher the k (Chen, 2015). Thus, factors (e.g., hydraulic gradient) that could potentially influence polymer clogging and elution may potentially affect the hydraulic conductivity of PMB GCLs. In this context, higher hydraulic gradient is hypothesized to promote elution of the polymer hydrogel. As indicated on Fig. 5.1, most previous studies on PMB GCLs have employed hydraulic gradients much higher than expected in the field (e.g., between 100 and 200) and limited studies have conducted hydraulic conductivity tests with low hydraulic gradients.

5.3 MATERIALS AND METHODS

5.3.1. Geosynthetic Clay Liners

The GCL used in this study is a commercial available PMB GCL containing a dry blend of granular Na-bentonite and a proprietary polymer. The PMB GCL has an average initial thickness of 9.37 mm, water content of 5.6%, and the PMB is encapsulated between a woven and a nonwoven geotextile by needle punching. Cation exchange capacity (CEC) of the PMB is 89.6 cmol⁺/kg, with the following bound cation mole fraction: Na (0.14), K (0.01), Ca (0.13), and Mg (0.04) determined by ASTM D7503. X-ray diffraction shows that the mineralogy of the PMB consists of 79% montmorillonite, along with measureable quantities of quartz, feldspar and mica (Chen *et al.*, 2015). Polymer loading was estimated to be 5.1% by loss on ignition (LOI) accounting for loss of strongly bound water molecules, calcite, and organic matter associated with the bentonite fraction (Scalia *et al.*, 2014; Tian *et al.*, 2016).

5.3.2. Permeant Liquids

Two types of permeant solutions were selected for hydraulic conductivity testing in this study. A single-species divalent cation salt solution - 50 mM CaCl₂; and a synthetic leachate - Trona ash, with the chemical characteristic shown in Table 5.1. The latter was synthesized from CCP leachate data base representative of conditions encountered in CCP disposal facilities throughout the USA (EPRI 2006 and 2009).

5.3.3. Hydraulic Conductivity Testing

Hydraulic conductivity tests on the PMB GCLs were performed employing both the falling-head method and the constant-flow method. Tests were conducted using the falling head method with average hydraulic gradient of 40, 50, 80, 90, 120, 160, 190 and 380. Tests were conducted using the constant flow method with an average hydraulic gradient of 15.

5.3.3.1. Falling Head Method

Falling head hydraulic conductivity tests were conducted in flexible wall permeameters following ASTM D5084 Method B and ASTM D6766 Method B. Average hydraulic gradients with corresponding effective stress conditions for each test used in this study are summarized in Table 5.2. To achieve the desired average hydraulic gradient with comparable effective stress among each specimen, the elevation of inflow burette was varied along with the cell pressure. Cell pressures were applied by using a burette filled with water fixed on the wall at desired elevation. The reading range in the inflow 50-mL burette was also varied to have a comparable average effective stress (18.1~20.2 kPa). All tests were conducted on GCL specimens with a diameter of 15.24

centimeters. Prior to initiation of flow, GCL specimens were hydrated with the corresponding permeant for 48 hours at cell pressure (ranging from 20.7 – 26.5 kPa). Effluents were collected in 60-mL polyethylene bottles for analysis. Each permeameter has two influent lines, two effluent lines, and a connection to a cell pressure line. One pair of influent and effluent lines are closed during flow but are used for polymer flushing once clogging was detected.

5.3.3.2. Constant Flow Method

Constant flow hydraulic conductivity tests were conducted using flexible wall permeameters following ASTM D5048 Method D and ASTM D6766 Method D. A wide range of flow rates and hydraulic gradients were used in this study. Similar hydration method was applied as in falling head method. GCL specimens were hydrated with the permeant for 48 hours at an average cell pressure of 27 kPa before permeation. A photograph of the constant flow setup with captions can be found in Fig. 5.2. Both the influent and effluent lines were connected to a KDS 120 Legacy Dual Syringe, Single Cycle Push-Pull Syringe Pump. The influent line was connected to the push portion of the pump, while the effluent line was connected to the pull portion of the pump. This effectively forces the volume of inflow to equal the volume of outflow during testing. A differential pressure transducer was connected to the inflow and outflow lines to measure the flow-induced head loss. A one-way pressure transducer was connected to the inflow line to calculate the effective stress by considering the inflow pressure and the measured differential pressure. There is a two-way valve connecting the inflow and outflow that is used to initialize (zero out) the differential transducer prior to testing. After the influent syringe has been emptied into the permeameter and the effluent syringe has been filled,

the effluent is then pushed into a polyethylene bottle for analysis, while the influent is recharged with fresh permeant using a bottle connected to the influent syringe. The hydraulic gradients were relatively high at the first 5 PVF because the unexpectedly low hydraulic conductivity values resulting in the difficulty of control, despite using the lowest allowable flow rate.

5.3.4. Termination Criteria

Equilibrium was defined using the hydraulic and chemical equilibrium criteria described in ASTM D 6766, according to which, hydraulic equilibrium is established when steady hydraulic conductivity has been maintained for three consecutive measurements with no significant change. The volumetric outflow to inflow ratio (Q_{out}/Q_{in}) should be within 1.0 ± 0.25 . Chemical equilibrium is defined in ASTM D6766 as the ratio of effluent to influent pH (pH_{out}/pH_{in}), and electrical conductivity (EC_{out}/EC_{in}) are within 1.0 ± 0.1 . In addition, concentrations of major cations (Ca^{2+} , Mg^{2+} , Na^+ , K^+) are also required to be within 1.0 ± 0.1 . These were analyzed using Varian MPX inductively coupled plasma atomic emission spectroscopy (ICP-AES) in accordance with method 6010B defined by the U.S. Environmental Protection Agency (EPA). In this study, equilibrium hydraulic conductivities were reported by taking the average of the last three consecutive readings at steady state. Chemical equilibrium upon termination was evaluated test-to-test basis (detailed results will be discussed in the following section).

5.3.5. Total Organic Carbon (TOC) Analysis

Effluents and declogged samples from PMB GCLs were analyzed periodically for total organic carbon (TOC) to quantify the amount of polymer elution. TOC concentrations

were analyzed using a Shimadzu TOC-VCSH (Shimadzu Scientific Instruments, Columbia, MD) with a measurement range for NPOC from 4 ppb to 25000 ppm in accordance with ASTM D4839-03. A calibration curve was set manually with dilution from a standard 100 ppm glucose ($C_6H_{12}O_6$) consisting of five points (5, 10, 25, 50, and 100 ppm) with a blank (UHP Milli-Q water). The calibration curve fit was linear with a minimum R^2 accepted at 0.999. Effluent samples were set on an end-over-end shaker for 24 hours, and diluted 25 times to disperse any polymer globules in the solutions and to ensure homogeneous solutions within the appropriate standard range. The total carbon of the sample contains the inorganic content in solution and organic content from polymer backbone chain. Prior to measurement, the inorganic carbon content was removed by sparging with CO_2 -free gas. The total organic carbon content was measured by detecting the amount of CO_2 , which was converted by combusting the sample. Thus, the TOC measured herein was considered as polymer concentration (organic content of solution). A standard solution (100 ppm glucose) was checked every 20 measurements to ensure the accuracy of measurement. The injection volume used was the same as that used for the calibration curve (50 μ L).

5.3.6. Loss on Ignition (LOI)

Polymer loading of the PMB was calculated by loss on ignition (LOI) determined in accordance with ASTM D7348. Materials were dried in an oven to constant mass at 105 ± 5 °C, then placed into pre-heated crucibles and subjected to sequential heating up to 550 °C in a furnace for 4 hours. After ignition, the crucibles were allowed to cool in a sealed container with desiccant. The mass loss after heating was then recorded at room

temperature. The end member bentonite and polymer used in this study have measured LOI values of 1.29% and 84.8%, respectively.

An average LOI value of 5.1% was measured for the PMB GCL used in this study. Samples of pre-permeation LOI were obtained by extracting PMB from a portion of the GCL roll located immediately adjacent to the location of the sample cut from the roll for permeability testing. Post-permeation LOI was conducted on multiple samples extracted from the GCL specimen after permeation. Samples were cut into 'pie' slices (Fig. 5.10, 5.11) to obtain an indication of post-test polymer spatial distribution. Percentage polymer loss (%) was calculated for each 'pie' section by deducting post-permeation-LOI from pre-permeation LOI. Standard deviation was calculated on polymer loss to quantify the amount of variation of polymer loss for GCL at each hydraulic gradient.

5.4 RESULTS AND DISCUSSION

Hydraulic conductivity tests were conducted with different hydraulic gradients for each permeant solution. Tests with 50 mM CaCl_2 were conducted with average hydraulic gradient of 40, 50, 80, 90, 120, and 160 with the falling head method, along with an average hydraulic gradient at 15 with the constant flow method. Tests using hydraulic gradient of 40 and 50 were testing for two years and then were increased to a hydraulic gradient of 190 for two months. Test with the Trona leachate were conducted at average gradient of 40, 80, 120 and 190. Tests at initial i of 40, 80 and 120 continued for around 18 months, whereupon hydraulic gradient was increased to 190, allowed to achieve steady state (600 days), and then gradient was doubled to 380. Overall testing duration for each hydraulic gradient is summarized in Table 5.3.

5.4.1. PMB GCLs permeated with 50 mM CaCl₂

5.4.1.1. Evolution of hydraulic conductivity

Hydraulic conductivity of the GCLs to 50 mM CaCl₂ solution is shown in Fig.5.3 as a function of pore volumes of flow (PVF) at various hydraulic gradients. The hydraulic conductivity values generally increase with higher hydraulic gradient at early PVFs, and reach the order of 10⁻⁸ m/s when sufficient PVF (~12 PVF) have passed. Hydraulic conductivity obtained by constant-flow tests are 2 orders of magnitude smaller for 0-8.5 PVF, then increase significantly after about 20 PVF to 10⁻⁸ m/s. The exact reasoning for the prolonged low k measured by the constant flow method is not known with full confidence. It is hypothesized that the large difference in hydraulic conductivity might be attributed to the decrease in pore volume of GCLs with constant flow method compared to that with falling head method. Reybrock (2017) found a slight change in pore volume by subtracting the cumulative outflow from the cumulative inflow. The constant flow method has an equal amount of inflow and outflow during permeation, while the falling head method doesn't impose this constraint until steady state is achieved. Calcium ions in permeant solution will replace the sodium ions that initially reside in the interlamellar space of the bentonite (Mitchell and Soga, 2005), which will cause the thickness of diffuse double layer to decrease and contribute to a higher portion of water molecules entering the intergranular space. Because of the constraint on equal inflow and outflow, pore pressure builds up within the GCL as cation exchange occurs, causing a higher portion of water molecules to enter the intergranular pore space; whereas, the falling head method allows this pressure to dissipate quickly. It would thus take a longer amount of time for the pressure to dissipate within the GCL tested with constant flow method and

hydraulic conductivity values would remain low during this period. At longer term, however, the difference in hydraulic conductivity values for the two test types is within 1 order of magnitude.

Tests were terminated when the GCLs reached hydraulic conductivity of 10^{-8} m/s after 8 months. Low hydraulic conductivity (10^{-12} m/s) was maintained and little PVF had been reached (around 1-2 PVF) for tests with hydraulic gradients of 40 and 55. Permeation was continued at the same hydraulic gradient for another 15 months, where the hydraulic conductivity rarely changed and PVF remained low (5.25 for i at 40, 1.21 for i at 55). Hydraulic gradient was then increased to 190 and specimens were permeated for two months. A sharp increase in hydraulic conductivity was observed with hydraulic gradient of 40 right after the increase in gradient, and k increased to $\sim 10^{-8}$ m/s within a short time period (Table 5.3), suggesting potential formation of preferential flow paths. Hydraulic conductivity remained low (10^{-11} m/s) for the test with hydraulic gradient of 55, although one order of magnitude increase in k was observed after the abrupt increase in hydraulic gradient. The results suggest that hydraulic gradient has an effect on hydraulic conductivity of PMB GCLs, where higher hydraulic gradient tends to result in higher measured hydraulic conductivity under comparable test and effective stress conditions.

It should be noted that a decrease in k was observed with the test at hydraulic gradient of 120 between the PVF from 12 to 18. This was caused by the polymer clogging as the $Q_{\text{outflow}}/Q_{\text{inflow}}$ ratio during this period was measured to be much less than unity. The hydraulic conductivity re-elevated to the 10^{-8} m/s within a short period of time after declogging of the permeameter system. This is discussed subsequently.

5.4.1.2. Chemical equilibrium

Trends in EC ratio (EC_{out}/EC_{in}), pH ratio (pH_{out}/pH_{in}), Ca concentration ratio (Ca_{out}/Ca_{in}) and effluent Na concentration are shown in Fig.5.4 (a), (b), (c) and (d) plotted with PVF respectively. After 5 PVF, the EC (a) and pH (b) ratio were 1.0 ± 0.1 , where the hydraulic conductivity had not reached steady state. Analysis of chemical composition of effluents indicates the gradual exchange of Na^+ by Ca^{2+} in the GCLs with tests under any hydraulic gradient because Ca_{out}/Ca_{in} ratios are close to unity and the Na concentration in the effluent decreases. Chemical equilibrium was reached after 45 PVF with hydraulic gradient of 160 using the falling head method, as shown in Fig.5.4 (b) and (c). However, the hydraulic conductivity reached steady state after 12 PVF. Unlike the significant increase in hydraulic conductivity of Na-bentonite that occurs when Na^+ in the exchange complex is replaced by Ca^{2+} in permeant solution, the hydraulic conductivity reached steady state prior to completion of cation exchange. This suggests that polymer elution governs the onset of hydraulic equilibrium for PMB GCLs.

5.4.1.3. Polymer elution

Fig.5.5 shows the TOC concentration of effluents (a) and calculated cumulative polymer elution (b) plotted with PVF. The measured effluent TOC concentrations were higher at initial PVF (0-8.5), and diminished gradually to 12 PVF, then leveled off (after 12 PVF) corresponding to the points at which the hydraulic conductivity have little change (Fig.5.3). Fig.5.5 (b) shows the cumulative polymer elution as a function of PVF, showing more polymer elution with higher gradient at initial PVF (0-8.5). A steeper slope of cumulative polymer elution to PVF was observed with tests at hydraulic gradient of 40 and 55, indicating more polymer was eluted at early PVFs (~ 2). It is hypothesized that the

flow was more uniformly penetrating the GCLs at lower hydraulic gradient (i.e., minimal preferential flow paths). The resistance encountered during permeation is the same within the whole area of GCL, if the low hydraulic gradient is less likely to cause preferential flow. It thus takes longer time for solution to flow through the GCL at lower hydraulic gradient and results in more polymer elution with same PVF compared to GCL permeated at higher hydraulic gradient. Once preferential flow forms, the polymer elution slope decreases to a value lower than the one exhibited at high hydraulic gradient, suggesting there was no longer elutable polymer present in the GCL. The polymer elution slope is higher at hydraulic gradient at 120, suggesting the existence of preferential flow similar to the GCL permeated at hydraulic gradient of 150.

Fig.5.6 shows hydraulic conductivity versus cumulative polymer elution with tests at different hydraulic gradient. The hydraulic conductivity corresponds directly to the mass of polymer eluted. An increase in hydraulic conductivity can be observed with increasing cumulative polymer elution. The drop in measured hydraulic conductivity observed at hydraulic gradient at 40, 55, and 120 is attributed to polymer clogging, since hydraulic conductivity increased after declogging of the permeameter system plumbing. Note that the test conducted with the constant flow method has a sharp increase in hydraulic conductivity with a relatively small amount of polymer elution. This might be explained by the frequent declogging processes conducted during permeation, in which, large amount of polymer was forced to flush out of the GCL. Therefore, hydraulic conductivity was high because significant amount of polymer had been eluted from GCL by either elution with outflow or declogging. Unfortunately, the liquids from declogging of the flow cell effluent

plumbing were not saved with GCLs permeated with 50 mM CaCl₂; thus, no data are available for estimating the amount of polymer by declogging the permeant system.

5.4.2. PMB-GCLs permeated with Trona leachate

5.4.2.1. Evolution of hydraulic conductivity

Hydraulic conductivity results for PMB GCLs permeated with Trona leachate are plotted with PVF in Fig.5.7 (a) and (b). For tests with average hydraulic gradient of 40, 90 and 120, the results are similar to those obtained for PMB GCLs permeated with 50 mM CaCl₂. After 16 months of permeation, the test at hydraulic gradient of 120 reaches 48 PVF, whereas the test at hydraulic gradient of 40 reaches less than 2 PVF. After 16 months, hydraulic gradient was increased to 190 for all three tests (Fig.5.7b). Abrupt increases in hydraulic conductivity were observed after the increase of hydraulic gradient. The test with i initially at 40 increased two orders of magnitude; the test with i initially at 90 increased 1.4 times, and the test with i initially at 120 increased one order of magnitude, ultimately reaching 10^{-7} m/s.

For the test with average hydraulic gradient of 190, there was a large increase in hydraulic conductivity from approximately 4 – 7 PVF. This is believed to be a result of sidewall leakage. Consequently, the permeameter was taken apart and reassembled with a new flexible membrane. After that, the hydraulic conductivity remained essentially constant from 10 – 20 PVF. The average hydraulic gradient was then increased from 190 to 380 after PVF of 20 and the hydraulic conductivity quickly increased by 3 orders of magnitude. It was hypothesized that the sudden increase in hydraulic gradient would promote polymer elution, which in turn would create localized preferential flow paths and

a subsequent increase in hydraulic conductivity. Reybrock (2017) found that there was a significant increase in effluent TOC in the first measurement after an abrupt increase in hydraulic gradient, followed by a significant decrease in TOC in subsequent measurements. The initial increase in TOC supports the hypothesis that an increase in polymer elution results in preferential flow and causes an increase in hydraulic conductivity. The subsequent decrease in TOC suggests that there is no longer significant polymer blocking the flow (i.e., the majority of mobile polymer has been eluted) such that elution thereafter significantly decreases. These results provide evidence to indicate that higher hydraulic gradient tends to elute polymer from PMB GCLs, which in turn forms localized preferential flow paths and an increase in hydraulic conductivity. A lower hydraulic gradient, the volume of pore fluid moving through the specimen (PVF) accumulates slowly because the flow is impeded and otherwise mobile polymer remains retained and blocks/clogs the porosity.

5.4.2.2. Chemical equilibrium

Fig.5.8 is a plot of EC ratio (EC_{out}/EC_{in}) and pH ratio (pH_{out}/pH_{in}) versus PVF for PMB GCLs permeated with Trona leachate. After 1 PVF, the EC ratio for all three tests is 1.0 ± 0.1 , although the hydraulic conductivity has not reached a steady value (Fig. 5.7). None of the three tests have pH ratio within 1.0 ± 0.1 , although 30 PVF passed through the GCL with hydraulic gradient of 120 and the hydraulic conductivity has little or no change after approximately 10 PVF. The EC and pH results from chemical analysis of effluents indicate the criterion used for determining equilibrium/completion of hydraulic conductivity test for conventional Na-bentonite may not effectively apply to PMB GCLs.

5.4.2.3. Implication of polymer clogging

Fig. 5.9 shows the pictures of polymer clogging in the outflow tube (b), inflow fitting (c), outflow side of geosynthetic fabric (d), permeameter plate (e), and inflow burette (d), respectively. Liquids obtained from periodic declogging of the flow cell effluent plumbing in the suite of tests permeated with Trona leachate were retained for TOC analysis. Mass of polymer elution, hydraulic conductivity and cumulative polymer elution without and with accounting for polymer content in the declogging fluid are plotted for $PVF < 20$ in Fig. 5.10 (a), (b) and (c), respectively. It may be noted that each apparent increase in hydraulic conductivity is followed by a significant amount of polymer elution detected in the effluent, or in the declogging liquid. Permeameter declogging was not required after increasing the hydraulic gradient to 190.

Fig.5.10 (c) compares the cumulative polymer elution calculated from effluent solution to cumulative polymer elution without including polymers in the declogging liquid. This result shows that a significant amount of polymer was detected in the declogging liquid for tests with all hydraulic gradients. The difference between the two plots (for example on the test with hydraulic gradient at 120) can be used to quantify the amount of polymer eluted by declogging. The mass of declogged polymer accounts half of the total polymer mass eluted at initial PVF (0-3), and a quarter of the polymer mass eluted over the term of the test. Declogging was not required once the difference in cumulative polymer elution became constant, which corresponds to the PVF where hydraulic conductivity has no or little change. This observation provides more support to the hypothesis that polymer clogging in the porosity of the GCL contributes to low hydraulic conductivity of PMB GCLs.

5.5 POST-PERMEATION POLYMER CONTENT

Prior to termination of hydraulic conductivity testing, 2 mL of Rhodamine dye tracer at concentration of 0.05 wt.% was introduced to the inflow burette mixed with 48 mL testing liquid to visually the distribution of flow through the GCL after test disassembly. Pink dye was observed on the surface of GCL indicating the flow pattern during permeation (Fig.5.11, Fig.5.12). The GCL was then cut into 'pie' slices and polymer content of the each slice was measured by LOI to calculate post-permeation spatial distribution of polymer content and polymer loss during permeation. The polymer loss was calculated as:

$$\text{Polymer loss (\%)} = \text{LOI}_{\text{Pre-permeation}} - \text{LOI}_{\text{Post-permeation}}$$

where $\text{LOI}_{\text{Pre-permeation}}$ is the LOI value obtained before permeation and $\text{LOI}_{\text{Post-permeation}}$ is the LOI value measured after permeation.

Fig. 5.11 shows the distribution of polymer loss for the PMB GCL permeated with 50 mM CaCl_2 . Higher polymer loss was generally observed to correspond to "pie slices" dyed pink by the tracer solution, indicating a correlation between polymer loss (elution) and preferential flow. For the GCLs tested at hydraulic gradient of 120 and 150, where the hydraulic conductivity reached 10^{-7} m/s, the average polymer loss (average of all pie slices) is significantly higher (1.72 and 1.90 respectively). The standard deviations of polymer loss among the pie slices for these two GCLs are also high, indicating that the difference in polymer loss among the slices was high, which can be considered an additional indicator of significant preferential flow. The GCLs tested at hydraulic gradient of 80, 90, and 135 exhibit similar average polymer loss and standard deviation values, and the hydraulic conductivity values are also similar. The GCLs tested at hydraulic

gradient of 40 and 55 have the same average polymer loss; however, the hydraulic conductivity of the two GCLs are quite different. This observation can be attributed to the difference in standard deviation of polymer loss. The GCL tested at hydraulic gradient of 55 exhibited the lowest standard deviation value among all the tests, suggesting the polymer loss was evenly distributed through the GCL. This is in accord with the observation that there was a maximum flow pattern area with the GCL exhibiting the lowest hydraulic conductivity (Fig. 5.3) and the highest polymer elution slope (Fig. 5.5b). Therefore, it can be concluded that the average polymer loss can be used to quantify the amount of polymer elution, while the standard deviation can be used as an indicator to assess the impact of preferential flow on hydraulic conductivity for PMB GCLs. The results presented in this section support the hypothesis that higher hydraulic gradient tends to elute polymer from PMB GCLs, trigger preferential flow, and increase hydraulic conductivity. Lower hydraulic gradient improves polymer retention in the GCL and results in a more uniform flow pattern, thus maintaining low hydraulic conductivity for longer PVF.

Fig. 5.12 shows post-permeation photographs and polymer loss values from tests permeated with the Trona solution. The average polymer loss is higher for GCLs permeated with Trona than those permeated with CaCl_2 . This is interpreted to indicate that polymer hydrogel formation and polymer-bentonite interaction was weaker in the Trona solution due to its high ionic strength (755mM). These factors can be assessed by index tests with PMB (e.g., viscosity, modified water content). Average polymer losses are close among the GCLs tested at hydraulic gradient of 40, 90 and 120. The difference in hydraulic conductivity observed in these tests can be explained by the extent of preferential flow, as evidenced by the standard deviation in polymer loss. The GCL tested

at hydraulic gradient of 120 has the highest standard deviation, indicating the largest degree of preferential flow among the three tests. The GCL tested at hydraulic gradient of 90 has the lowest standard deviation, where the degree of preferential flow was lowest. Hydraulic conductivity was the highest and lowest in the former and latter. The similar average polymer loss value can be attributed to fact that the GCL tested at hydraulic gradient of 90 had the longest cumulative permeation time (Table 5.3). Thus, although polymer elution required more PVF, the cumulative elution was significant.

Fig. 5.13 plots the hydraulic conductivity versus standard deviation of polymer loss for each PMB GCL that evaluated in this study. A trendline is found to fit the data set:

$$\log k = 6.3 \log \sigma - 6.0$$

where k is the hydraulic conductivity (m/s) of PMB GCL, σ is the standard deviation of polymer loss (%) for each GCL. This trend shows that higher hydraulic conductivity can be observed with a PMB GCL exhibiting larger standard deviation of polymer loss.

Results from the post-permeation polymer loss analysis indicate that the hydraulic conductivity of PMB GCLs is dominated by two factors: the amount of polymer elution and preferential flow. The former can be quantified by the average polymer loss obtained from post-permeation LOI and is primarily controlled by leachate characteristics that affect the quality of polymer hydrogel and strength of polymer-bentonite interaction. The latter can be assessed by the standard deviation of polymer loss, where a higher value suggests a larger degree of preferential flow. High hydraulic gradient tends to promote a higher standard deviation value in polymer loss due to an unevenly distributed flow

pattern, and thus has higher potential for high hydraulic conductivity than at lower hydraulic gradient when permeated with the same liquid.

5.6 POLYMER ELUTION INDEX

Since polymer elution is essential in determining the hydraulic conductivity of PMB GCLs, an elution index is introduced to characterize the potential of polymer elution from PMB in different solutions. The elution index, I_E , is defined here as

$$I_E = \frac{PL_{\text{initial}} - PL_{\text{final}}}{PL_{\text{initial}}}$$

where the PL_{initial} and PL_{final} are the polymer loading at “initial” and “final” conditions, respectively. Polymer loading is calculated by assuming the mass loss upon ignition of bentonite (m_b), pure polymer (m_p) and bentonite-polymer mixture (m_b+m_p) are independent and therefore additive. Polymer loading is calculated as

$$PL = \frac{m_p}{m_b + m_p} = \frac{LOI_{B-P} - LOI_{\text{bentonite}}}{LOI_{\text{polymer}} - LOI_{\text{bentonite}}} * 100 (\%)$$

where $LOI_{\text{bentonite}}$, LOI_{polymer} and LOI_{B-P} represent the LOI values obtained from end member bentonite, end member polymer and bentonite-polymer mixture, respectively.

“Initial” polymer loading in the above equation is defined as that corresponding to raw PMB sampled from a fresh (unpermeated) GCL. Modified water content procedures (Chapter 4) are used to obtain material to define “final” polymer loading. As described in Chapter 4, PMB is mixed with testing liquid at a solid-to-liquid ratio of 10% and centrifuged to separate the solids from liquids. The ‘solid’ part after centrifugation is retained for LOI analysis to determine “final” polymer loading.

Fig. 5.14 is a plot of hydraulic conductivity for PMB GCLs versus elution index in different solutions. Theoretically, a higher elution index indicates a lower final polymer loading, which can be attributed to greater separation of the bentonite and polymer fractions during centrifugation in the modified water content test procedure. It may be observed that elution index values are smaller than 0.2 for tests with extremely aggressive solutions (ionic strength greater than 1000 mM or divalent cation concentration greater than 100 mM). Hydraulic conductivity decreases with increasing elution index. The low elution index with extremely aggressive solution may be attributed to polymer chains that formed contracted coils. Polymer with coiled conformation continues to exist in the bentonite pores when conducting LOI measurement but are likely mobile and eluted in presence of seepage force. As illustrated in Fig. 5.15a, contracted polymer coils would be eluted from GCLs and trigger preferential flow resulting in high hydraulic conductivity during permeation. The hydraulic conductivity results obtained with extreme solutions are very high and are within the same order of magnitude. The opposite trend observed here could be caused by uneven polymer distribution in the GCL rolls, where the total amount of polymer, rather than the amount of polymer elution, governs hydraulic conductivity since the small polymer coils will likely be eluted.

For elution indices greater than 0.2, hydraulic conductivity results varied greatly and are divided into two portions in the plot. For GCLs permeated with solutions that have hydraulic conductivity greater than 10^{-10} m/s, polymer in the GCLs may form large polymer globules that would separate from bentonite particles. In this case, little polymer-bentonite interaction is present (Fig. 5.15c) and the flow will not be blocked by polymer in the bentonite intergranular pores. However, for the GCLs permeated with solutions that have

a hydraulic conductivity value lower than 10^{-10} m/s, clogging of the permeameter system was frequently detected. Polymer is hypothesized to have conformation of medium sized polymer coils in these solutions, as shown in Fig.5.15b, and the medium sized polymer may still clog the pores. After system declogging, the polymer coils may be mobilized and contribute to high hydraulic conductivity.

While there is scatter in the relation due to system clogging, results on Fig. 5.14 suggest that a relationship can be used to estimate hydraulic conductivity of PMB GCLs as a function of elution index without considering the clogging and in extreme aggressive solutions. A trendline fit through the data is in the form:

$$\log k = 7.213 \log I_E - 6.699$$

Where k is the hydraulic conductivity (m/s) and I_E is elution index. An increased hydraulic conductivity observed with increasing elution index, where the relationship fits the empirical model.

Fig. 5.14 highlights results at low and high hydraulic gradient, respectively. Though the elution index is similar with the same testing solution, the hydraulic conductivity is quite different with low and high hydraulic gradient. This indicates that the polymer tends to be retained in the GCL and clogs bentonite pores at low hydraulic gradient, whereas, the high hydraulic gradient pushed the clogging polymer out and resulted in a high hydraulic conductivity. This observation is consistent with the observation presented and discussed in above section.

5.7 CONCLUSIONS AND RECOMMENDATIONS

The effect of hydraulic gradient applied in laboratory permeation tests was evaluated in the context of polymer elution and subsequent hydraulic conductivity for PMB GCLs with two permeant solutions of different chemical characteristics. Hydraulic gradients ranging from 10-380 were applied employing the constant-flow method and falling-head method to achieve the series of target hydraulic gradients. Polymer uniformity was assessed by measuring post-permeation LOI to assess the spatial variability of polymer elution and preferential flow. An elution index was proposed to characterize the potential for polymer elution from PMB GCLs in a given test solution. The following conclusions and recommendations are drawn based on the findings of this study:

- The constant-flow method can be employed to achieve low hydraulic gradient ($i \sim 10-30$) in a shorter time period than the falling-head method.
- Pore volumes of flow accumulate more rapidly with higher hydraulic gradient for PMB GCLs permeated with both 50 mM CaCl_2 and Trona leachate using the falling-head method. Hydraulic conductivity is lower with low hydraulic gradient, and increases with increasing hydraulic gradient. A five-order-of-magnitude difference in hydraulic conductivity is observed for PMB GCLs permeated with the same solution at different hydraulic gradients.
- Termination criteria applied to conventional Na-B GCLs may not be effective for representing the equilibrium condition for PMB GCLs due to the effects of polymer elution and preferential flow. Hydraulic conductivity remains essentially constant once preferential flow occurs and reaches steady state much earlier than the achievement of chemical equilibrium. Chemical analysis of effluents to account for

polymer elution, e.g. TOC analysis, are necessary to assess the equilibrium status of hydraulic conductivity tests for PMB GCLs.

- Hydraulic conductivity is dominated by two factors: the amount of polymer elution and the degree of preferential flow. High hydraulic conductivity can be caused by either large amount of polymer elution from PMB GCLs or by significant preferential flow. The former is dominated by characteristics of the permeant solution, which can be assessed by index tests, and quantified by the average polymer loss calculated from post-permeation LOI. Hydraulic gradient has an effect on the latter factor when permeated with the same solution.
- High hydraulic gradient tends to elute polymer from PMB GCLs, reopen bentonite pores clogged by polymer, trigger preferential flow, and result in high hydraulic conductivity. Low hydraulic gradient results in a more uniform flow pattern (maximum flow area) because the seepage force is not sufficient to trigger preferential flow.
- Increase in hydraulic gradient has the potential to increase hydraulic conductivity of PMB GCLs by causing preferential flow; however, the long term (permeation > 2 years) effect on hydraulic conductivity under low hydraulic gradient (e.g., $i=40$) stays unclear. Future study is needed to evaluate polymer elution and hydraulic conductivity for PMB GCLs with low hydraulic gradient for long term permeation.
- Standard deviation in polymer loss obtained from post-permeation LOI measurements can be used to assess the degree of preferential flow. The larger the standard deviation value, the more significant preferential flow in the GCL. A

relationship was found between hydraulic conductivity of PMB GCL and standard deviation of polymer loss.

- Elution index can be used to evaluate the potential of polymer elution from bentonite with any permeant solution. Correlation between elution index and hydraulic conductivity of PMB GCLs supports the hypothesis that polymer clogging is a primary mechanism by which PMB GCLs maintain low hydraulic conductivity. Future study is recommended to classify elution index more specifically with polymer conformation and polymer bentonite interaction for $I_E > 0.2$.
- Polymer may also clog parts of the testing apparatus and result in significant changes in measured hydraulic conductivity. A modified hydraulic conductivity test apparatus is recommended to minimize polymer clogging in testing apparatus.

5.8 REFERENCES

- Ashmawy, A., Darwish, E., Sotelo, N., and Muhammad, N. (2002) Hydraulic performance of untreated and polymer-treated bentonite in inorganic landfill leachates. *Clays and Clay Miner.*, 50(5), 546-552.
- Benson, C., Kucukkirca, E., and Scalia, J. (2010) Properties of geosynthetics exhumed from a final cover at a solid waste landfill. *Geotext. Geomembr.*, 28, 536-546.
- Benson, C., Chen, J., and Edil, T. (2013) Hydraulic conductivity of geosynthetic clay liners to coal combustion product leachates, *interim report*. Sustainability Report No. OS-13-07, Office of Sustainability, University of Wisconsin-Madison, Madison, WI.
- Chen, J. (2015). Compatibility of Geosynthetic Clay Liners with Leachate from CCP Management Facilities. (Doctor of Philosophy) University of Wisconsin-Madison.
- Dunn, J. R., and Mitchell, J. K. (1984). Fluid Conductivity Testing of Fine-Grained Soils. *Journal of Geotechnical Engineering*, 110(11), 1648-1665.
- Daniel, D.E., Shan, H.-Y., and Anderson, J.D., 1993. Effects of partial wetting on the performance of the bentonite component of a geosynthetic clay liner. *Geosynthetics '93*, IFAI, St. Paul, MN, Vol. 3, pp. 1482-1496.
- Didier, G., Comeaga, L., (1997). Influence of initial hydration conditions on GCL leachate permeability. In: Well, L.W. (Ed.), *Testing and Acceptance Criteria for Geosynthetic Clay Liners*, ASTM STP 1308.ASTM, West Conshohocken, PA, pp. 181-195.

- Di Emedio, G., Van Impe, W., and Flores, V. (2011) Advances in geosynthetic clay liners: polymer enhanced clays. GeoFrontiers 2011. Advances in Geotechnical Engineering, American Society of Civil Engineers, Reston, USA, 1931-1940.
- EPA. (2001). Geosynthetic Clay Liners Used in Municipal Solid Waste Landfills. United States Environmental Protection Agency.
- EPRI (2006). Characterization of field leachates at coal combustion product management sites, Electric Power Research Institute, Palo Alto, CA.1012578.
- EPRI (2009). Coal ash: characteristics, management, and environmental issues. Electric Power Research Institute, Palo Alto, CA.1019022.
- Kolstad, D., Benson, C., Edil, T., and Jo, H. (2004) Hydraulic conductivity of dense prehydrated GCL permeated with aggressive inorganic solutions. Geosynth. Int., 11(3).
- Katsumi, T., Ishimori, Ho, Onikata, M., and Fukagawa, R. (2008) Long-term barrier performance of modified bentonite materials against sodium and calcium permeant solutions. Geotext. and Geomembranes 26(1), 14-30.
- Lin, L., 1998. Effect of wet-dry cycling on swelling and hydraulic conductivity of geosynthetic clay liners. MS Thesis. University of Wisconsin-Madison.
- Lin, L., Katsunami, T., Kamon, M., Benson, C., Onikata, M., and Kondo, M. (2000) Evaluation of chemical-resistant bentonite for landfill barrier application. Annals of Disas. Prev. Res. Inst., Kyoto Univ., No. 43 B-2, 525-533.

- McRory, J., and Ashmawy, A. (2005) Polymer treatment of bentonite clay for contaminant resistant barriers. GSP 142 Waste Containment and Remediation, 1-11.
- Mitchell, J. K., & Soga, K. (2005). *Fundamental of Soil Behavior*, Third Edition. Hoboken, New Jersey: John Wiley & Sons, Inc.
- Petrov, R.J., Rowe, R.K., (1997). Geosynthetic clay liner (GCL) chemical compatibility by hydraulic conductivity testing and factors impacting its performance. *Canadian Geotechnical Journal* 34, 863-885.
- Petrov, R.J., Rowe, R.K., Quigley, R.M., (1997a). Comparison of laboratory-measured GCL hydraulic conductivity based on three permeameter types. *Geotechnical Testing Journal*, ASTM, West Conshohocken, PA, 20 (1), 49-62.
- Petrov, R.J., Rowe, R.K., Quigley, R.M., (1997b). Selected factors influencing GCL hydraulic conductivity. *Journal of Geotechnical and Geoenvironmental Engineering*, ASCE, Reston, VA 123 (8), 683-695.
- Quaranta, J.D., Gabr, M.A., Bowders, J.J., (1997). First-exposure performance of the bentonite component of a GCL in a low-pH, calcium-enriched environment. In: Well, L.W. (Ed.), *Testing and Acceptance Criteria for Geosynthetic Clay Liners*, ASTM STP 1308. ASTM, West Conshohocken, PA, pp. 162-177.
- Rad, N.S., Jacobson, B.D., Bachus, R.C., (1994). Compatibility of geosynthetic clay liners with organic and inorganic permeants, *Proc. Fifth International Conference on Geotextiles, Geomembranes and Related Products*, pp. 1165-1168.

- Reybrock, W. (2017). Methods for Testing the Effect of Hydraulic Gradient on the Polymer Elution of Polymer GCLs. (Thesis, Master of Science) University of Wisconsin-Madison.
- Ruhl, J.L., Daniel, D.E., (1997). Geosynthetic clay liners permeated with chemical solutions and leachates. *Journal of Geotechnical and Geoenvironmental Engineering*, ASCE, Reston, VA 123 (4), 369-381.
- Salihoglu, H. (2015), Behavior of Polymer-Modified Bentonites with Aggressive leachates, (Thesis, Master of Science) University of Wisconsin-Madison.
- Scalia, J., Benson, C., Bohnhoff, G., Edil, T., and Shackelford, C. (2014) Long-term hydraulic conductivity of a bentonite-polymer composite permeated with aggressive inorganic solutions. *J. Geotech. Geoenviron. Eng.*, 140(3), 1-13.
- Scalia, J., and Benson, C. (2014) Barrier Performance of Bentonite-Polyacrylate Nanocomposite to Artificial Ocean Water. *Proceedings, Geo-Congress 2014 Geo-Characterization and Modeling for Sustainability*, GSP No. 234, ASCE, Reston, VA.
- Shackelford, C., Benson, C., Katsumi, T., Edil, T., and Lin, L. (2000). Evaluating the hydraulic conductivity of GCLs permeated with non-standard liquids. *Geotext. and Geomembranes*, 18(2-3), 133-161.
- Shan, H.-Y., Daniel, D.E., (1991). Results of laboratory tests on a geotextile/bentonite liner material. *Geosynthetics*, IFAI, St. Paul, MN, Vol. 2, pp. 517-535.

Tian, K. (2015). Long-Term Performance of Geosynthetic Liner Materials in Low-Level Radioactive Waste Disposal Facilities. (Doctor of Philosophy) University of Wisconsin-Madison.

Trauger R., and Darlington J. (2000) Next-generation geosynthetic clay liners for improved durability and performance. TR-220. Colloid Environmental Technologies Company, Arlington Heights, 2-14.

5.9 TABLES

Table 5.1. Characteristics of Trona Leachate

Major Cation and Anion Concentrations (mM)		BULK characteristics	
Ca	12.5	TOC (mg/L)	0.95
Na	645	EC (S/m)	41.3
Mg	6.3	pH	11.0±0.5
K	5.1	Ionic strength, <i>I</i> (mM)	755
Chloride	-	RMD (M ^{1/2})	4.40
Sulfate	343	Anion Ratio (Cl ⁻ /SO ₄ ²⁻)	0.0

Table 5.2. Effective Stress Conditions of Tests with Different Gradient

Hydraulic Gradient Effective Stress		40	55	80	90	120	135	150
		Inflow Side	Minimum	15.6	14.3	11.6	11.1	12.4
Maximum	17.6		17.4	13.7	13.2	14.5	14.7	16.1
Outflow Side		19.2	20.3	20.6	21.1	25.5	25.6	26.9
Average		18.1	18.1	16.6	16.6	19.5	19.6	20.2

Table 5.3. Hydraulic conductivity of GCLs permeated at different hydraulic gradient

Hydraulic Gradient	PVF	Permeation Time (d)	Hydraulic Conductivity (m/s)
Permeate to 50mM CaCl ₂			
40	5.25	600.4	5.8×10^{-11}
190 (increased from 40)	27.75	0.7	5.7×10^{-8}
55	1.21	584.5	1.8×10^{-12}
190 (increased from 55)	2.02	79.3	1.0×10^{-11}
80	43.37	19.8	4.9×10^{-8}
90	44.22	19.6	5.6×10^{-8}
120	43.25	2.3	2.5×10^{-7}
135	46.03	6.1	6.9×10^{-8}
150	60.35	0.5	2.8×10^{-7}
15 (constant Flow)	69.42	-	2.8×10^{-7}
Permeate to Trona			
40	1.47	411.2	6.3×10^{-11}
190 (increased from 40)	21.6	4.0	3.4×10^{-9}
90	7.95	397.4	5.3×10^{-12}
190 (increased from 90)	2.01	76.0	7.1×10^{-12}
120	47.34	117.5	2.6×10^{-8}
190 (increased from 120)	8.4	0.04	1.5×10^{-7}
190	19.81	980.8	3.7×10^{-12}
380 (increased from 190)	18.2	17.1	8.8×10^{-9}

Note: Permeation time refers to cumulative permeation time in unit of days.

5.10 FIGURES

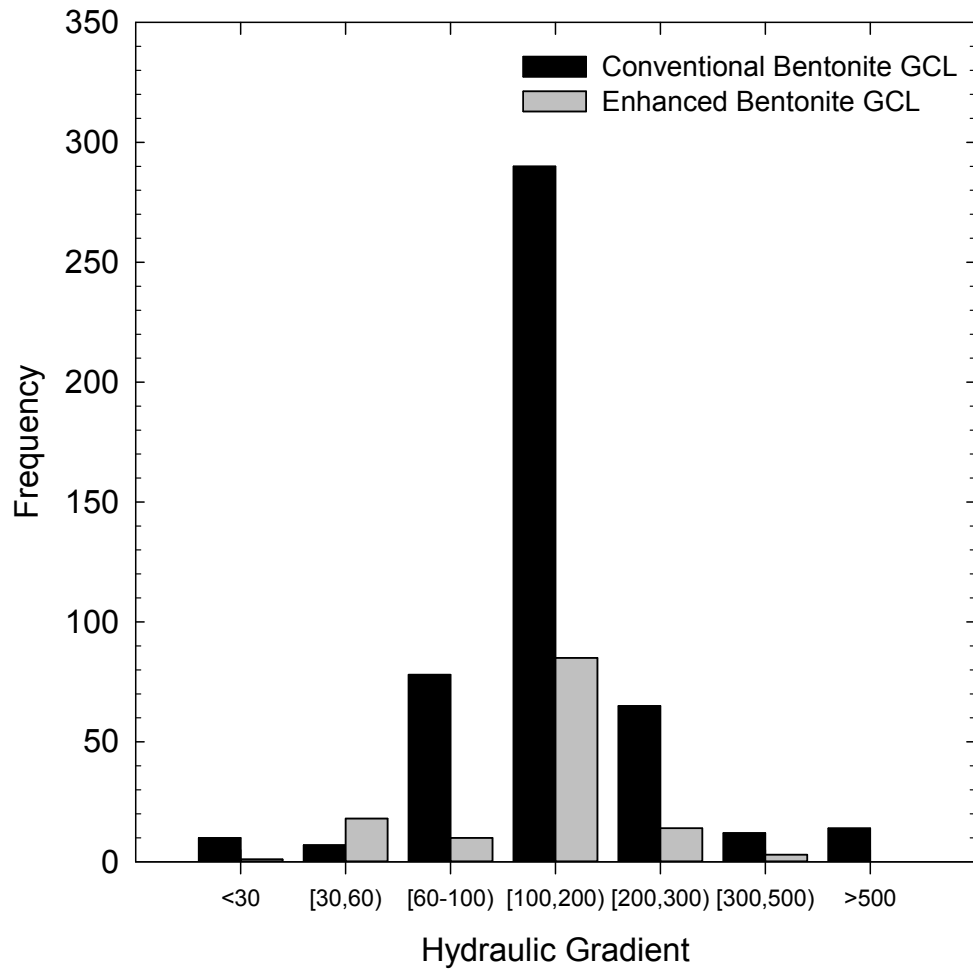


Figure 5.1. Hydraulic gradients used in previous studies and this study for conventional bentonite GCLs and enhanced bentonite GCLs.

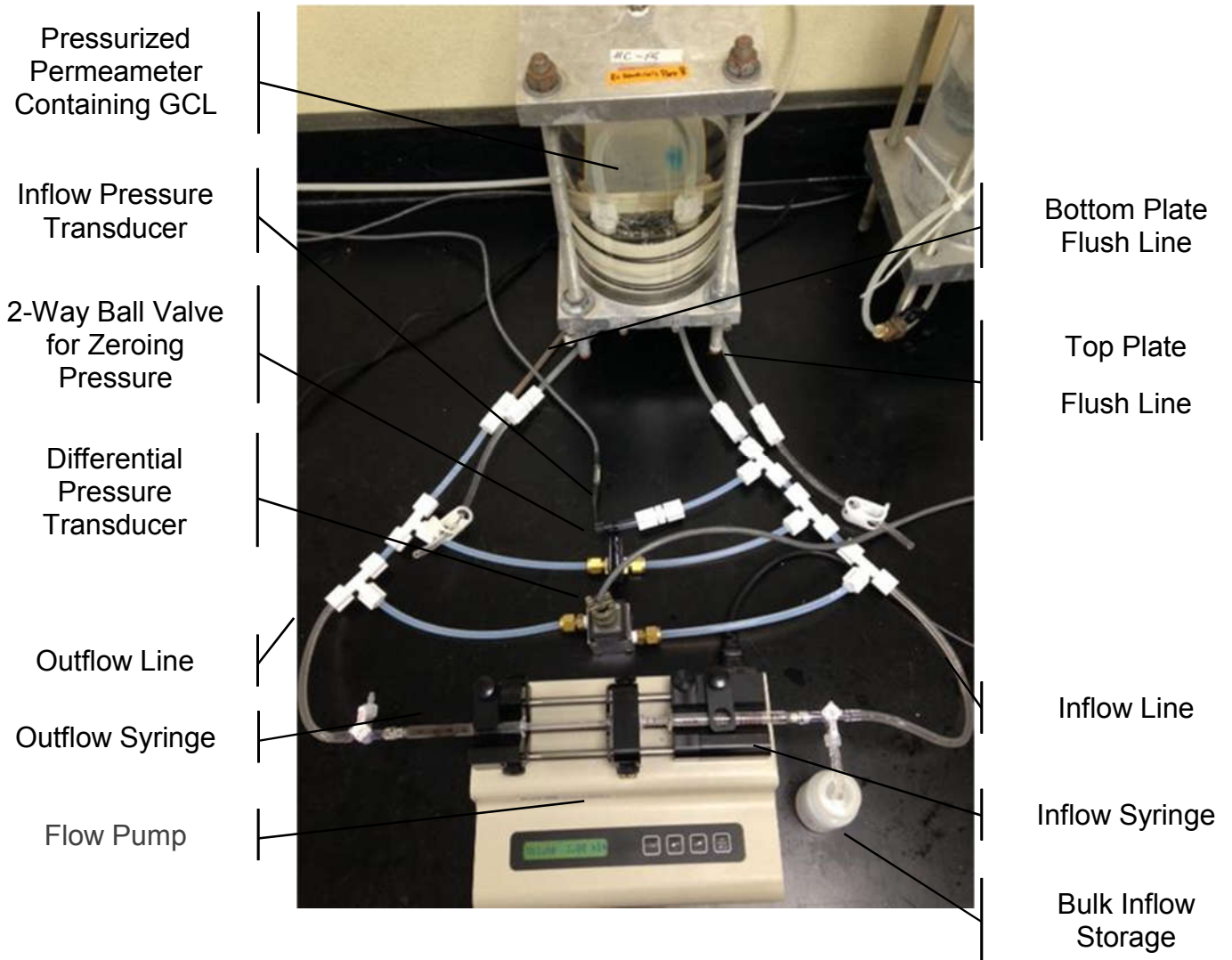


Figure 5.2. Photograph with main components of constant-flow pump apparatus

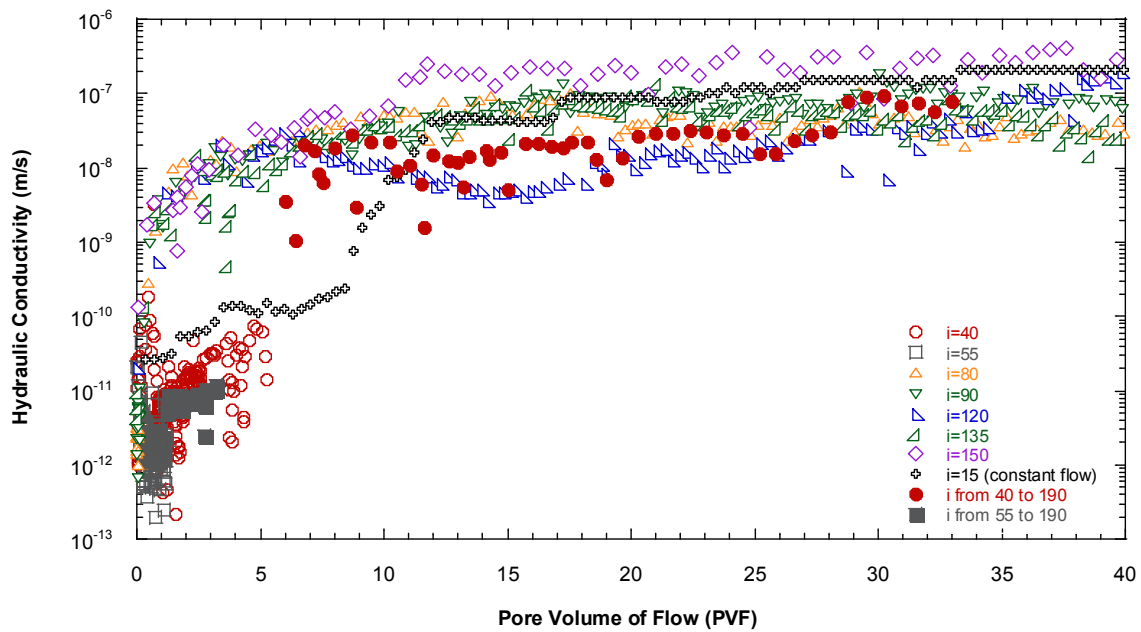


Figure 5.3. Hydraulic conductivity values plotted with PVF at varying average hydraulic gradients for PMB GCLs permeated with 50 mM CaCl_2 .

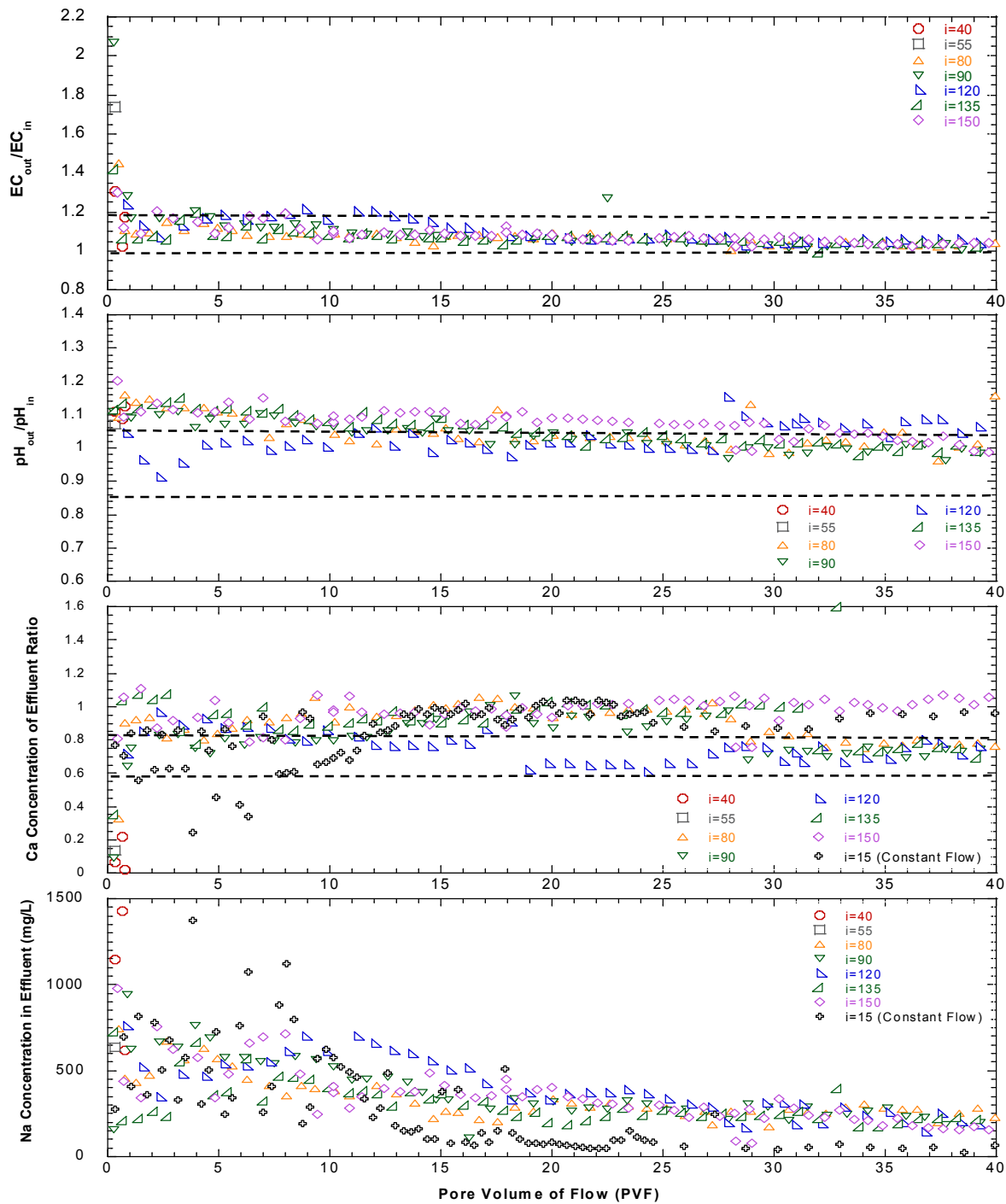


Figure 5.4. Chemical analysis data of effluents from hydraulic conductivity tests on (a) EC ratio (b) pH ratio, (c) concentration of Ca ratio, and (d) concentration of Na permeated to 50 mM CaCl₂.

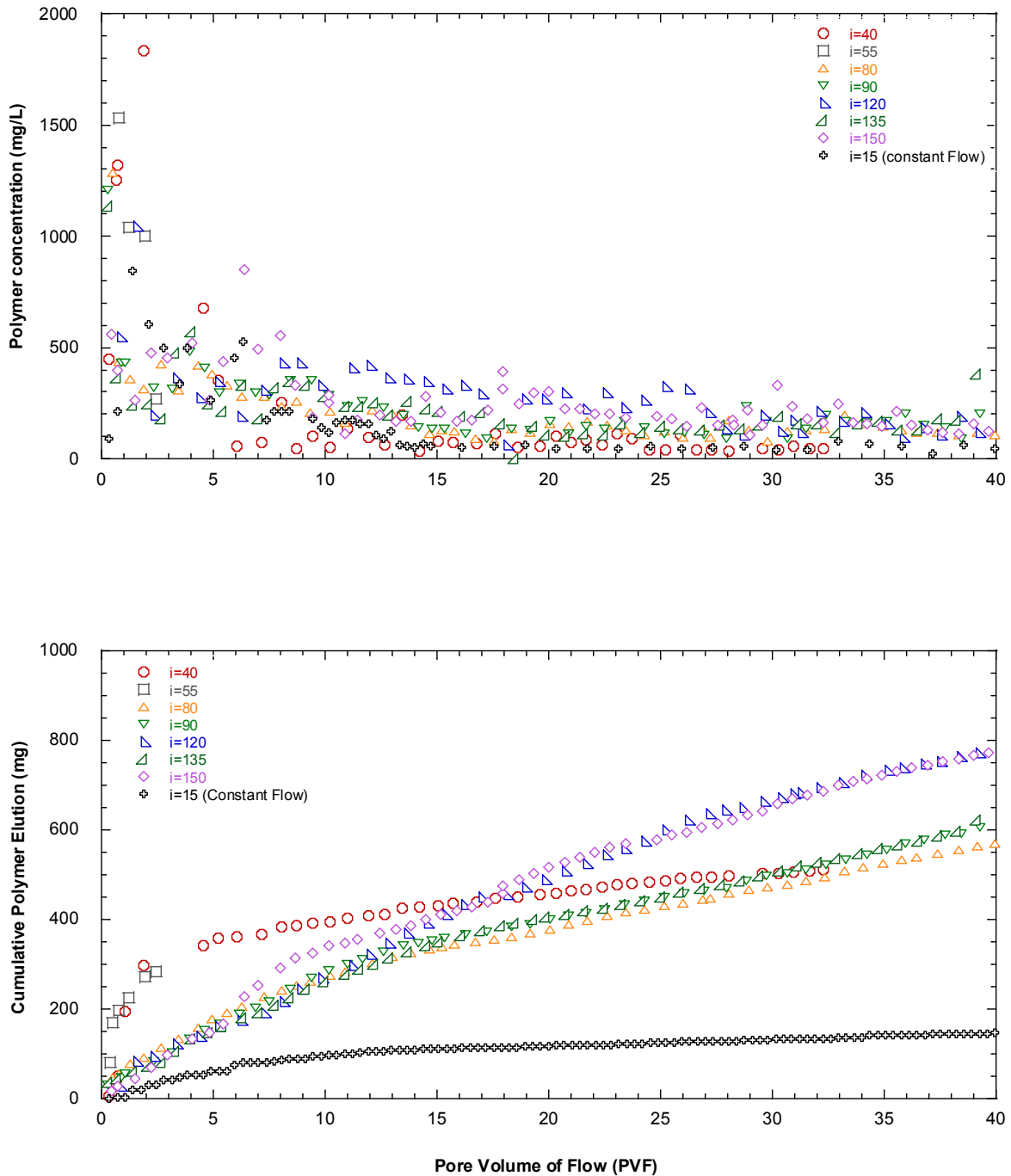


Figure 5.5. Hydraulic Conductivity (a) and cumulative polymer elution (b) of PMB GCLs permeated with 50 mM CaCl₂.

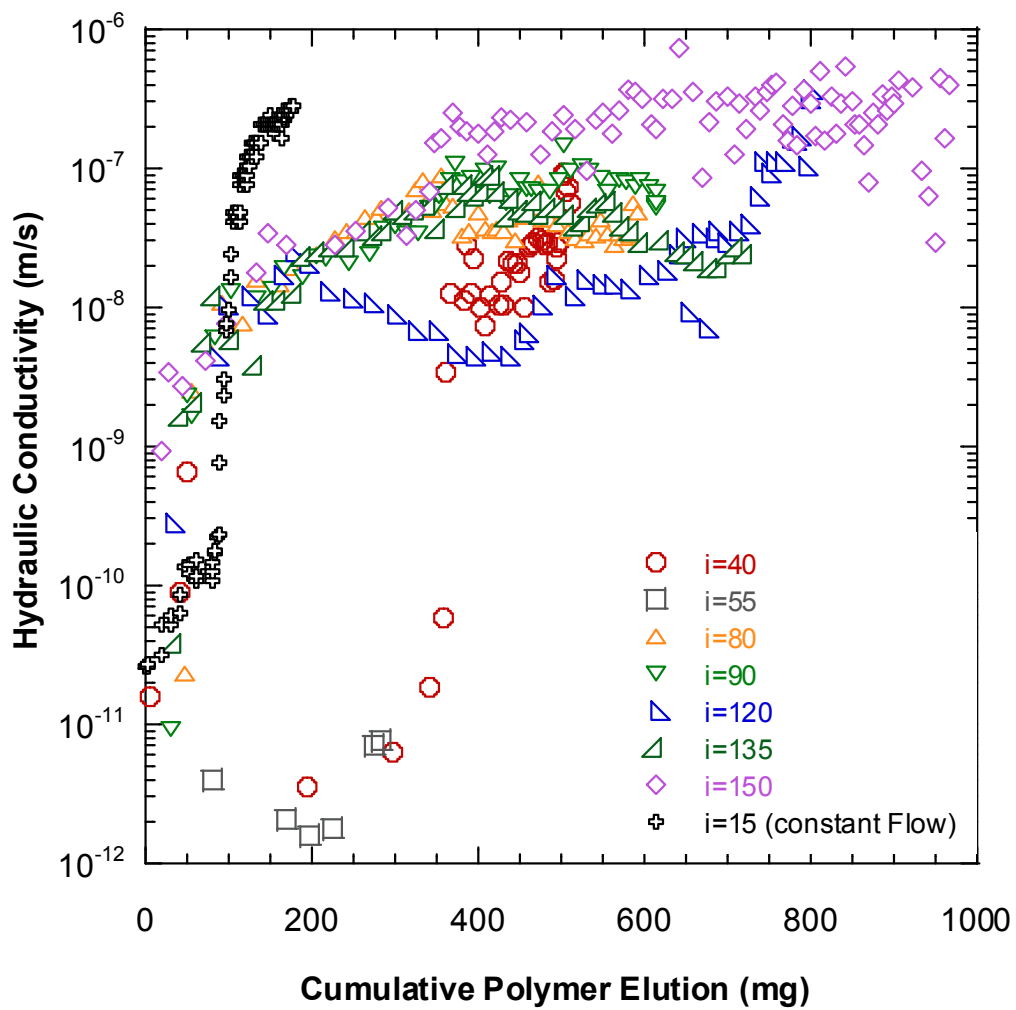


Figure 5.6. Hydraulic Conductivity versus cumulative polymer elution of PMB GCLs permeated with 50 mM CaCl_2 .

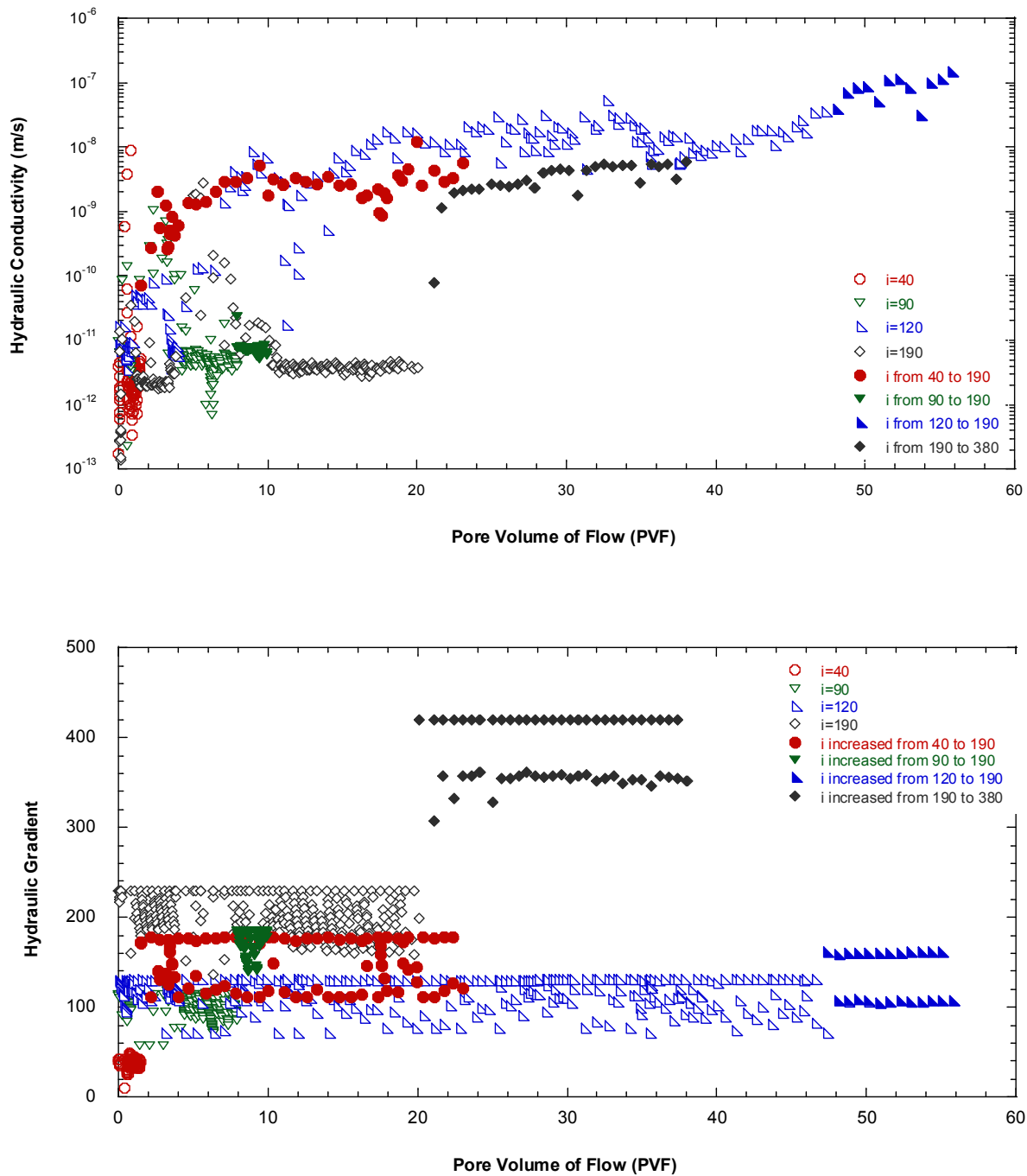


Figure 5.7. Hydraulic conductivity (a) and hydraulic gradient (b) plotted with PVF with falling head methods at varying average hydraulic gradients for PMB GCLs permeated with Trona leachate.

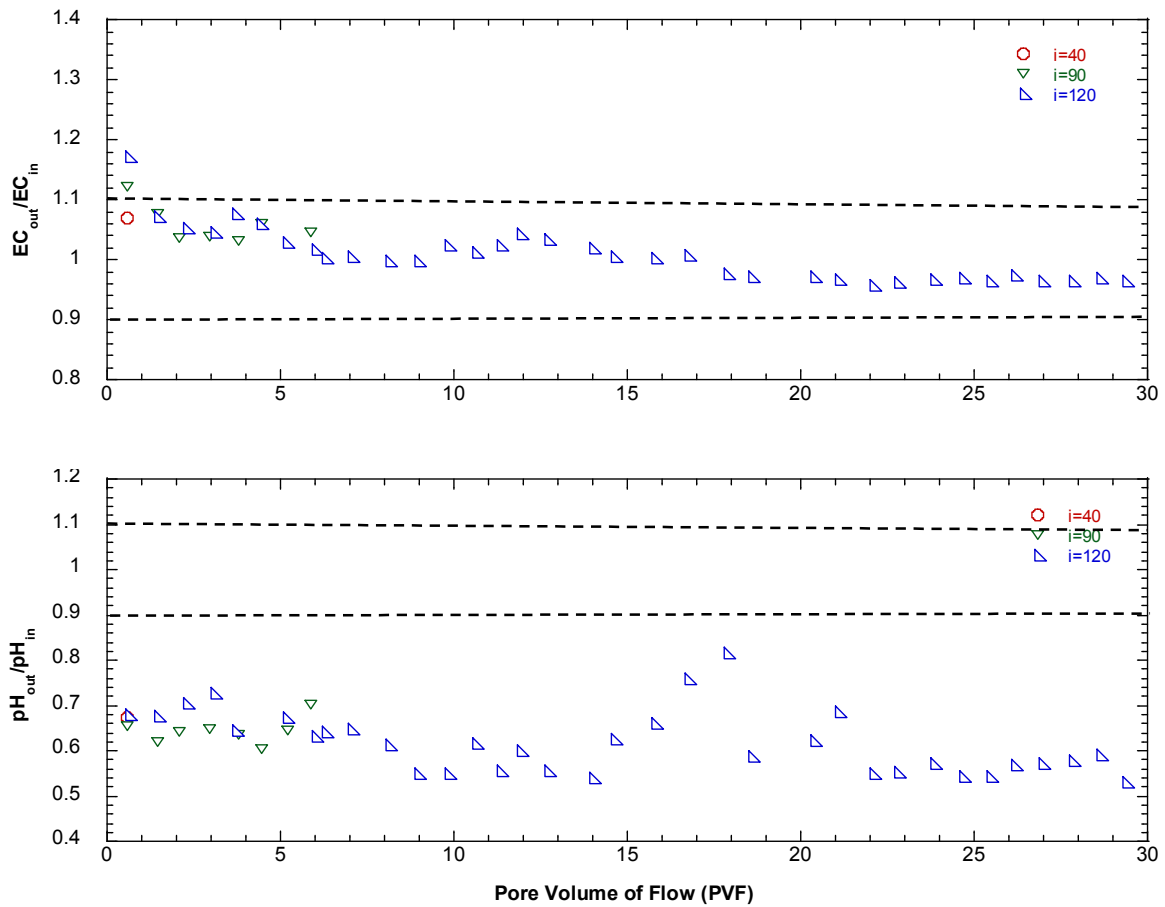


Figure 5.8. Chemical analysis data of effluents from hydraulic conductivity tests on (a) EC ratio, and (b) pH ratio permeated to Trona leachate.

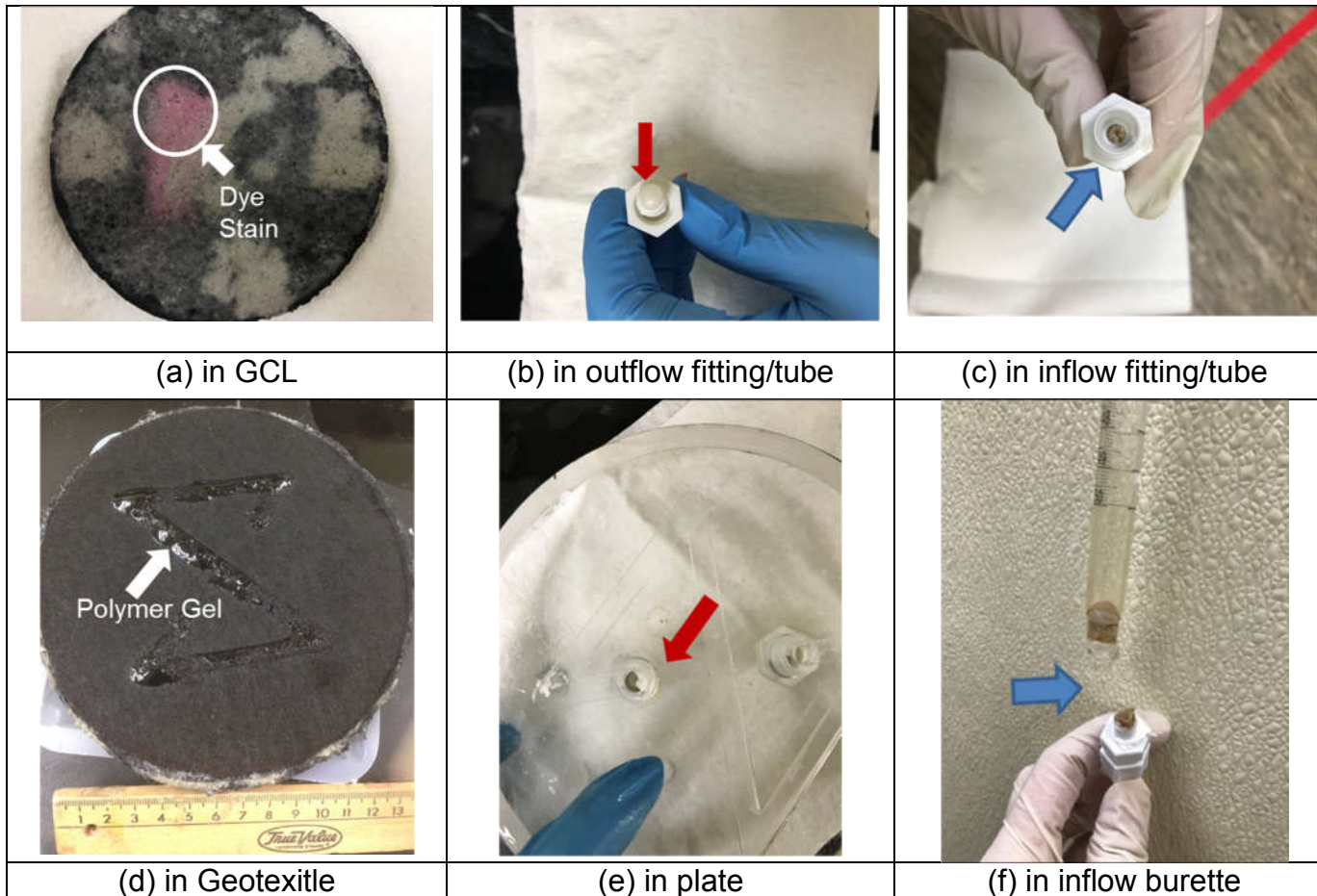


Figure 5.9. Photographs of polymer clogging observed: (a) in GCL specimen with dye marking preferential flow path, (b) in outflow fitting/tube, (c) in inflow fitting/tubes, (d) in geosynthetic fabric, (e) in outflow plate, and (f) in inflow burette.

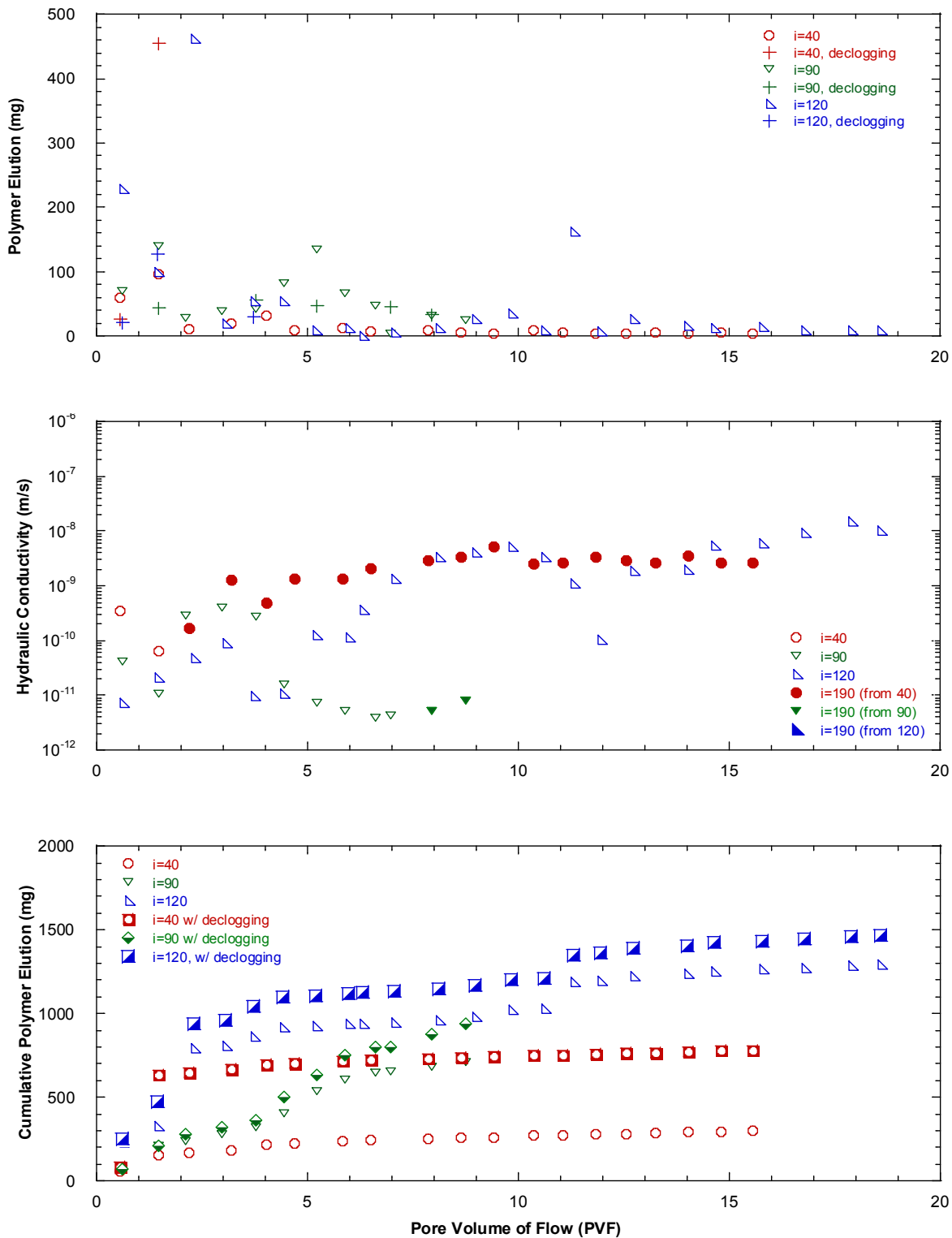
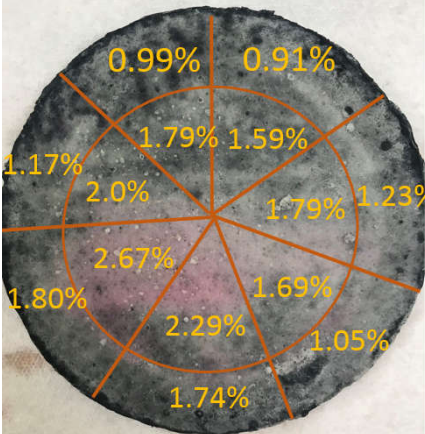
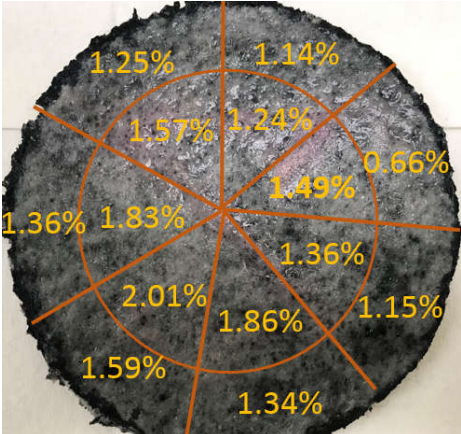


Figure 5.10. Polymer elution in effluents and declogging liquids (a), hydraulic conductivity (b) and cumulative polymer elution (c) plotted with pore volume of flow permeated with Trona.

Hydraulic Gradient	40	55
Pre-LOI (%)	5.68	5.68
Post -LOI		
Polymer loss (%)	1.62±0.51	1.62±0.35
Final k (m/s)	5.7 x 10 ⁻⁸	1.0 x 10 ⁻¹¹

NOTE: Numbers in each 'pie' section indicate the polymer loss.

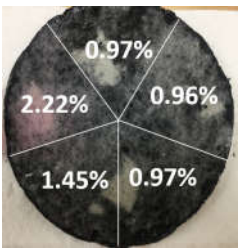
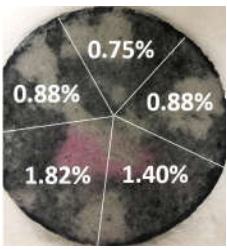

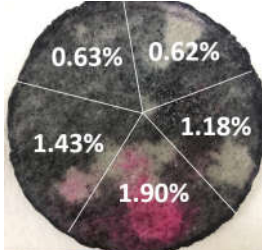
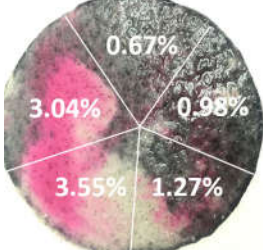
Hydraulic Gradient	80	90	120	135	150
Pre-LOI (%)	5.56	5.24	4.51	5.31	5.30
Post -LOI					
Polymer loss (%)	1.32±0.55	1.15±0.45	1.72±0.73	1.15±0.55	1.90±1.30
Final k (m/s)	4.9 x 10 ⁻⁸	5.6 x 10 ⁻⁸	2.5 x 10 ⁻⁷	6.9 x 10 ⁻⁸	2.8 x 10 ⁻⁷

Figure 5.11. Pictures of PMB GCL taken after permeation with Rhodamine dye staining and polymer loss calculated from post-permeation LOI permeate to 50 mM CaCl₂ at various hydraulic gradients.

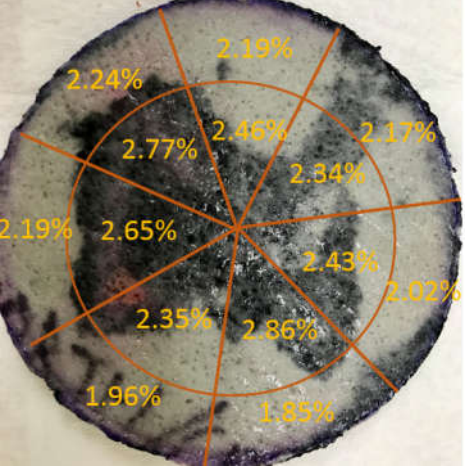
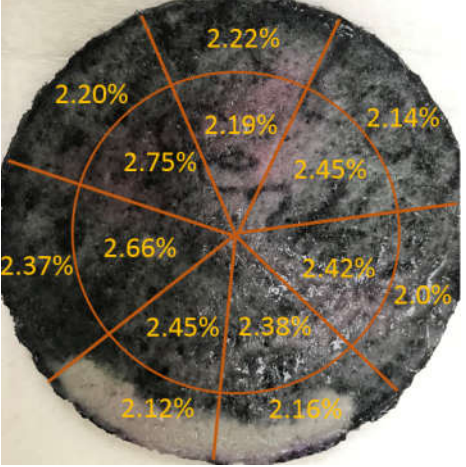
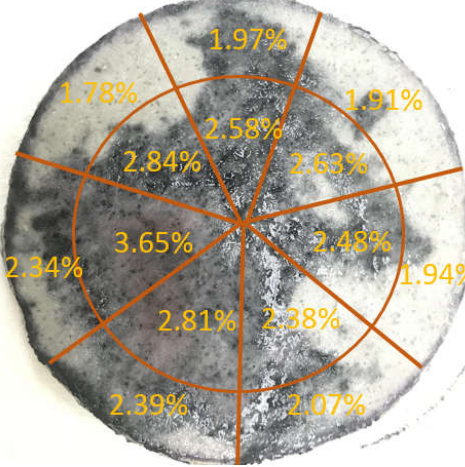
Hydraulic Gradient	40	90	120
Pre-LOI (%)	5.10	5.10	5.10
Post -LOI			
Polymer loss (%)	2.31±0.30	2.32±0.21	2.41±0.49
Final k (m/s)	3.4 x 10 ⁻⁹	7.1 x 10 ⁻¹²	1.5 x 10 ⁻⁷

Figure 5.12. Pictures of PMB GCL taken after permeation with Rhodamine dye staining and polymer loss calculated from post-permeation LOI permeate to Trona at hydraulic gradients of 40, 90, and 120.

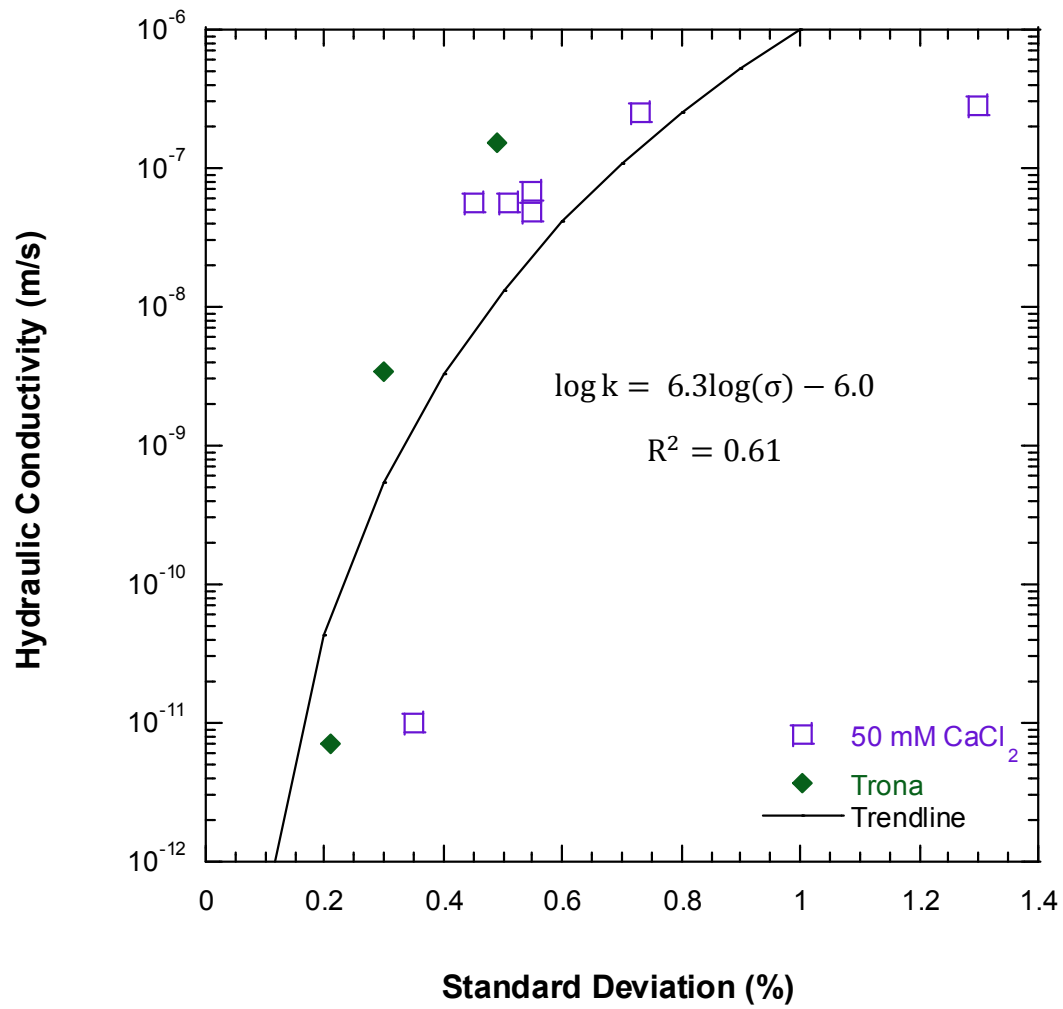


Figure 5.13. Hydraulic conductivity versus standard deviation of polymer loss after permeation on PMB GCLs.

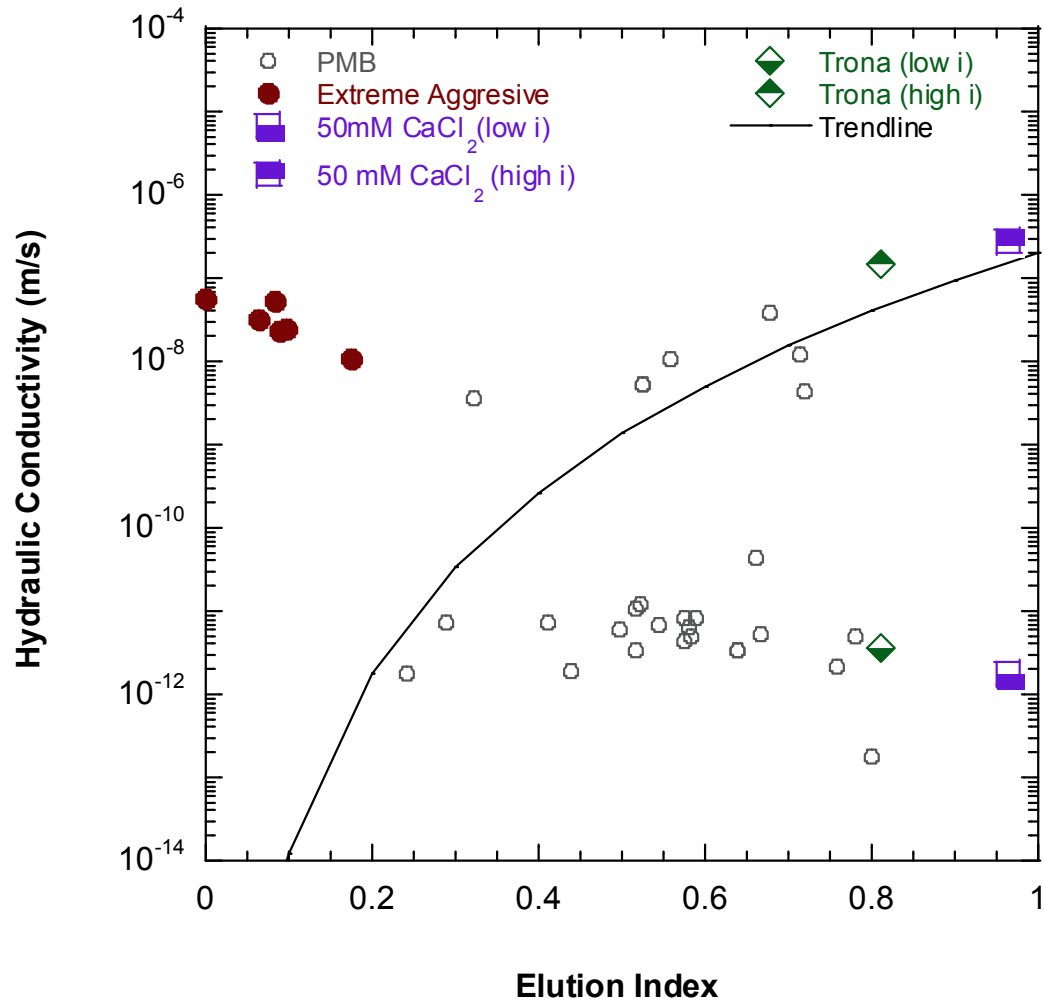


Figure 5.14. Hydraulic conductivity versus elution index of polymer bentonite mixture.

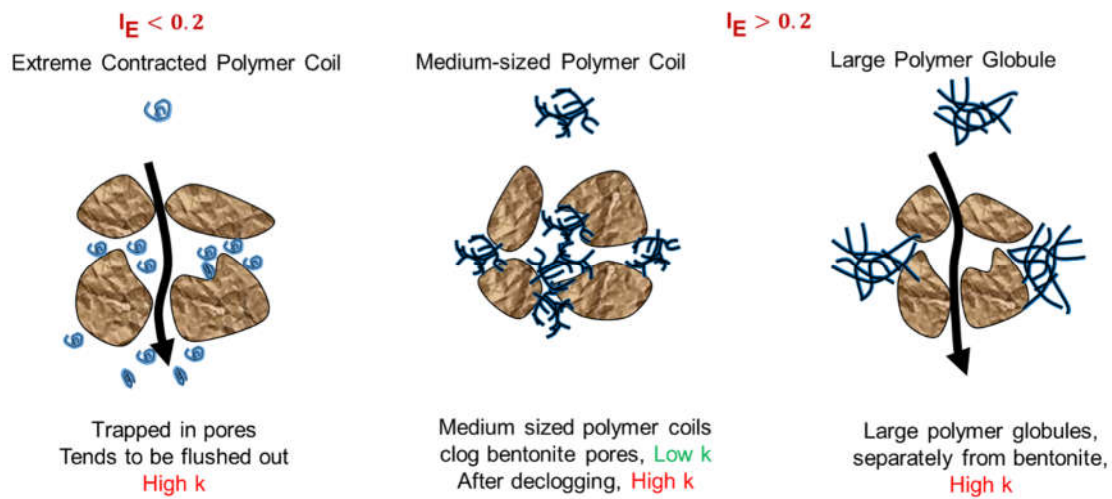


Figure 5.15. Conceptual representation of polymer modified bentonite in poor solutions (i.e. high ionic strength, low RMD), indicating the polymer conformation, polymer bentonite interaction and potential flow path in relationship with elution index.

CHAPTER SIX

EFFECT OF ANIONS ON HYDRAULIC CONDUCTIVITY OF POLYMER MODIFIED BENTONITE GEOSYNTHETIC CLAY LINERS

ABSTRACT

Previous studies have indicated that anion species affect the hydraulic conductivity of polymer modified bentonite (PMB) geosynthetic clay liners (GCLs). Experiments were conducted to evaluate the turbidity, viscosity, free swell, and modified water content of polymer and polymer-bentonite suspensions and the hydraulic conductivity of PMB-GCLs for a suite of single species anion solutions selected from the Hofmeister anion ranking series. Turbidity and viscosity of polymer suspensions showed similar trends according to anion type. Free swelling, viscosity, and modified water content for polymer-bentonite mixtures also showed consistent trends, but different than those observed for the polymer suspensions. Results suggest that polymer-bentonite interaction is the dominating factor that determines these characteristics of polymer-bentonite suspensions and that this behavior is affected by anion type. Hydraulic conductivity of PMB-GCLs is dominated by bentonite fraction at the initial stage of permeation, then by polymer-bentonite interaction as permeation continues, and ultimately by polymer elution. Anion type influences all three factors, and thus is considered an essential factor in influencing the hydraulic conductivity of PMB-GCLs.

6.1 INTRODUCTION

Geosynthetic clay liners (GCLs) are widely used for liners and covers in waste containment systems containing a variety of leachate compositions (Shackelford et al. 2000, Benson et al. 2010, Scalia et al. 2014). A number of studies have focused on the effect of cation type (e.g., monovalent vs. divalent) on the hydraulic conductivity of Na-B and PMB GCLs (Jo et al. 2001, Kolstad et al. 2004 a,b, Scalia et al. 2014), while only limited study has been conducted to evaluate the effects of anion type. Tian et al. (2017) found that the hydraulic conductivity of a PMB GCL can increase up to three orders of magnitude with solutions having a fixed cation, but with a changing ratio in anions (SO_4^{2-} and Cl^-), and hypothesized that the sensitivity of PMB GCL to anion ratio was due to collapse of polymer in Cl^- -rich solutions. Results from Chapter 4 in this thesis show that the chemical composition of a test solution determines the polymer conformation and the quality of polymer hydrogel, and thus influences the hydraulic performance of PMB-GCLs by altering the polymer-bentonite network structure. In this chapter, experiments were conducted to evaluate how anion species affects the behavior of pure polymer suspensions and suspensions of PMB. Seven single-species sodium solutions with different anions were selected to evaluate the turbidity and viscosity of polymer suspensions, behaviors of PMB suspensions, and the hydraulic conductivity of PMB-GCLs.

6.2 BACKGROUND

6.2.1. Anion Fraction in Leachates

A literature review was conducted to summarize anion composition in typical leachates chemistries. Fig. 6.1 summarizes the anion ratio ($[\text{Cl}^-]/[\text{SO}_4^{2-}]$) of mining

leachate, acid mine drainage (AMD), CCP leachate, low-level radioactive-waste leachate, municipal solid waste leachate, incineration ash leachate, and hazardous waste leachate. The anion ratio in these leachates ranges from Cl^- rich to SO_4^{2-} rich conditions due to composition of the wastes and various industrial processes. For example, acidic sulfur-rich wastewater is commonly generated as the byproduct of mining process because sulfuric acid is commonly used in the heap leaching process to extract the metal out of copper, nickel, or gold ore. AMD is also generated during mining process because sulfide-bearing material is exposed to oxygen and water (e.g., oxidation of pyrite) (Akcil and Koldas 2006).

6.2.2. Hofmeister Series on Anion Rank

Hofmeister that discovered specific ions (cation and anion) have an effect on precipitation of purified egg white, and ranked the ions in an order according to the efficiency of the ions, known as the Hofmeister series. A typical rank on anions is in the series (Cereser, 2010): CO_3^{2-} > SO_4^{2-} > F^- > Cl^- > Br^- > NO_3^- > I^- > SCN^- . Proteins are natural polymers of amino acids and exhibit some trends in aqueous solution with the above anions (from left to right), e.g. decreased surface tension and protein stability, and increased solubility and protein denaturation. Zhang and Cremer (2006) found that kosmotropic ions (anions to the left of Cl^-) have stabilizing and salting-out effects both on proteins and on macromolecules. There is a motivation to systematically study the anion effect on polymer suspensions, and to understand if the anions exhibit rank as Hofmeister.

6.3 MATERIALS AND METHODS

6.3.1. Geosynthetic Clay Liner

Tests were conducted on a GCL containing a polymer modified bentonite (PMB). Properties of the GCL are summarized in Table 1.1. The major mineral component of the bentonite is montmorillonite (79%), as determined by X-ray diffraction (XRD) using the methods in Scalia et al. (2014). Swell index of the PMB in DI water is 27 mL/2 g following the procedures in ASTM D5890. Polymer loading of the PMB-GCL is 5.1% as determined by the difference in loss on ignition (LOI) between the PMBs and the base bentonite, as suggested by Scalia et al. (2014). This approach is based on the assumption that the polymer is completely combusted during the LOI test conducted using the procedure in ASTM D7348 (Tian et al. 2016). LOI of the unamended Na-B was 1.6%, and is attributed to loss of strongly bounded water molecules, calcite, and organic matter (Scalia et al. 2014, Tian et al. 2016).

6.3.2. Testing Liquids

Test solutions for the anion series study were Na solutions at fixed concentration of 300 mM with various single anion species: CO_3^{2-} , OH^- , NO_3^- , Cl^- , F^- , I^- . Solutions were prepared with reagent grade salts (e.g., NaCl and Na_2SO_4) mixed in Type II DI water per ASTM D1193. Anion ratio solutions described in Chapter 3 (Table 3.1) were also used for conducting modified water content tests for PMBs. The R defined as the molar concentration ratio of Cl^- to SO_4^{2-} is referred to as the anion ratio, and solutions were prepared with a fixed cation concentration (e.g., 300 mM Na^+ , 300 mM K^+ , and 50 mM Mg^{2+}) and $R = 0$ (pure SO_4^{2-}), 0.2, 1, 5, 20, and ∞ (pure Cl^-).

6.3.3. Hydraulic Conductivity Testing

Hydraulic conductivity tests on the GCL specimens were conducted in flexible-wall permeameters using the falling headwater-constant tailwater method described in ASTM D6766. GCL specimens were hydrated with the permeant liquid in the permeameter for 48 hr at an effective confining stress of 10 kPa and without a hydraulic gradient. After hydration, the effective confining stress was increased to 20 kPa and the hydraulic gradient was set at 150. Influent for the tests was contained in 50-mL burettes sealed with parafilm to prevent evaporation. Effluent was collected in 60-mL polyethylene bottles. Samples of the influent and effluent solutions were analyzed periodically for elemental concentrations by inductively coupled plasma-optical emission spectroscopy (ICP-OES) following USEPA Method 6010.

Equilibrium was defined using the hydraulic and chemical equilibrium criteria in by ASTM D6766 along with the additional criteria for influent and effluent concentrations described in Bradshaw and Benson (2014) and Tian et al. (2016). The termination criteria in D6766 require hydraulic conductivity within 25% of the mean for three consecutive measurements and no temporal trend. The ratio of outflow (Q_{out}) to inflow (Q_{in}) must also be within $\pm 25\%$ for at least three measurements. The electrical conductivity of the effluent (EC_{out}) show no temporal trend and fall within 10% of the electrical conductivity of the influent (EC_{in}). pH of the effluent and influent was monitored in the study as a supplement to chemical equilibrium. Similar to the EC measurement, pH of the effluent were required to be within 10% of the pH of the influent.

6.3.4. Total Organic Carbon Analysis

Total organic carbon (TOC) analysis was conducted on effluent from the hydraulic conductivity tests to quantify the mass of polymer eluted from the PMB-GCLs during

permeation. TOC was measured in accordance with ASTM D4839 using a Shimadzu TOC analyzer (TOC-VCSH, Shimadzu, Kyoto, Japan). Samples were acidified with HCl to achieve pH = 2 prior to analysis. The inorganic carbon component of the sample was removed by sparging with CO₂-free gas. The remaining organic carbon fraction was converted to CO₂ by combusting the sample. Calibration solutions were prepared using anhydrous potassium hydrogen phthalate to various concentrations with DI water.

6.3.5. Viscosity Testing

The methods used for viscosity tests on polymer and PMB suspensions with a solid-to-liquid mass ratio of 0.5% and 10% respectively are detailed in Chapter 3. Shear rate for these tests was controlled at a torque speed of 100 RPM and for a maximum measured time of 20 minutes. PMB granules were removed from GCL, placed in a beaker with the corresponding test solution, and continuously stirred using a blunt-bladed mixing paddle powered by an external motor. Mixing time was considered complete when uniform suspensions were achieved by manual visual observation. Viscosity tests in all cases were conducted immediately after mixing.

6.3.6. Modified Water Content Testing

Modified water content tests were conducted on PMB extracted from PMB-GCLs with permeant solutions at solid-to-liquid ratio at 10%. Prior to test, the PMB slurries were centrifuged as described in Chapter 4. The 'solid' part and 'liquid' part were separated by gravity, then the 'solid' part was transferred and measured for water content following ASTM D2216.

6.3.7. Turbidity Testing

The methods for measuring turbidity of polymer suspension are described in Chapter 3. Polymer suspensions were mixed with test solutions at solid-to-liquid ratio of 0.5% by using an end-over-end shaker for 48 hrs. Turbidity measurements were taken at room temperature with a Hach 21000N Laboratory Turbidity Meter (Cole-Parmer) (Fig. 4.5) in accordance with EPA method 180.1.

6.4 RESULTS AND DISCUSSION

6.4.1. Behavior of Polymer Suspensions

Fig. 6.2 shows turbidity results for polymer suspensions in single species Na solutions at ionic strength of 150 mM, 300m M and 600 mM, respectively. For a certain anion solution, lower turbidity corresponds to higher ionic strength, indicating a thinner formation of polymer gel with increased ionic strength. At a given ionic strength, the turbidity of polymer suspensions increases in the solutions following a certain rank: NaOH < Na₂CO₃ < NaNO₃ < NaF < Na₂SO₄ (< NaI), indicating an increased thickness of polymer gel, where a better polymer networked structure is maintained. Note that NaI is an exception because of the brownish color of NaI solution (and thus the turbidity results with NaI will not be discussed herein). As discussed in Chapter 4, the higher turbidity value indicates a well-formed polymer network structure in the solution, where more intramolecular forces are present. The turbidity results of polymer suspensions presented a rank of anions in an order that is different than the conventional Hofmeister rank.

Fig. 6.3 plots the viscosity results at solid-to-liquid ratio of 0.5% polymer suspension in Na solutions at ionic strength of 150 mM, 300 mM and 600 mM in an anion order exhibiting turbidity results from low to high. In each solution, viscosity of polymer suspension has a general decreasing trend as ionic strength increases. This is interpreted

to indicate a collapsed polymer structure, where less intermolecular forces are present in higher ionic strength solutions. At each ionic strength, e.g., at ionic strength of 300 mM, the viscosity of polymer suspension decreases in a trend of anion order, indicating a thinner polymer gel in solutions shifting from left to right (to Na_2SO_4). As described in Chapter 3, the lower viscosity indicates that less intermolecular forces are present due to the aqueous chemistries, and thus more susceptible to shear. However, the viscosity decreases as turbidity increases at fixed ionic strength. This unexpected trend could be due to the higher ionic strength for divalent anion solutions at fixed Na concentration ($I=450$ mM for Na_2CO_3 and Na_2SO_4), suggesting viscosity of polymer suspension tends to be more sensitive to ionic strength than to anion. Future measurements are suggested to conduct on the viscosity of polymer suspensions with solutions of comparable ionic strength to address this hypothesis.

6.4.2. Anion Effect on Behaviors of Polymer Bentonite Suspensions

Fig. 6.4 shows the results, including free swell, viscosity, modified water content, and hydraulic conductivity (before significant polymer elution was detected) of polymer bentonite suspensions with the Na solutions of different anions. Table 6.1 summarizes results for swell index, viscosity, and modified water content as well as the hydraulic conductivity in each solution. Results conducted with 300 mM NaOH were not available due to permeameter corrosion in the high alkaline solution. Results with DI water are presented here as a reference. Viscosity and modified water content measurements were conducted with polymer bentonite suspensions at solid-to-liquid ratio of 10%, and hydraulic conductivity tests were permeated for 15 months. Viscosity results correlate well with modified water content but not necessary with swell index, because the free swell

test does not capture the behavior of polymers in bentonite matrix as described in previous chapters. From low to high on hydraulic conductivity, the PMB GCLs exhibited a trend of behaviors (e.g. modified water content, hydraulic conductivity) with Na solutions in the following anion order: DI>NaF>Na₂SO₄> NaI>NaNO₃> Na₂CO₃>NaCl. This is a different order as the pure polymer suspension and is not the Hofmeister order, suggesting polymer is not the dominating fraction in determining this behavior of polymer bentonite suspensions. In the solutions where PMB exhibits high viscosity and modified water content, e.g., DI, NaF, and Na₂SO₄, the results indicate the presence of either a thick polymer gel or a stronger polymer bentonite interaction. However, Fig. 6.3 shows the low viscosity results of polymer suspension with NaF and Na₂SO₄. This is interpreted to indicate that polymer bentonite interaction dominates behaviors of polymer bentonite suspension.

6.4.3. Implication of Anion Ratio on Polymer Bentonite Interaction

Modified water content tests were conducted with anion ratio solutions to understand the anion effect on polymer bentonite interaction with specific to Cl⁻ and SO₄²⁻. The results in Fig. 6.5 show that the modified water content of PMB is higher in SO₄²⁻ solutions than in Cl⁻ solutions, indicating the water-holding capacity of PMB is higher in sulfate rich solutions. With the exception of solutions of 300 mM Na⁺ and K⁺, the decreasing modified water content trend was observed in 50 m Mg²⁺ solutions with increasing R, despite the fact that an increased turbidity trend was exhibited with polymer suspension in 50 m Mg²⁺ solutions. The change of modified water content of polymer bentonite mixture indicates the water-holding capacity of PMB is higher in sulfate rich solution, suggesting that SO₄²⁻ has a pronounced effect in either promoting stronger

polymer bentonite interaction or increasing the water-holding capacity for bentonite. This is further supported by increased hydraulic conductivity results of PMB-GCLs permeated with sulfate rich solutions reported by Tian et al. (2017).

6.5 SUMMARY AND CONCLUSIONS

This chapter evaluated the effect of anions from Hofmeister Rank on polymer suspension, polymer bentonite suspension, and hydraulic conductivity of PMB-GCL. Anion has effect on behaviors of polymer suspension in the following order: NaOH, Na₂CO₃, NaNO₃, NaF, Na₂SO₄, (NaI) (turbidity from low to high, viscosity from high to low) at a given ionic strength, which is a different order as described in the conventional Hofmeister rank. This suggests that anion type has a profound effect on turbidity of polymer suspension, where a well-formed polymer network structure tends to be present in solutions containing anions on the right side of the ranking order. Viscosity of polymer suspensions decreases following the above order, indicating that the viscosity of polymer suspension is more sensitive to ionic strength than anion type. Additional viscosity measurements are recommended for polymer suspensions with solutions of comparable ionic strength to address this issue.

Anion exhibits influence on behaviors of polymer bentonite suspension in the order: NaF > Na₂SO₄ > NaI > NaNO₃ > Na₂CO₃ > NaCl, where viscosity and modified water content decrease from left to right (F⁻ to Cl⁻). This is a different order presented by the polymer suspension, suggesting polymer is not the dominating fraction in determining these aspects of behavior of polymer bentonite suspensions. Combined with the viscosity results of polymer suspension, it shows that polymer bentonite interaction dominates the

behaviors of polymer bentonite suspension. A supplementary modified water content measurement study with anion ratio solutions supports the above conclusion by showing that SO_4^{2-} is more effective in promoting polymer bentonite interaction. Future study is recommended on developing quantitative methods to evaluate the polymer bentonite interaction.

6.6 REFERENCE

- Akcil, A. and Koldas, S. (2006). Acid Mine Drainage (AMD): causes, treatment and case studies, *J. of Cleaner Production*, 14(12), 1139-1145
- Benson, C., Kucukkirca, E., and Scalia, J. (2010). Properties of geosynthetics exhumed from a final cover at a solid waste landfill. *Geotext. Geomembr.*, 28, 536-546.
- Bradshaw, S., & Benson, C. (2014). Effect of municipal solid waste leachate on hydraulic conductivity and exchange complex of geosynthetic clay liners. *J. Geotech. and Geoenvironmental Eng.*, 140(4), 04013038.
- Cereser, A. (2010). The rheometer as a tool to study a section of the Hofmeister Series. Available at: http://www.membranes.nbi.dk/thesis-pdf/2010_Project_AlbertoCereser.pdf
- Hofmeister F: Zur Lehre von der Wirkung der Salze. *Arch Exp Pathol Pharmacol* 1888, 24:247-260. [Title translation: About the science of the effect of salts.]
- Jo, H., Katsumi, T., Benson, C., and Edil, T. (2001). Hydraulic conductivity and swelling of non-prehydrated GCLs permeated with single species salt solutions. *J. Geotech. Geoenviron. Eng.*, 127(7), 557-567.
- Kolstad, D. Benson, C., and Edil, T. (2004a). Hydraulic conductivity and swell of nonprehydrated GCLs permeated with multispecies inorganic solutions. *J. Geotechnical and Geoenvironmental Engineering*, 130(12), 1236-1249.
- Kolstad, D., Benson, C., Edil, T., and Jo, H. (2004b) Hydraulic conductivity of dense prehydrated GCL permeated with aggressive inorganic solutions. *Geosynth. Int.*, 11(3).

- Piazza, R and Pierno, M. (2000). Protein interactions near crystallization: a microscopic approach to the Hofmeister series. *Journal of Physics: Condensed Matter*, Volume 12.
- Scalia, J., Benson, C., Bohnhoff, G., Edil, T., and Shackelford, C. (2014). Long-term hydraulic conductivity of a bentonite-polymer composite permeated with aggressive inorganic solutions. *J. Geotech. Geoenviron. Eng.*, 140(3), 1-13.
- Shackelford, C., Benson, C., Katsumi, T., Edil, T., and Lin, L. (2000). Evaluating the hydraulic conductivity of GCLs permeated with non-standard liquids. *Geotext. and Geomembranes*, 18(2-3), 133-161.
- Tian, K, Benson, C., and Likos, W. (2016). Hydraulic conductivity of geosynthetic clay liners to low-level radiative waste leachate. *J. Geotechnical and Geoenvironmental Engineering*, DOI: 10.1061/(ASCE)GT.1943-5606.0001495
- Tian, K., Benson, C., & Likos, W. (2017). Effect of anion ratio on the hydraulic conductivity of a bentonite-polymer geosynthetic clay liner. Proceedings, *Geo-Frontiers 2017*, GSP No. 276, ASCE, Reston, VA.
- Zhang, Y and Cremer, P.S. (2006). Interactions between macromolecules and ions: the Hofmeister series. *Current Opinion in Chemical Biology*, Volume 10.

6.7 TABLES

Table 6.1. Tests results with PMBs in Anion Solutions

300 mM Na solution characteristics			Index Tests Results			Hydraulic Conductivity (m/s)		
Salts (Anions)	pH	Ionic Strength (mM)	Viscosity (cP)	Modified Water Content (%)	Free Swelling (mL/2g)	Initially	During Permeation	Ultimately
NaF	7.45	300	1000	500.0	18.0	2.21×10^{-11}	1.62×10^{-12}	4.92×10^{-12}
Na ₂ SO ₄	6.57	450	972	433.3	22.3	-	2.90×10^{-12}	3.37×10^{-12}
NaI	6.27	450	315	238.5	14.5	4.48×10^{-11}	5.44×10^{-12}	1.15×10^{-11}
NaNO ₃	7.27	300	325	217.1	11.0	1.10×10^{-11}	1.58×10^{-11}	1.98×10^{-11}
Na ₂ CO ₃	11.38	300	245	247.5	22.5	3.09×10^{-11}	4.80×10^{-11}	2.49×10^{-12}
NaCl	5.67	300	170	150.1	22.3	2.09×10^{-11}	6.90×10^{-11}	1.03×10^{-11}
DI water	7.00	0	1672	884.9	27.0	-	1.75×10^{-13}	-

6.8 FIGURES

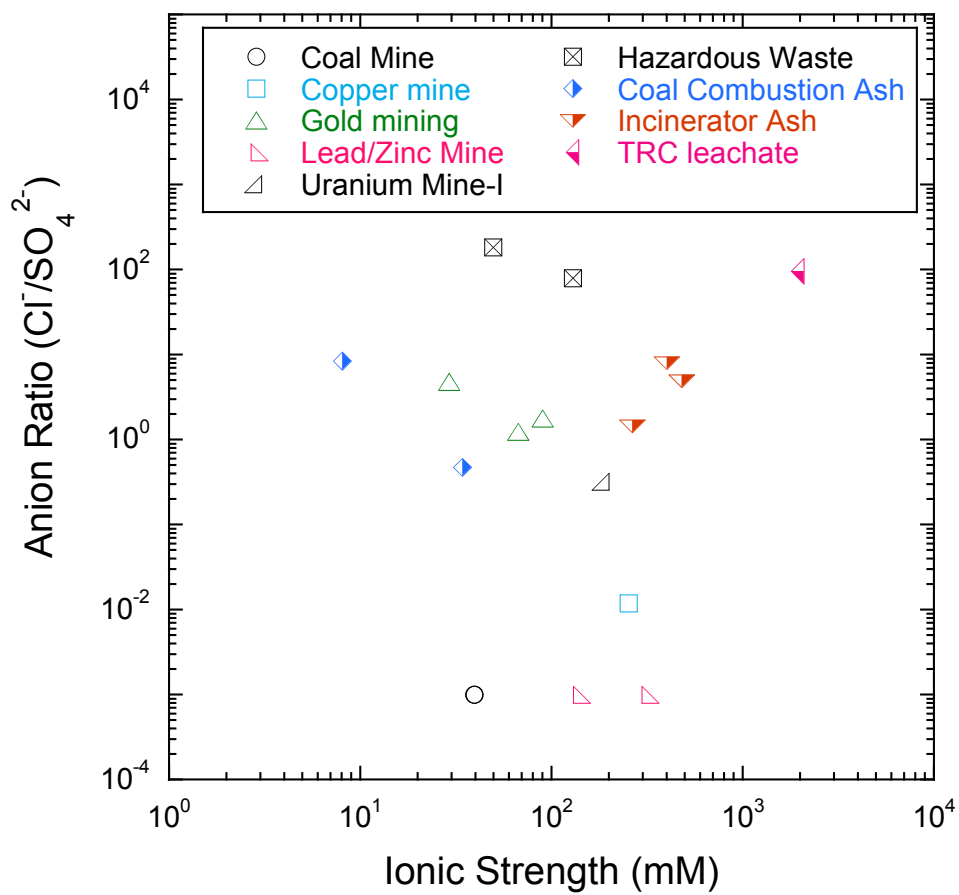


Figure 6.1. Summary of anion ratio and ionic strength of coal mine, copper mine, gold mining, lead/zinc mine, uranium mine, hazardous waste, coal combustion ash, incinerator ash, and TRC leachate. (From Tian et al. 2017)

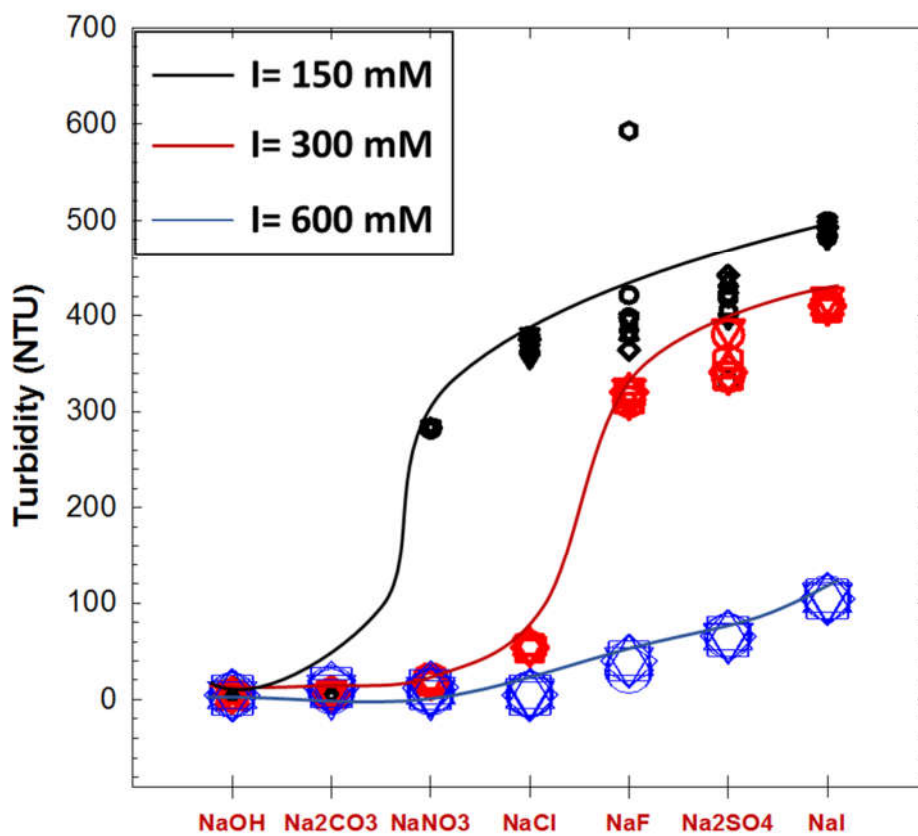


Figure 6.2. Turbidity of polymer suspension at 0.5% in anion series solutions at ionic strength of 150 mM, 300 mM and 600mM.

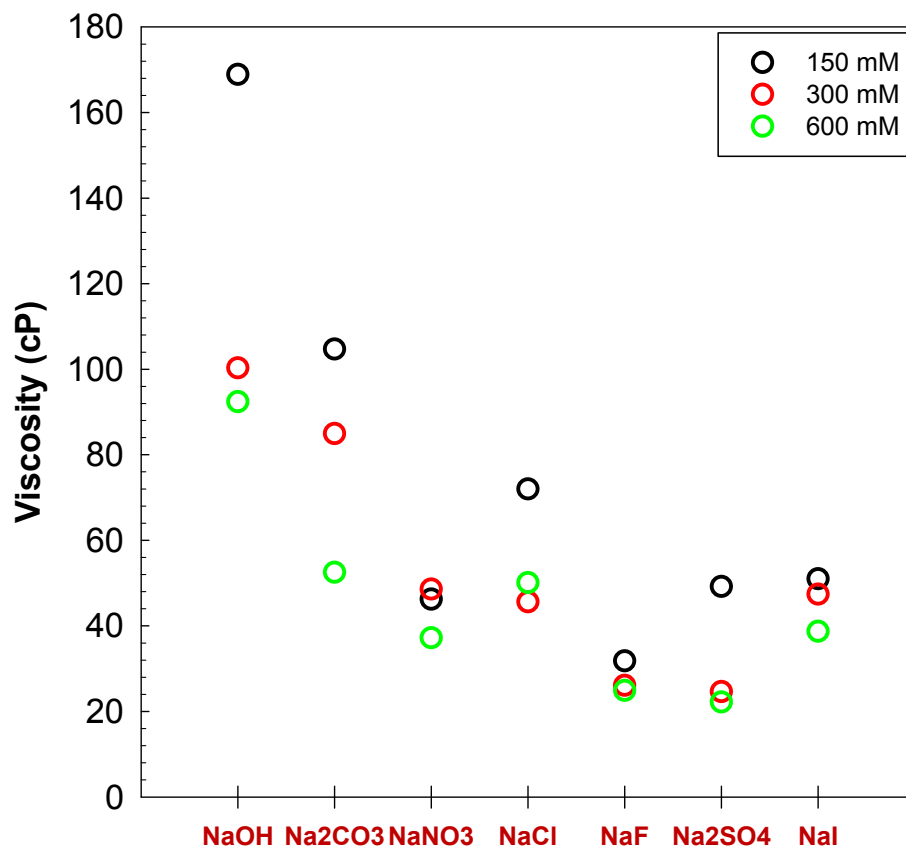


Figure 6.3. Viscosity of polymer suspension at 0.5 % in anion series solutions at ionic strength of 150 mM, 300 mM and 600mM.

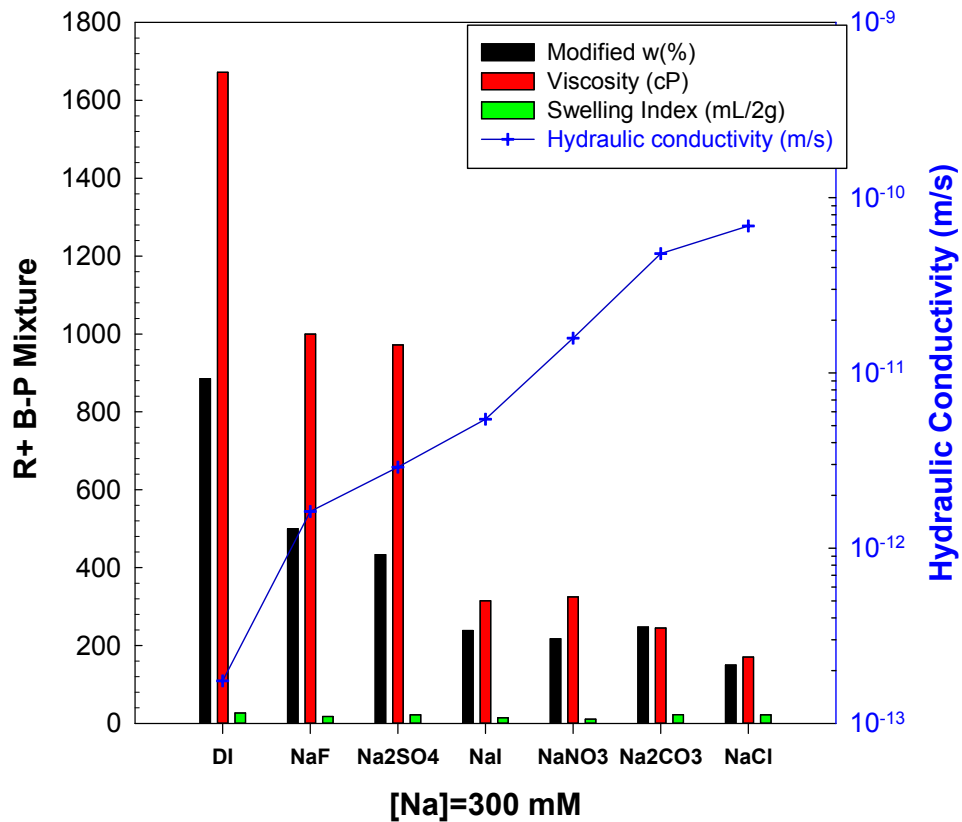


Figure 6.4. Summary of test results with polymer bentonite suspensions and hydraulic conductivity with PMB-GCLs in anion series solutions.

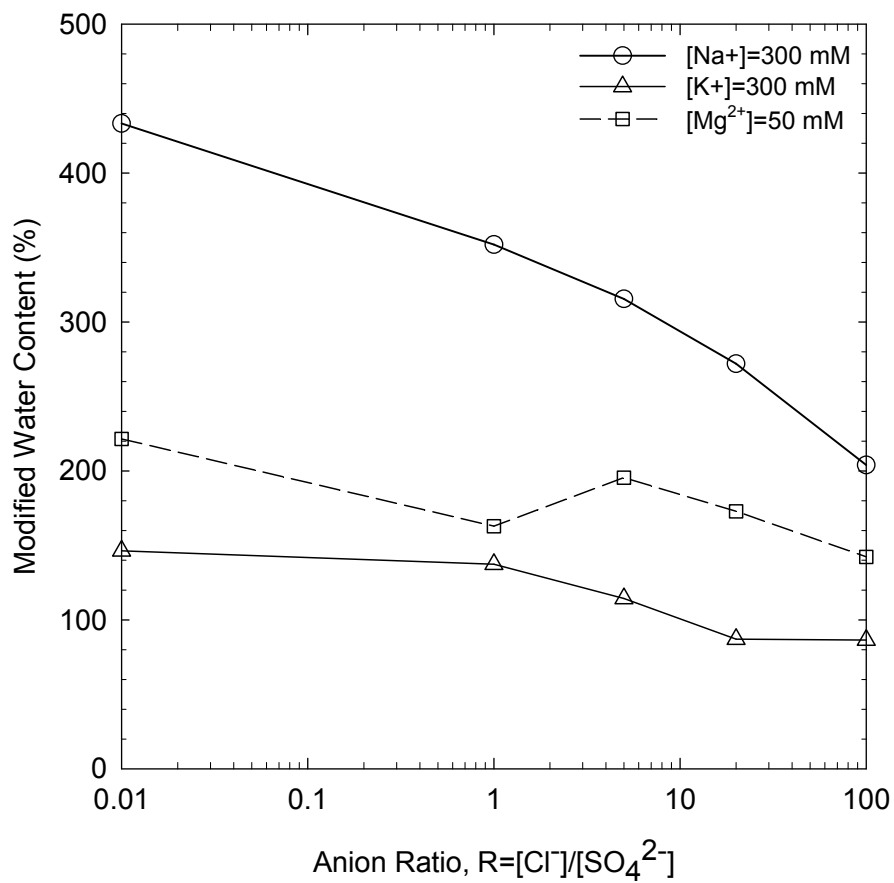


Figure 6.5. Modified water content of polymer bentonite suspension at solid-to-liquid ratio of 10% in 300 mM K^+ and Na^+ solutions, and 50 mM Mg^{2+} solutions as a function of anion ratio.

CHAPTER 7

EFFECT OF ANION TYPE ON HYDRAULIC CONDUCTIVITY OF SODIUM BENTONITE GEOSYNTHETIC CLAY LINERS

ABSTRACT

Hydraulic conductivity tests were conducted on sodium bentonite (Na-B) geosynthetic clay liners (GCL) using solutions with two suites of single monovalent cation (Na^+ and K^+) solutions and varying anion ratio, R , defined as the molar concentration ratio of Cl^- and SO_4^{2-} . An increased hydraulic conductivity was observed with Na-B in solutions rich in SO_4^{2-} regardless of decreasing ionic strength. Two suites of swell index tests were conducted with Na-B in the solutions of 150 mM SO_4^{2-} and 300 mM Cl^- with pure Na^+ solutions, pure K^+ solutions, and solutions of equal amount of Na^+ and K^+ . Swell index results show a higher Na-B swelling in 150 mM SO_4^{2-} solutions regardless of cation type. Chemical analysis of effluents from hydraulic conductivity tests indicates that Na^+ would tend to elute from GCL as the solutions become Cl^- rich. A conceptual framework is proposed on anion adsorption of Na bentonite.

7.1 INTRODUCTION

Previous studies have focused on the effect of cations on the hydraulic conductivity of Na-B GCLs (Jo et al. 2001, Kolstad et al. 2004 a,b), and have indicated that the low hydraulic conductivity of GCLs is primarily due to osmotic swelling of montmorillonite (e.g., >20 mL/ 2 g). Osmotic swelling of montmorillonite requires that cations in the exchange complex must be primarily monovalent (e.g., Na⁺, Li⁺) and the permeant solution must have an ionic strength less than 300 mM (Norrish and Quirk 1954, Jo et al. 2001). However, limited studies have evaluated the effect of anion type and concentration in permeant solution on the hydraulic conductivity of Na-B GCL. Chapter 6 conducted a series of anion studies on PMB- GCLs and observed that the anion in permeant solution has a profound effect on the chemical compatibility and hydraulic conductivity of PMB. Viscosity and modified water content decreased in solutions with certain anions, e.g. Cl⁻, where high polymer elution and high hydraulic conductivity were also exhibited. In the anion series study, it was found that bentonite was the dominant factor determining the hydraulic conductivity of PMB-GCLs at initial stage of permeation, and anion influenced the viscosity of bentonite. Thus, there is a motivation to evaluate if the anion would have effect on sodium bentonite. This chapter evaluates the effects of anion type of behaviors of Na-B using anion ratio solutions. Hydraulic conductivity results and chemical compatibility of effluents including EC, pH and cation concentrations are presented and discussed herein. A conceptual framework is proposed and future study is recommended.

7.2 MATERIALS AND METHODS

7.2.1. Geosynthetic Clay Liners

Tests were conducted on a conventional Na-B GCL with the properties summarized in Table 1.1. The major mineral component of the bentonite is montmorillonite (84%), as determined by X-ray diffraction (XRD) using the methods in Scalia et al. (2014), and the swell index in DI water is 32 mL/2 g.

7.2.2. Testing Liquids

Test solutions used in this study are the anion ratio solutions with [Na] and [K] described in Chapter 3. Single monovalent cation (Na^+ or K^+) solutions were prepared with fixed cation concentration at 300 mM, and anion ratio $R = 0$ (pure SO_4^{2-}), 0.2, 1, 5, 20, and ∞ (pure Cl^-), where R is the molar concentration ratio of Cl^- to SO_4^{2-} . Solutions were prepared with reagent grade salts (e.g., NaCl and Na_2SO_4) mixed in Type II DI water per ASTM D1193.

7.2.3. Free Swell Test

Swell index with Na-B were conducted following the procedure in D5890. Na-B was oven-dried first to remove water at 105 ± 5 °C, and then conducted in a 100-mL graduated cylinder using 2.0 g material with each solution.

7.2.4. Hydraulic Conductivity Testing

Hydraulic conductivity tests were conducted with Na-B GCL specimens following ASTM D 6766. Effluent was collected in 60-mL polyethylene bottles, and analyzed for elemental concentration by inductively coupled plasma-optical emission spectroscopy (ICP-OES) following USEPA Method 6010.

Equilibrium was defined using the criteria defined by ASTM D6766 along with additional criteria for influent and effluent concentrations. Cumulative Na from effluents were calculated from measured Na concentration of each collected effluent bottle.

7.3 RESULTS AND DISCUSSION

7.3.1. Swell Index of Sodium Bentonite

Swell index tests were conducted with Na-B in solutions at a fixed cation (Na and/or K) concentration of 300 mM with single anion SO_4^{2-} (150 mM) or Cl^- (300 mM). As shown in Fig. 7.1, swell index increases with the solution switches from pure Na^+ to pure K^+ , which is consistent with Jo et al. (2001), who reported that Na-B swells more in Na solution than in K solutions due to osmotic swelling. In addition, Na-B exhibits an overall lower swelling in Cl^- solutions than in SO_4^{2-} solution with same cation conditions, e.g. 27 mL/2g in 150 mM Na_2SO_4 and 20 mL/2g in 300 mM NaCl , though the latter one has a lower ionic strength. This result suggests that Na-B swells more in SO_4^{2-} solutions than in Cl^- solutions at same cation concentration.

7.3.2. Hydraulic Conductivity of Na-B GCLs

Hydraulic conductivity of Na-B GCLs permeated with 300 mM Na^+ and 300 mM K^+ solutions is shown in Fig. 7.2. Similar to the results observed with PMB-GCLs, hydraulic conductivity of Na-B GCLs increases systematically as R increases in both Na^+ and K^+ solutions (i.e. relative abundance of Cl^- increases) though the ionic strength of permeation solution decreases. At the same cation concentration, the hydraulic conductivity increases three orders of magnitude in Na^+ solution and one order of magnitude in K^+ solution, as anion ratio increases (from pure SO_4^{2-} solution to pure Cl^- solution). Contrary

to the results found by previous studies (Daniel et al. 1997, Jo et al. 2001, Tian et al. 2016) stating that the hydraulic conductivity of conventional Na-B GCL was sensitive to the cations but not to anion species, the results here indicate the hydraulic conductivity is also sensitive to anion species, at least to SO_4^{2-} and Cl^- .

Fig. 7.3 plots the effluent to influent ratio of pH and EC versus cumulative inflow in K^+ (a) and Na^+ (b) anion ratio solutions, respectively. The chemical equilibrium criteria in D6766 require the electrical conductivity of the effluent (EC_{out}) show no temporal trend and fall within 10% of the electrical conductivity of the influent (EC_{in}). Similar to EC measurement, pH of the effluent are required to be within 10% of the pH of the influent. According to the criteria, no test in this study has achieved the chemical equilibrium as none of them reached $\text{pH}_{\text{out}}/\text{pH}_{\text{in}}$ ratio within 1.0 ± 0.1 . However, in both of Na^+ and K^+ solutions, the initial ratio of EC and pH fall much closer to the value of 1.0 with decreased anion ratio (SO_4^{2-} rich), suggesting that those effluents were not significantly changed when permeated with SO_4^{2-} rich solutions than with Cl^- rich ones. That is, Cl^- more effectively affects the bentonite surface chemistry.

7.3.3. Sodium Elution

Na concentration of collected effluents permeated with 300 mM K^+ solutions were obtained from ICP-OES and are plotted as a function of cumulative inflow in Fig. 7.4 (a). The eluted Na is higher with Na-B permeated with solutions of higher R (Cl^- rich), indicating that the Na^+ originally existed in the bentonite interlayer was more effectively replaced by K^+ in the Cl^- rich solutions.

Cumulative Na elution in the effluent is shown versus cumulative inflow in Fig. 7.4 (b). At cumulative inflow of 1500 mL, the cumulative Na elution permeated with R=0 (pure

SO_4^{2-}) is 312 mg; whereas, the cumulative Na elution permeated with $R = \infty$ (pure Cl^-) is 3655 mg. This discrepancy between cumulative Na elution suggests that Na^+ in the bentonite interlayer would be more effectively replaced by K^+ in the permeant solution for the Cl^- rich condition.

7.4 CONCEPTUAL FRAMEWORK

Fig. 7.5 presents a conceptual framework for interaction of anion and Na-bentonite. Swelling of Na-B occurs in the interlayer space primarily due to osmotic swelling (Norrish and Quirk 1964, Jo et al. 2001, Kolstad et al. 2004), shown in Fig. 7.5-a. It is hypothesized that SO_4^{2-} ion can be more strongly adsorbed by the bentonite edge surface than Cl^- under comparable conditions, which makes the negative charge density of bentonite larger due to its divalency. This may result in a higher capacity for cation adsorption with the bentonite basal surface, thus promoting enhanced osmotic swelling (Fig.7.5-b) resulting in a higher swell index and lower hydraulic conductivity. When permeated to K solutions, SO_4^{2-} has a stronger affinity to Na^+ than K^+ as the ionic radius of Na^+ is larger than K^+ , i.e. 0.102 nm for Na^+ , 0.138nm for K^+ (Database of Ionic Radii from Imperial College London). Therefore, the presence of SO_4^{2-} prevents the cation exchange of K^+ for Na^+ in the interlayer, thus there is less Na eluted (Fig.7.4). Future study is recommended for validating this proposed conceptual framework.

7.5 REFERENCE

Database of Ionic Radii from Imperial College London, available at:

<http://abulafia.mt.ic.ac.uk/shannon/ptable.php>

Jo, H., Katsumi, T., Benson, C., and Edil, T. 2001. Hydraulic conductivity and swelling of non-prehydrated GCLs permeated with single species salt solutions. *J. Geotechnical and Geoenvironmental Engineering*, 127 (7), 557–567.

Geotechnical and Geoenvironmental Engineering, 127 (7), 557–567.

Kolstad, D. Benson, C., and Edil, T. 2004a. Hydraulic conductivity and swell of nonprehydrated GCLs permeated with multispecies inorganic solutions. *J. Geotechnical and Geoenvironmental Engineering*, 130(12), 1236-1249.

Geotechnical and Geoenvironmental Engineering, 130(12), 1236-1249.

Kolstad, D., Benson, C., Edil, T., & Jo, H. (2004b). Hydraulic conductivity of dense prehydrated GCL permeated with aggressive inorganic solutions. *Geosynth. Int.*, 11(3).

Norrish, K. and Quirk, J. P. (1954). Crystalline swelling of montmorillonite. Use of electrolytes to control swelling. *Nature*, 173, 255-256.

Tian, K., Benson, C., & Likos, W. (2017). Effect of anion ratio on the hydraulic conductivity of a bentonite-polymer geosynthetic clay liner. *Proceedings, Geo-Frontiers 2017*, GSP No. 276, ASCE, Reston, VA.

7.6 FIGURES

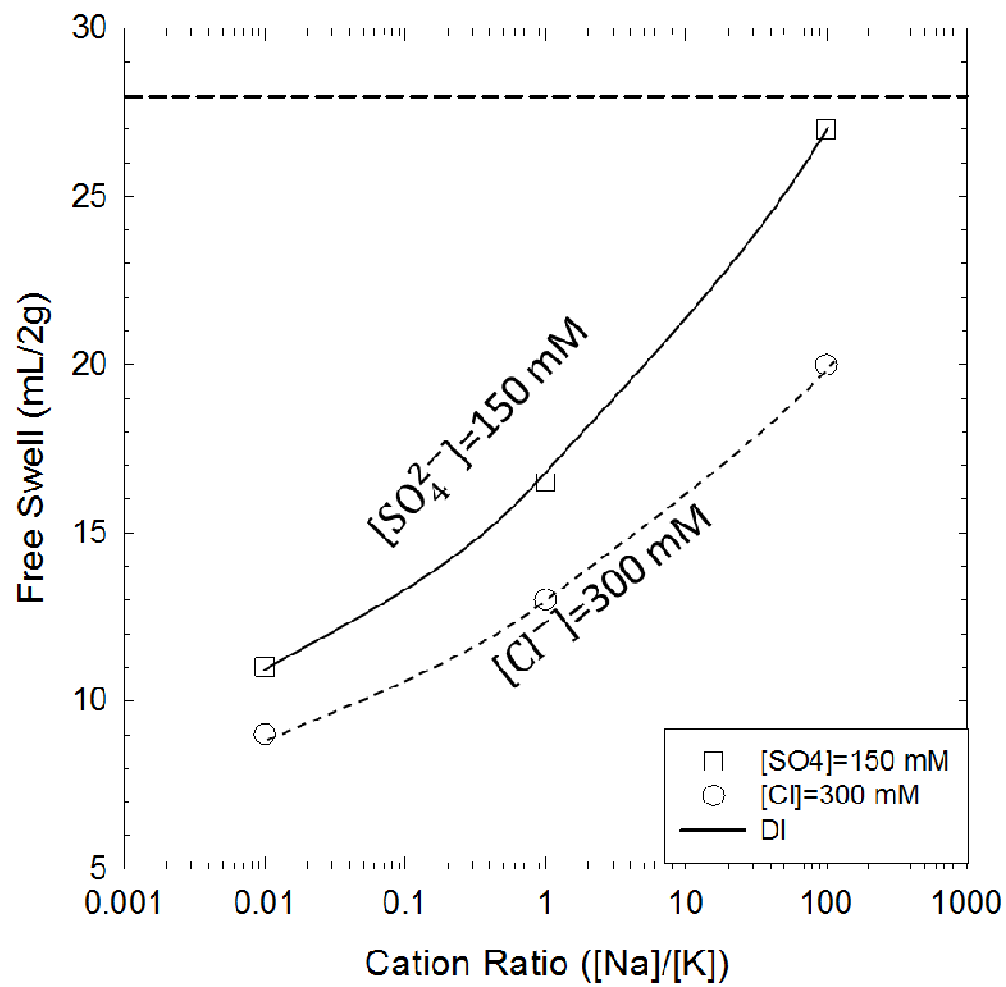


Figure 7.1. Swell index of Na-B in 300 mM cation with single species anion solutions.

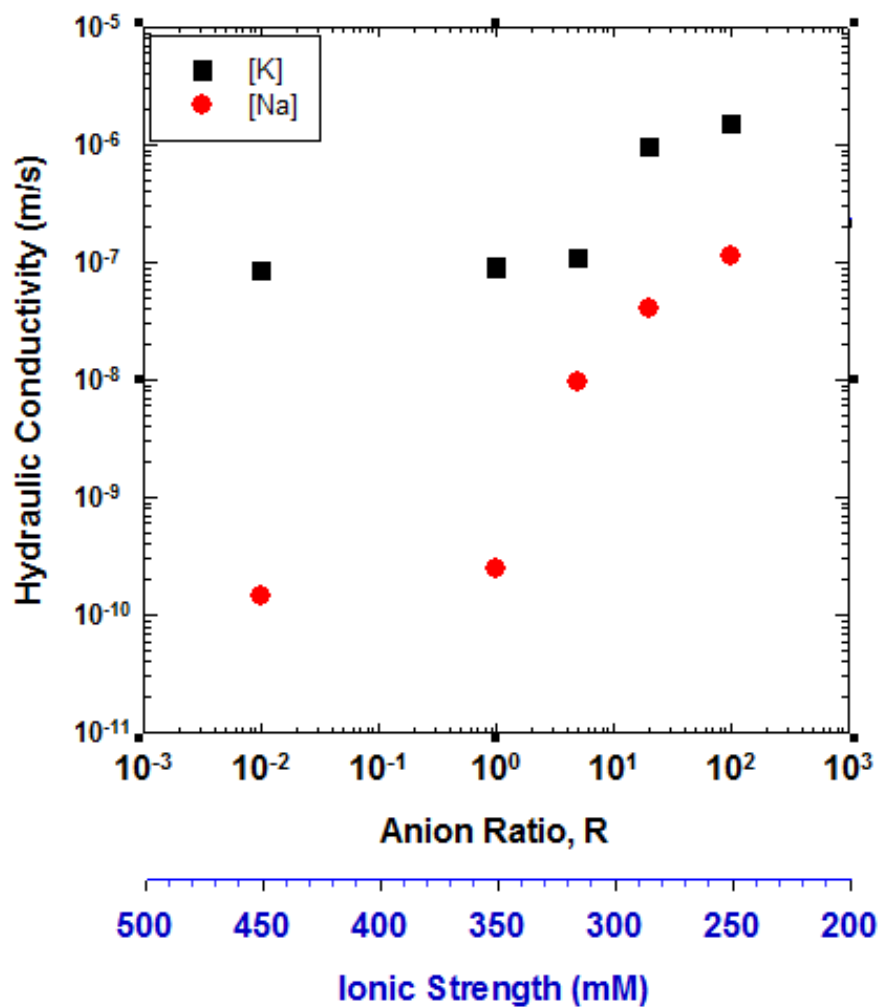


Figure 7.2. Hydraulic conductivity of Na-B permeated with a fixed 300 mM Na⁺ and K⁺ solutions with various anion ratios, along with pure Cl⁻ and SO₄²⁻.

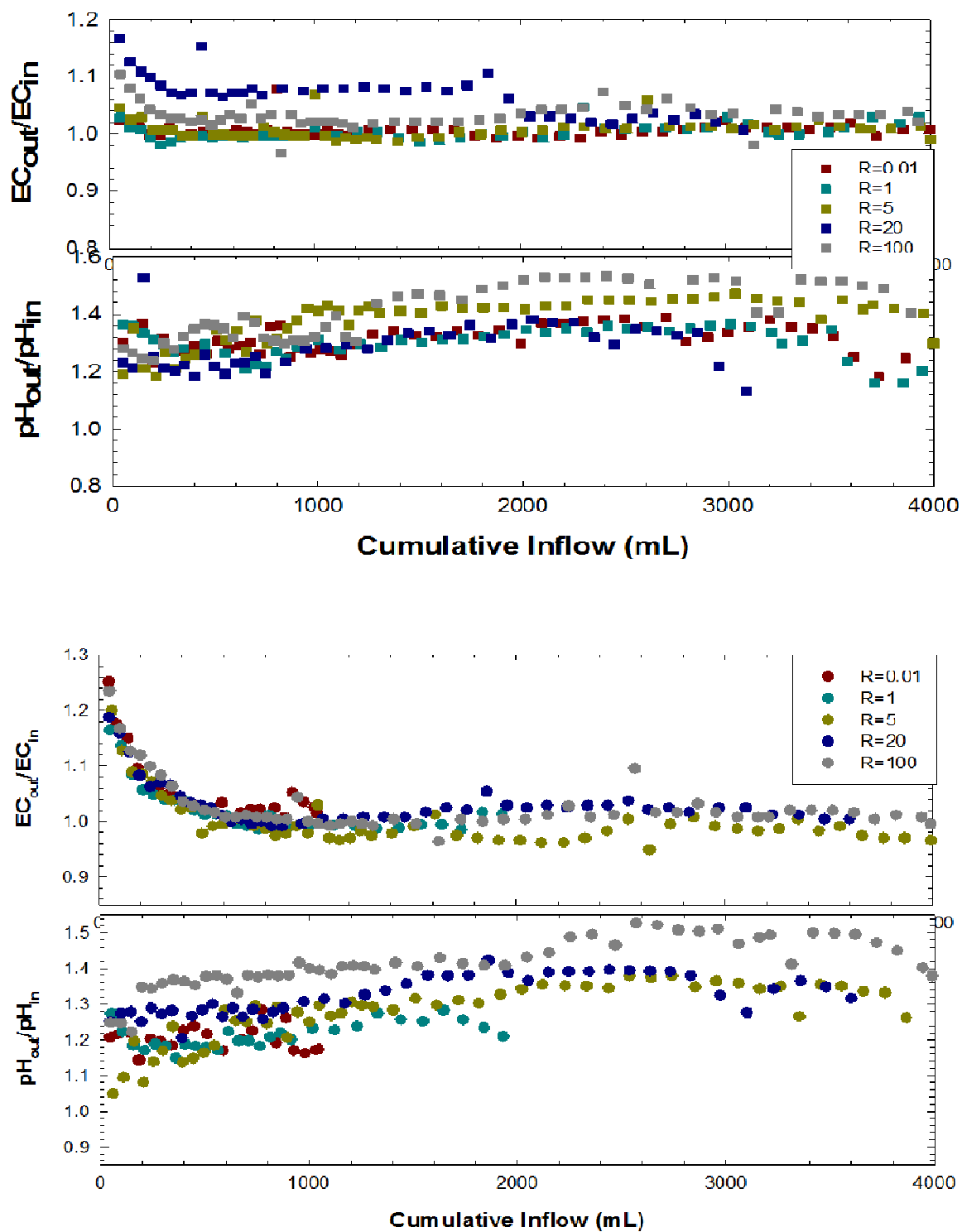


Figure 7.3. Chemical equilibrium condition, ratio of incremental outflow to inflow, pH and EC from tests on Na-B permeated to 300 mM K solutions (a), and 300 mM Na solutions (b).

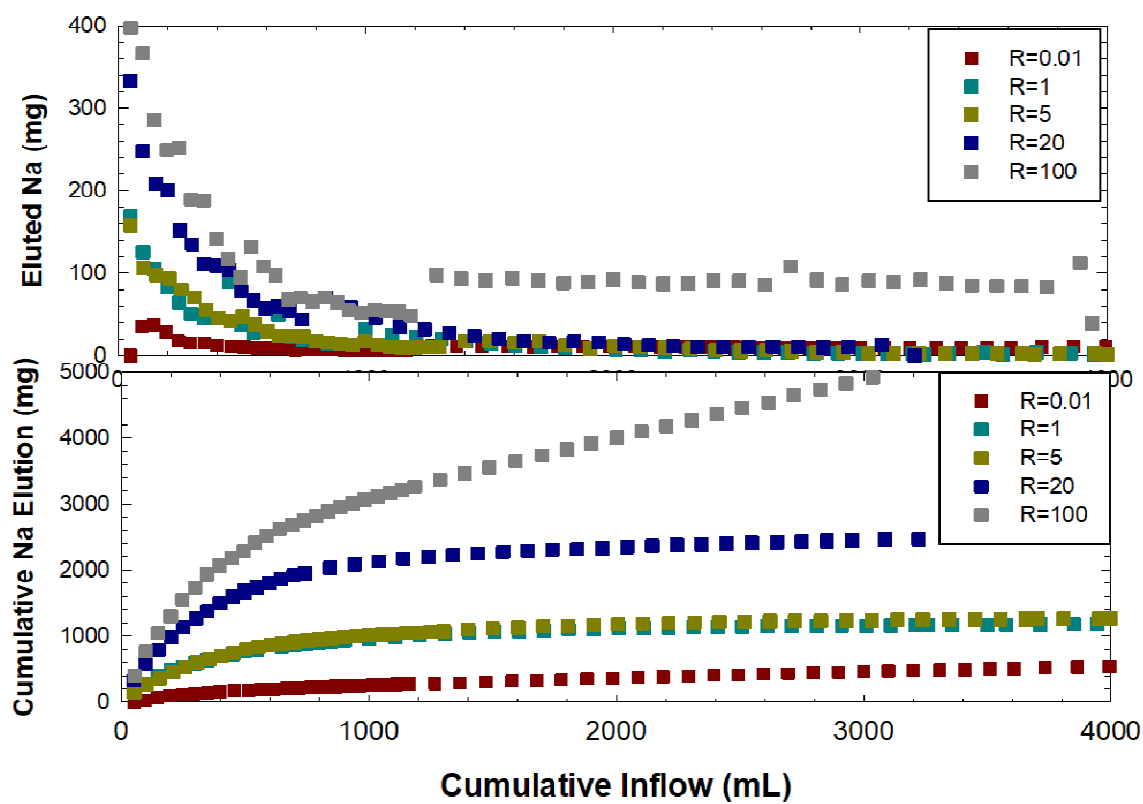


Figure 7.4. Eluted Na as a function of cumulative inflow (mL) for Na-B permeated with 300 mM K⁺ anion ratio solutions (a), and cumulative Na elution as a function of cumulative inflow (mL) permeated with 300 mM K⁺ anion ratio solutions (b).

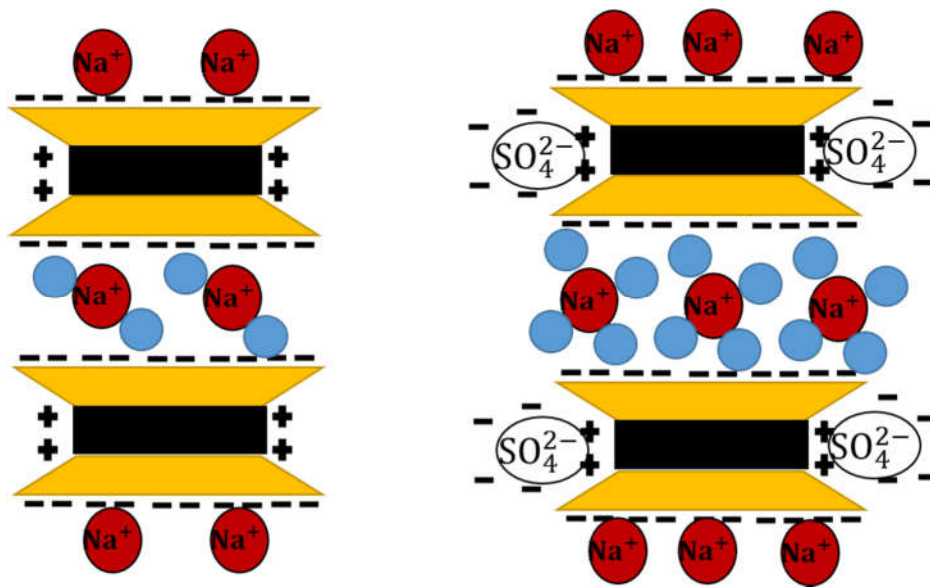


Figure 7.5. Conceptual framework of Na in bentonite interlayer space (a), and enhanced osmotic swelling caused by anion adsorption effect (b).